Design optimization of grid-tied solar Photo-Voltaic (PV) systems for flat roofs

By

K. M. Emtiaz Salim

A thesis submitted in partial fulfillment of the requirements for the degree of

Master of Science

in

Construction Engineering and Management

Department of Civil and Environmental Engineering

University of Alberta

ABSTRACT

In flat roof solar PV projects, design is one of the most important and challenging processes. PV design is challenging in that it requires various aspects to be considered (such as weather, location, purpose of use), and standard guidelines for building a solar PV system are not currently available. More challenging still is the task of improving the design of a solar PV system in order to optimize energy generation in a cost-effective manner. In the present research, in order to determine the optimal system size in terms of cost-effectiveness and power generation capacity for a flat roof solar PV system, optimization of the parameters is carried out. This optimization focuses on the design stage parameters, which must be determined prior to system implementation. In this research, through multi-objective optimization, the solar PV system design process is improved by optimizing the tilt angle and the space between rows (row distance) of solar PV modules. An objective function is developed based on the total solar energy generation from the PV system and energy generation per unit PV in order to improve cost effectiveness. The goal is to maximize these two outputs of the objective function. Particle Swarm Optimization (PSO) is utilized to carry out the optimization. Given that the two objectives are different and have both equal and opposite effects on one another, modifications of the PSO are made. Finally, the outputs of the optimization model are compared and validated by real-world data. The model presented in this thesis will assist designers as well as users to determine the optimal size for a solar PV system. Additionally, this model will assist users in decision making based on the technical output and financial aspects of the system.

ACKNOWLEDGMENTS

First, thanks to ALLAH. I would like to thank my supervisor, Dr. Mustafa Gül, for his support, direction, and encouragement for this work. Without his tutelage and constant motivation, this work would not have been possible. I would especially like to thank him for his patience throughout the entire process.

I would also like to thank my co-supervisor, Dr. Mohamed Al-Hussein. I've learned much from him as he has helped me in my academic endeavors.

Dr. Haitao Yu from Landmark Group of Companies is very much appreciated for his support and knowledge sharing.

Special thanks also to my Department of Civil and Environmental Engineering for allowing me to conduct this research. And also to my friends and fellow students in the Construction Engineering and Management for the different ways we've all been able to assist one another.

Thanks to my Mother and Father for every achievement and every good thing in my life.

TABLE OF CONTENTS

LIST OF TABLES

LIST OF FIGURES

CHAPTER ONE: INTRODUCTION

The solar photovoltaic (PV) industry is one of the fastest growing industries in the world, given that the production volume of solar PVs has increased with a compound annual growth rate (CAGR) of over 40% in the last 15 years (Jäger-Waldau 2016). The demand for solar PV systems is determined by the PV cell (or module) production (Figure 1) as presented in the 2016 PV Status Report in the Joint Research Centre's Science and Policy Report (Jäger-Waldau 2016); this report also projects that worldwide installed PV power capacity could be double between 2015 (235 GW) and 2018.

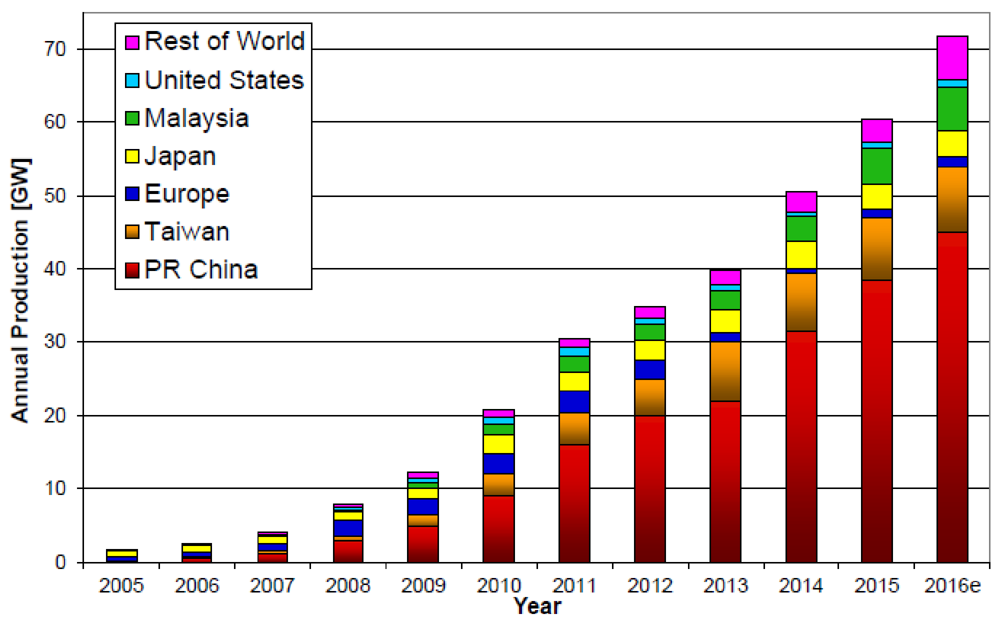

Figure 1: World PV cell/module production from 2005 to 2016 (Jäger-Waldau 2016)

The International Energy Agency (IEA) shows in their Photovoltaic Power Systems Programme (PVPS) T1-29:2016 report (PVPS IEA 2016) that, in Canada, 600 MW of new solar PV power systems were connected to the grid in 2016, increasing the total cumulative installed PV power capacity to 2.5 GW. Installed PV power capacity in MW by province in Canada is presented in Figure 2.

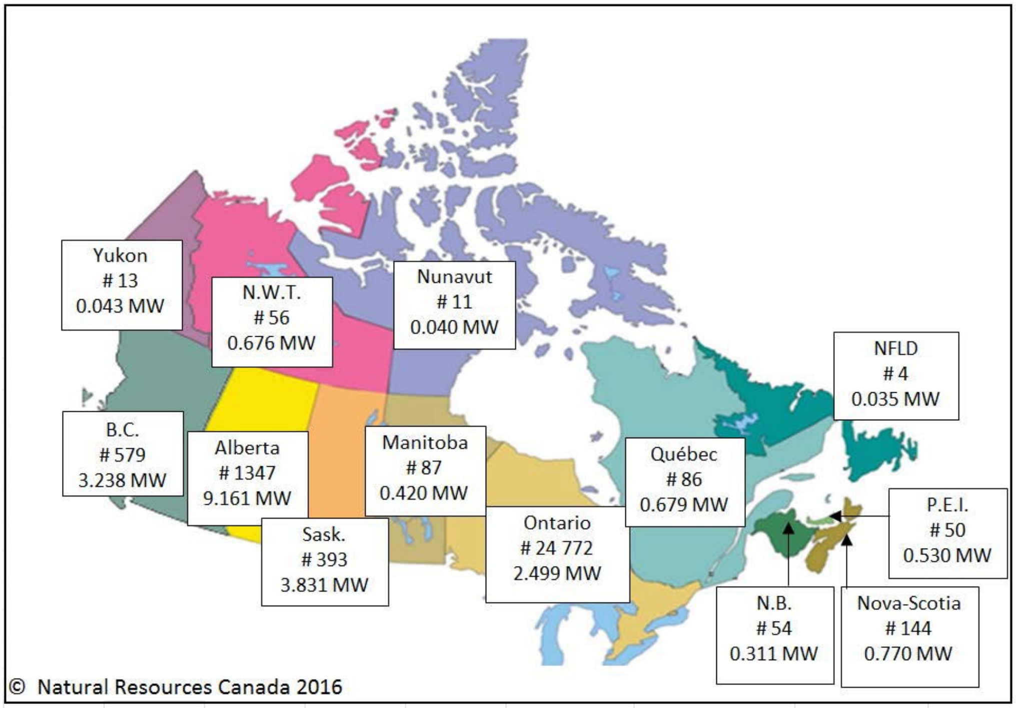

Figure 2: Total capacity of solar PV (MW) for Canadian provinces in 2015 (Poissant et al. 2016)

The number of installed solar PV systems in Alberta totalled 9.161 MW in 2015 and, as of March, 2017, this number has increased to 16.986 MW (Solar energy society of Alberta 2017). This growth of PV installation underscores the need to ensure optimum performance of these systems. Design is a key aspect for optimal solar PV performance; thus, to optimize the system performance, various parameters of the design must also be optimized.

Tilt angle of the solar PV module, shading effect, and total quantity of solar PV modules, among others, are key parameters through which design can be improved. In the case of a flat roof, solar PV modules can be installed in rows. In cases where more than one row is present in a system, the PV panels that constitute one row can cause shading and temperature effects on the adjacent row, depending on the row distance. Therefore, the row distance of the PV modules in a flat roof system is another important factor to consider in performance optimization.

Canada has a cold continental climate, but the solar radiation is high. Some regions, including Alberta, have an average annual sum of Direct Normal Irradiation of 1,500 kWh/m^2/year or greater. High solar radiation and low temperature make this region suitable for operation solar PV systems of various scales.

The factors mentioned above indicate that an effective solar PV system can be obtained through proper system design beginning at the early stage of the project. In an effort to improve the design at an early stage for a flat roof solar PV system, the research presented in this thesis focuses on the optimization of the design parameters. The primary objectives of this research are as follows:

1. Propose a novel optimization method using two key properties of solar PV power generation to comprehensively design the PV system.
2. Implement a multi-objective optimization with the goal of maximum electrical energy generation and energy per unit generation in order to determine the optimum design for solar PV system.

1.1 Problem statement

1.1.1 Rreview and analysis on design optimization

As borne out in a review of the relevant literature, most design optimizations are carried out using electrical and material parameters. Although some research has been carried out using the general parameters (electrical properties of solar cell, heat loss, inverter circuit configuration, etc.), little research exists that combines tilt angle, shading loss, and total number of panels in a flat roof design.

Calculating the solar potential assessment of roofs is a complex task, although roofs are a key part of the building envelope in the process of collecting renewable energy from solar irradiance. A robust strategy is needed in order to install PV modules correctly on flat roofs. PV modules are installed on flat roofs in order to achieve maximum total energy generation considering maximum energy generation of each solar PV panel. Several studies have noted the effects of mutual shading as an important parameter (Kornelakis and Marinakis 2010; Halasah et al. 2013; Strzalka et al. 2012; Quaschning and Hanitsch 1998). Mutual shading depends on the layout of the panels as well as the system, e.g., the position of the bypass diode and the serial/parallel panel connections (Kanters and Davidsson 2014).

1.1.2 Modelling the design of a PV system by tilt angle and mutual module distances

Depending on the project size and scale, the number of solar PV modules in a system can vary from ten to thousands. To determine the optimal arrangement pattern based on tilt angle and row distance in order to maximize power generation, an optimization method is proposed that can determine the ideal combination of tilt angle and spacing between two consecutive rows of panels to maximize energy output.

1.1.3 Design optimization based on PSO technique

Various methods have been proposed in previous literature regarding design optimization, and these will be analyzed in detail in chapter II. In the research presented in this thesis, total energy and energy per unit PV are used in a multi-objective optimization for the first time (to the knowledge of the author) to improve the design of the PV array in a typical grid-tied distributed inverter PV system.

1.2 Organization of the thesis

Chapter 1 of this thesis defines the research problem and the primary research objectives. This chapter provides background information and an outline of the thesis, elaborating on the key problems and how the thesis overcomes these issues.

Chapter 2 provides a comprehensive review of the solar cell/module and array configurations, and discusses the various devices and components used in the grid-connected and household PV systems. It provides the necessary context for understanding the problem statement and also provides a full review and detailed analysis of design optimization of PV systems. This chapter also describes the need for PV system design optimization and reviews previous work carried out in this regard; it then discusses limitations regarding some of the previous methods of PV module design.

Chapter 3 proposes a new method for design optimization of the PV system and the structure of that algorithm with objective functions. It also describes the mathematical analysis carried out to produce the calculations underlying the optimization model, and discusses the implementation of the model in MATLAB.

Chapter 4 presents the results and analysis. Validation is conducted for the new model on the basis of real data, and the validation results are also presented.

Chapter 5 presents the conclusion and discusses the research findings.

CHAPTER TWO: BACKGROUND OF COMPONENTS AND REVIEW OF PREVIOUS WORK ON SOLAR PV SYSTEM DESIGN OPTIMIZATION

The photovoltaic (PV) cell is the smallest unit within the PV system. A group of PV cells linked by a series of parallel connections forms a PV panel (module). Depending on the material and cell fabrication technology, several variations of PV panels are possible. These panels (modules) can be connected with one another in a series (in parallel), constituting a PV string. A PV array, in turn, is built using multiple PV strings connected internally. The components of a PV array are presented in Figure 3.

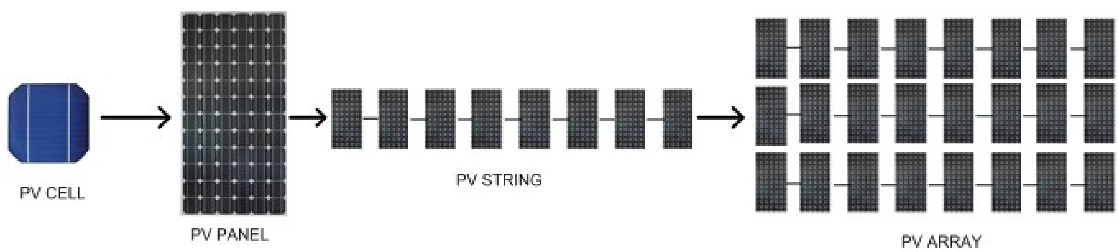

Figure 3: PV array nomenclature

A PV array generates direct current (DC) power from the sun's energy; however, most appliances and the main electricity grid in North America utilize alternating current (AC) power. Thus, after generation, DC power is converted into AC power through a DC to AC converter, which can also be used as the controller for battery storage and as the synchronizer to the grid. Most solar PV systems that have an electrical energy storage bank use a separate electrical charging controller for the battery storage system. Figure 4 illustrates a typical solar PV system that utilizes an energy storage bank and is connected to the grid.

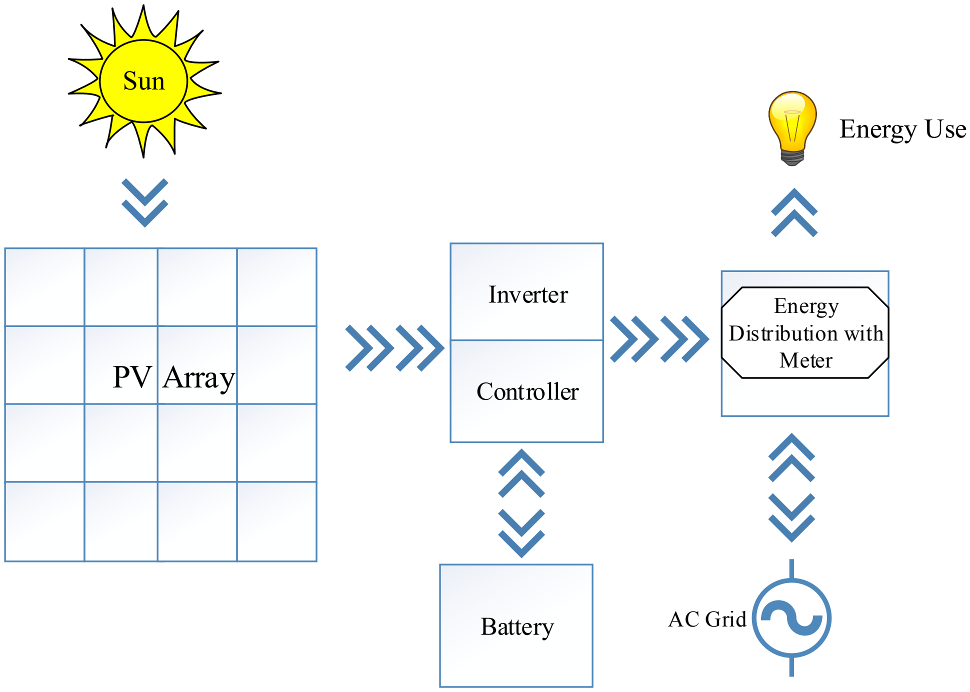

Figure 4: Typical solar PV system

Depending on the electricity grid connection and storage, there are three possible types of PV systems:

Grid-tied—the PV system is connected to the electricity grid and to the local load (Figure 5). To connect the PV array to the grid, it must be electrically synchronized with the grid power. This type of system has no storage capability to store the output power, but the grid functions as a storage system (Mondal and Islam 2011).

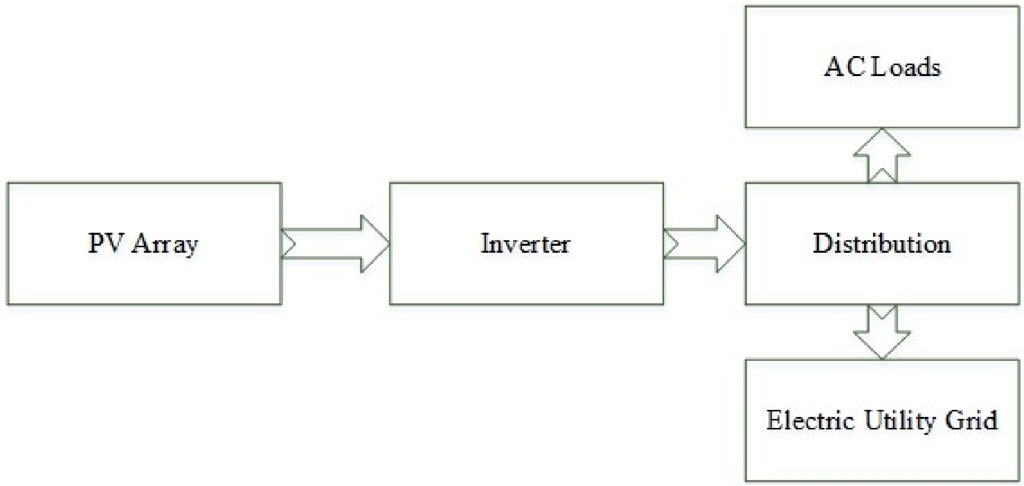

Figure 5: Grid-tied PV system block diagram

- **Stand-alone/Off-grid system**—This system has no electricity grid connection. Independent of the grid supply, stand-alone systems are designed to supply predetermined DC or AC electrical load. In general, stand-alone systems are designed to include an energy storage system (battery bank) (Figure 6). In some applications (e.g., water pump, water heater, ventilation fans, etc.) the PV array is directly connected to a DC load, called a direct coupled system. The direct coupled system load only operates when there is sunlight available.

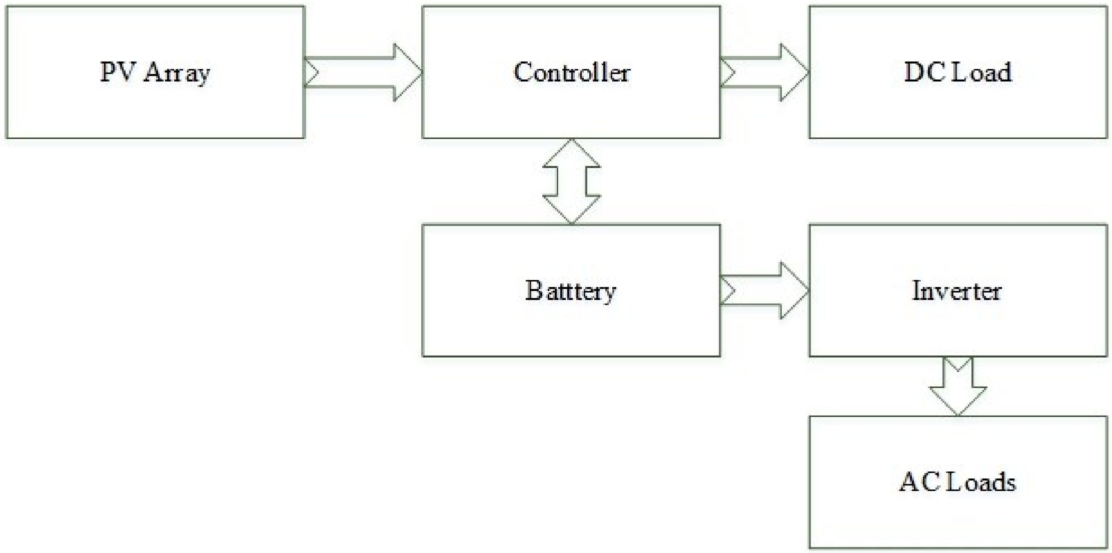

Figure 6: Stand-alone PV system block diagram

- **Hybrid PV system**—In this type of system, the PV array is connected to a storage system to supply the power to the load, and the electricity grid is also connected to the load as a back-up supply if necessary. Battery storage and the electricity grid are connected through a controlling channel. Figure 7 presents a block diagram of a hybrid PV system.

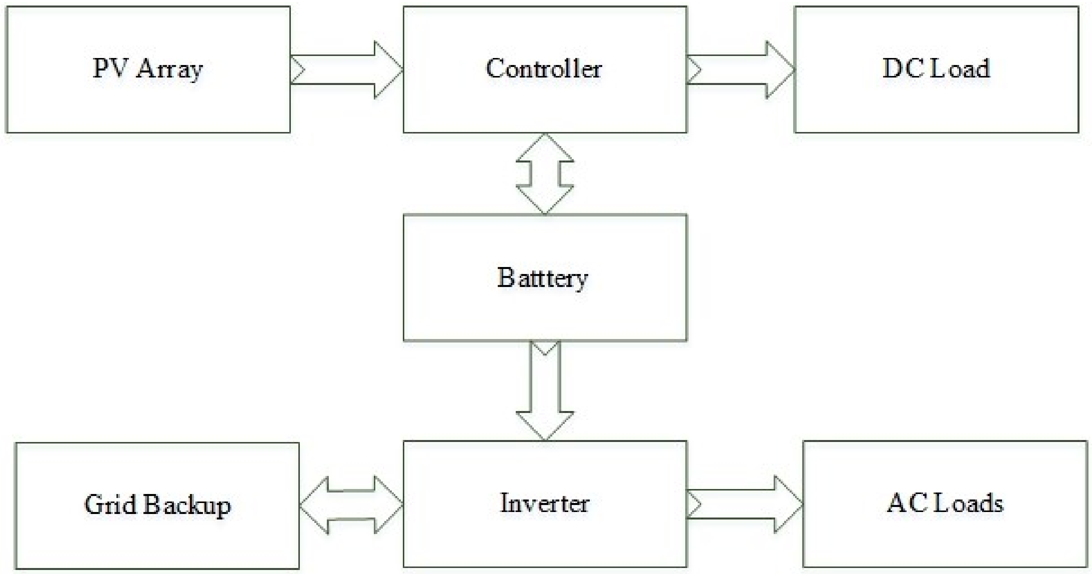

Figure 7: Hybrid PV system block diagram

2.1 Advantages and disadvantages of grid-tied system

In a grid-tied system, as the name suggests, the PV array is connected to the grid. It requires no local storage, it can feed excess energy generation to the grid, and at any non-sunny time the grid can supply electrical energy for household usage.

The grid-tied solar PV system is ubiquitous the world over as a renewable energy solution due to its many advantages, whether the application is a small solar PV system or a large solar PV power plant. The following are some of the advantages of the grid-tied solar PV system (RETScreen 2005; Anapode Solar):

1) It requires less electrical equipment and safety equipment for the electrical infrastructure, which facilitates easy design and implementation.
2) It is synchronized with the grid, which eliminates delays to the transmission and distribution network.

3) It is the most cost-effective among all solar PV systems.
4) It is simple, resulting in installation that is more straightforward and less time-consuming than other types of PV systems.
5) The payback period is shorter for the grid-tied system than for other types of PV systems.

There are drawbacks also for the grid-tied solar PV system (SolarGuy 2014), as summarized below:

1) In the case of a power outage, a grid-tied system stops it operation. Grid-tied solar PV systems cannot produce electricity during a power outage, regardless of whether the sun is shining or not.
2) Since there is no storage capability, it is not possible to use electrical energy from storage.
3) Grid-tied solar PV systems typically require government authorization, triggering extensive paperwork and approvals prior to connecting with the electrical line.
4) If there is an existing legislative framework governing the sale of renewable energy to the government, then the grid-tied solar PV system payback period will be long.

2.2 Major components of grid-tied solar PV system

2.2.1 Solar PV panel

The solar PV panel includes multiple layers of various materials, all of which are important and serve different functions. Figure 8 presents the layer structure of a crystalline PV panel. The first layer of the PV panel is typically glass that is transparent in order to allow solar light to pass through it. Beneath this layer is an Ethyl Vinyl Acetate (EVA) encapsulate, followed by the crystalline PV cell layer; the base layer is made of Polyvinyl Fluoride Film (PV EDUCATION.ORG 2017b).

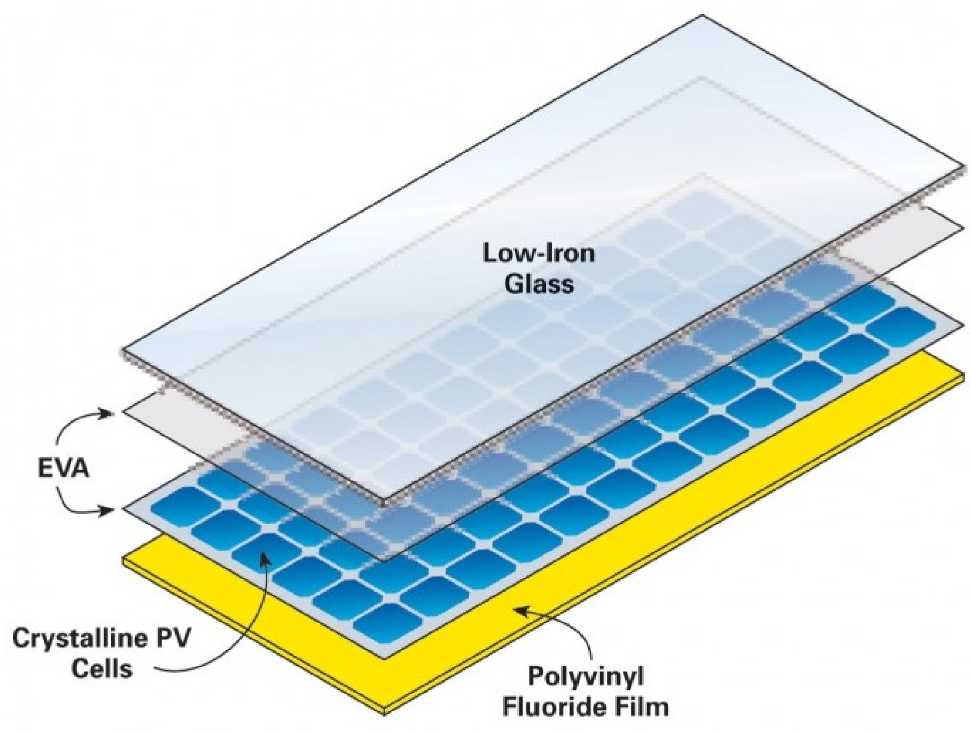

Figure 8: Typical structure of a crystalline PV module (Joe and Windy 2007)

Several properties are important to consider in the selection of materials for the various layers of a solar PV panel. The material forming the top layer should feature low-reflection properties and must be capable of high wavelength transmission (i.e., in the range of 350 nm to 1,200 nm). An anti-reflection coating is sometimes used to reduce the reflection. This layer should be rigid and impervious to water. Dust and dirt accumulation may hinder the passing of light into the PV cells, so this layer must not be prone to dust and dirt build-up. Polymers, acrylic, and glass are typical materials used for this layer. Low-cost PV panels use tempered glass with low-iron content, as this glass is strong, stable, highly transparent, impervious, and inexpensive.

The encapsulate (EVA) layer of the PV panel, as illustrated in Figure 8, provides adhesion between the top surface, the solar cells, and the bottom layer of the panel. The material of this layer must remain stable at high temperatures and during high ultraviolet light exposure. The base layer must be water- or moisture-resistant and should have low thermal resistance. For the bottom-most surface of the PV panel, a thin polymer sheet, polyvinyl fluoride (Tedler), is commonly used. Finally, an aluminum structure is used as the frame of the solar PV panel. This frame must be water- and dust-proof and must be strong and lightweight (PV EDUCATION.ORG 2017b).

2.2.2 Solar PV system inverters

The inverter converts DC power into AC power, thereby making it one of the most important pieces of equipment in the solar PV system. It has a direct influence on the efficiency and reliability of the system. The inverter includes a compound circuit component and a strong outer casing to withstand weather conditions and address other safety issues. In general, 220 VAC and 110 VAC are the typical power supply requirements to run regular electrical appliances; therefore, the solar PV system generates DC power and the solar inverter then converts this power to a 220 VAC or 110 VAC power supply. Solar PV inverters are generally rated based on the amount of AC power they can continuously supply (EnergyTrend 2011).

The solar inverter encompasses several necessary properties. It should have a high efficiency rating. It must be robust and have the necessary electrical protection circuits. Solar PV projects are built for long-term use, so the inverter must require little maintenance. As in the input side of the inverter, DC power from the PV panel varies greatly, so the inverter must have a high tolerance to DC input.

In solar PV systems, common inverters are the central inverter, string inverter, and module/micro-inverter. Figure 9 presents the configurations of these inverters.

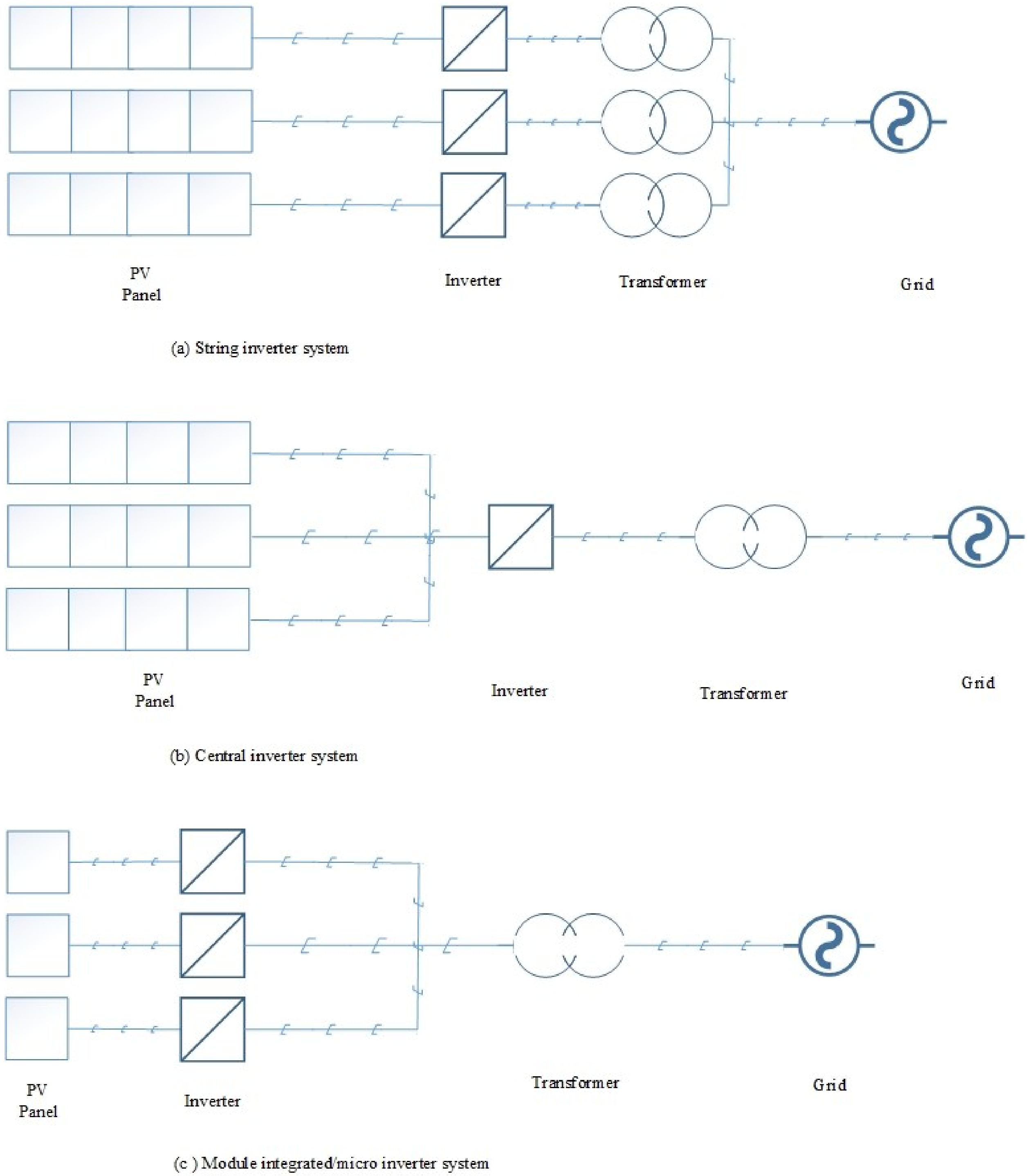

Figure 9: Common inverter configurations for solar PV systems

The central inverter is the most widely used due to the low capital costs associated with it. The disadvantage is monitoring of the each PV panel's condition is not possible. The micro-inverter configuration is costly, as it has a complex circuit and a small range, such that an inverter is required for each PV panel in the system. However, it is more reliable than other inverter systems. Micro-inverter use in solar PV systems has increased in recent years due to advancements in technology, and, given that it requires less space, it can be coupled with the PV panel (Solar Power Engineering 2010).

2.3 Some important factors of the solar PV system

2.3.1 Tilt angle

Tilt angle is the angle between the solar PV panel and the horizontal surface on which that panel is placed. This is an important factor in efforts to maximize the sun's rays. When the rays are perpendicular to the PV panel's surface, the PV panel will receive the maximum amount of solar light and thus the optimally efficient operation. Needless to say, the angle of the sun varies throughout the year and varies from one geographic location to another. Therefore, the optimal tilt angle of a solar PV system varies from one geographic location to another, as well as during different times of year. In Figure 10, angle β, located between the PV panel and the horizontal surface, is the tilt angle for the PV panel.

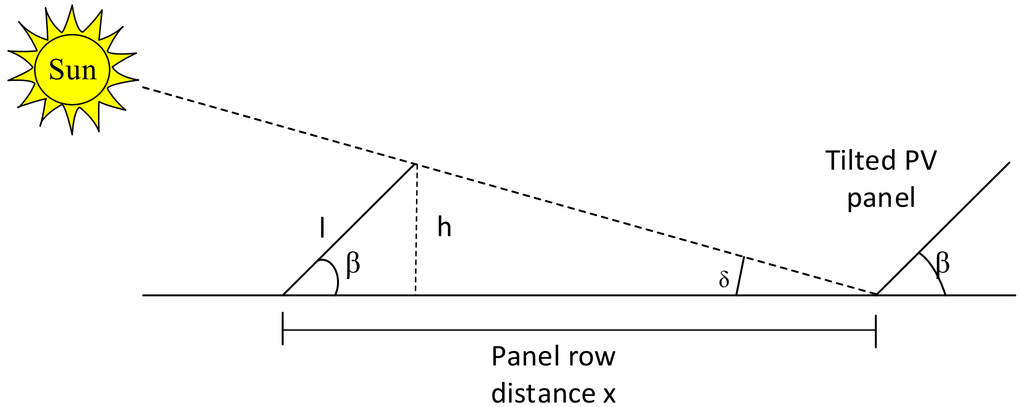

Figure 10: Tilt angle and other factors of solar PV system

2.3.2 Azimuth angle

The azimuth angle is a horizontal angle with reference to the meridian. The sun is directly south in the Northern Hemisphere and directly north in the Southern Hemisphere at solar noon. As the position of the sun changes depending on the time of the year and the geographic location, the azimuth angle also varies depending on the time and location (PV EDUCATION.ORG 2017a). In Figure 11, angle "a" is the azimuth angle of the PV panel with reference to true north.

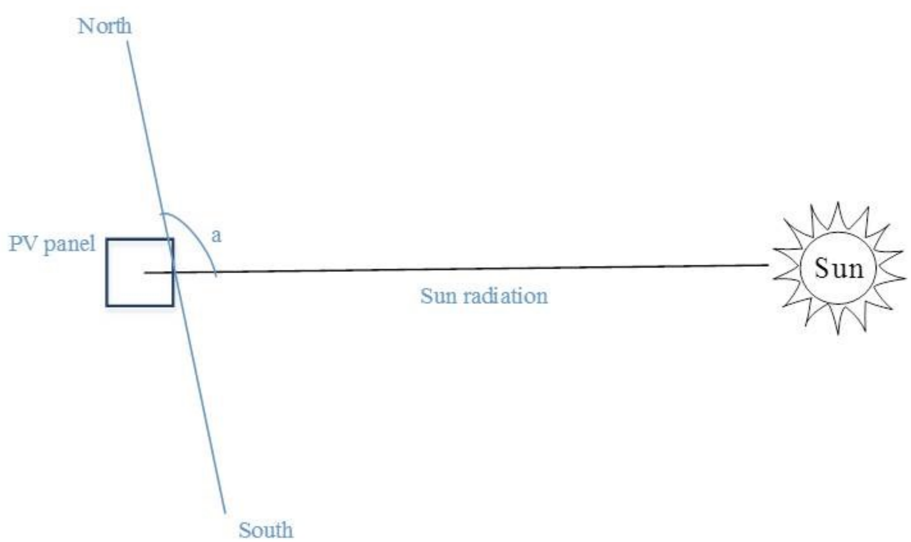

Figure 11: Top view of a rooftop solar PV system

2.3.3 Location

The operation of a solar PV system is entirely dependent upon the weather conditions, given that it generates power from sunlight. Of course, natural conditions such as weather vary in different geographic locations; therefore, location is an important factor in the context of solar PV systems.

2.3.4 Shading

Shading significantly affects solar PV panels. As mentioned above, a PV panel consists of solar PV cells connected either in series or in parallel. When a cell is in shading (cast by another panel, for instance) it is unable to generate power, thereby creating a problem for the entire string of cells or portion of the panel. Even minimal shading on a PV panel has a significant impact on the total power generation.

2.3.5 Solar PV design

The output of a solar PV system is random due to weather changes. Also, after the electrical energy is generated, various types of energy losses may occur which cannot be ignored. Proper design, taking into consideration the various key factors (tilt angle, system size, area, etc.) and necessary steps (proper number of panel calculation, accurate angle design, utilized area calculation, etc.), is imperative in designing a solar PV system that is efficient and cost-effective.

2.4 Review of previous work

French scientist, Edmond Becquerel, first discovered PV power in 1839. Forty-three years later, Charles Fritts successfully developed a working solar PV cell using gold-coated selenium. Moreover, the practice of generating electricity from solar PV cells has been widely utilized since the early 1900s. Mass production of crystalline silicon solar PV cells was first established in 1954 by Bell Telephone Laboratories. The efficiency of their solar PV cell's conversion of the sun's radiation to electrical energy conversion was 6%. In the late-20th century, the effects of global warming started to become a greater concern, while the demand for renewable energy increased. Scientists continued to improve the efficiency of the PV cell while maintaining low production costs. By the early 2000s, a solar cell with 24% efficiency had been developed. Currently, solar PV panel technology is cost-effective and easily accessible .

In this thesis, an in-depth literature review is carried out on recent research, and work on various salient topics in this area, including tilt angle for solar PV energy generation, shading effect on solar PV energy generation, and solar PV system design and optimization.

2.4.1 Tilt angle for solar PV energy generation

The tilt angle of solar PV panels is one of the primary variables determining solar radiation as well as solar PV output in a given geographic location. Several techniques are presented in the literature by which to estimate the solar radiation on horizontal surfaces (Bakirci 2009; Chandel and Aggarwal 2011; Chandel et al. 2005). Solar radiation on tilted surfaces is discussed by (El-Sebaii et al. 2010; Demain et al. 2013). Yang and Lu (Yang and Lu 2007) utilize an anisotropic sky model to determine the yearly optimum tilt angle in Hong Kong. Chen et al. (Chen et al. 2005) employ a genetic algorithm approach to determine the optimum tilt angle in Taiwan. (Hussein et al. 2004) predict the annual performance of mono-crystalline PV panels using a Fortran computer subprogram connected to the TRNSYS simulation program in order to find the optimum tilt angle of solar PVs in Cairo, Egypt. Calabrò (Calabrò 2009) uses a simulation tool to optimize tilt angle at varying latitudes ranging from 36° to 46°. Cheng et al. (Cheng et al. 2009) utilize a software package (PVSYST 3.41) in order to study the optimum tilt angle in various geographic locations and to establish a correlation between latitudes and tilt angle of solar PV. They find the optimum tilt angle to be nearly identical to the latitude of a given location for those south of the Tropic of Cancer. However, they find the optimum tilt angle to be smaller than the latitude of a given location for more northerly latitudes. In a study conducted by (Siraki and Pillay 2012), a simple method based on a modified sky model is used to calculate the optimum angle for PV panel installation. Shading due to surrounding buildings is considered in their model.

2.4.2 Shading effect on solar pv energy generation

In multiple-row solar PV plants, shadings cast from the PV panel reduce the amount of solar radiation to adjacent solar PV panels. To calculate this, shading effect must be considered in the design stage of the project. Several researchers have taken this aspect into consideration and have developed mathematical models by which to calculate and predict the shading effect at various times of day and year using available historical weather data (Appelbaum and Bany 1979; Bany and Appelbaum 1987; Groumpos and Khouzam 1987; Barra et al. 1977; Weinstock and Appelbaum 2004a). Spacing between two consecutive rows of solar panels, as well as other parameters such as orientation and location, it should be noted, significantly affect shading. In this regard, (Groumpos and Khouzam 1987) propose mathematical models by which to calculate the shading effect on solar panels. These models consider various types of tracking systems for solar collectors to calculate the optimal spacing between collectors. (Weinstock and Appelbaum 2004a) develop optimization models to maximize the energy and minimize the area of the solar collectors used in their research. (Appelbaum and Bany 1979) characterize the relationship between shaded area and solar PV panel length in the east-west direction. Other researchers have developed models to calculate the shading area cast on the solar collectors from adjacent collectors for various spacing distances. (Sadineni et al. 2008) present various shading areas of the collectors for various time periods. (Weinstock and Appelbaum 2009) add the azimuth angle of solar panels to their optimization as a variable and observe an increase in the efficiency of an array as a result of reducing the amount of shading. (Bourennani et al. 2010) seek to maximize electrical energy output for solar PV considering spacing and shading issues, using differential evolution and simulation as the optimization technique. (Deline et al. 2013) study the impact of partial shading on the performance of a large PV system. (Goss et al. 2014) develop an algorithm to calculate shading loss in a PV system considering two sub-models: irradiance incident on the cells and current-voltage for each PV panel. An optimization model to minimize the distance between the solar PV panels based on the exact calculation of the shadings based on the position of the sun is developed by (Castellano et al. 2015). (Ramaprabha and Mathur 2012) investigate the effects of partial shading on the energy output of different solar PV systems as well as the losses by incorporating a bypass diode. All of these studies underscore the importance of solar PV row spacing at the design stage.

2.4.3 Solar PV system design and optimization

There are primarily two types of grid-tied solar PV systems: building integrated PV system (BiPV) and distributed generation PV (DGPV) system. In the BiPV system, solar PV supplies a specific load and exports the excess energy to the grid. In the DGPV system, all the energy generated by the system is injected to the grid (Khatib et al. 2013). The design of the BiPV system is primarily dependent on the load demand of local use; the amount of power required to be exported to the grid is also sometimes considered. On the other hand, the design of DGPV is based only on the amount of power required to be exported to the grid. To fulfill this sizing design, researchers have considered various parameters such as PV panel type, PV array size, tilt angle, azimuth angle, and inverter size. Intuition based method is used to select the inverter size in a study conducted by (Fernández-Infantes et al. 2006) in which they optimize external (or self-) shading, wire losses, optimum orientation, and tilt angle for a PV system in Spain; however, they do not consider PV array size. In a study by (Notton et al. 2010), mathematical models for PV array, inverter type, and tilt angle are used. In these models, the variables which are optimized are PV type, inverter type, PV array inclinationand location for a grid-connected system. Four types of PV panels, three types of inverters, and several tilt angles are used in their models to identify the optimum selection. The impact of PV array, orientation, tilt angles, and inverter sizing ratio on the grid-connected solar PV is investigated by (Mondol et al. 2007), where real weather data and mathematical models are used in an iterative simulation to optimize these variables in a grid-connected system. (Kornelakis and Koutroulis 2009) use genetic algorithm (GA) techniques to optimize grid-connected PV systems. Real weather data is employed in their optimization model using iterative simulation. The optimal number and type of PV panels, inverter, tilt angle, optimal arrangement of PV array, and optimal distribution of the PV panels among DC/AC inverters are the objectives of their model.

Particle swarm optimization (PSO) is employed in various research fields due to its efficiency in solving complicated problems. (Kornelakis and Marinakis 2010) use PSO to optimize tilt angle and solar PV system design in their work. They take the electrical properties of the inverter and the system as input and calculate using the net present value (NPV). In their research, the results are economically evaluated in terms of payback period and rate of return. Their research thus contributes to the maximization of economic and environmental benefits.

A number of studies demonstrate the ability of PSO to handle diverse loads and solar irradiation in order to maximize the power output and number of panels used (Zhang et al. 2008; Wang and Singh 2007). In various solar PV and wind hybrid system studies, PSO is used as an optimization technique. (Belfkira et al. 2007; Abedi et al. 2011) use PSO to optimize the PV system, including the optimization of devices being used and the cost function, in a grid-connected system. (Tudu et al. 2011) present a comparative analysis which indicates that PSO technique performs better than Genetic Algorithm (GA) for the sizing problem in terms of the number of iterations and CPU utilization time. In a study conducted by (T.V. et al. 2016), PSO estimators are used to determine the optimum tilt angle on an annual basis, with the results compared with an artificial neural network (ANN) estimator and RETScreen software data.

2.4.4 Solar PV system design method used by solar PV farms

Solar PV system installation or setup companies use various software tools to design the system. To design the required parameters and accessories for solar PV, output simulation and economic evaluation software tools are used. Some of the best-known software are System Advisor Model (SAM), RETScreen, HOMER Legacy v2.68, SKELION, HYBRID2, PVComplete, PVSYST, PVWATTS (Photovoltaic 2014). Typically in these software interfaces the user must input the tilt angle, azimuth angle, PV panel and other electrical components specifications and locations. Then, the software simulates the system showing the energy production and economic analysis.

What follows are the basic design steps commonly followed at solar farms (IFC 2015; Society of Research Administrators 2015):

- Tilt Angle Calculation: The most suitable tilt angle for the solar PV panel in a system is calculated based on the highest radiation and the highest energy production from the PV panel. Using commercially available software and in-house databases, solar PV farms determine the tilt angle and the amount of output power in a given location.
- Row-to-row Distance calculation: Depending on the height of the panel, calculated tilt angle and azimuth angle, consecutive row distance is estimated to prevent shading from one row of panels on to others. This row distance is determined in consideration of winter solstice (when the sun is at its lowest point above the horizon and casts the longest shading). Maintenance space is also considered for the row distance.
- Other Shading Loss: Calculation of shading loss due to skyscraper or trees is carried out using the simulation tools.
- Total Size: Size of the system or number of panels is estimated based on the given area or required power output.
- Mounting Structure design: Analyzing the weight and size of the panel, the mounting structure is designed.
- Electrical Design: Depending on the power output and system size, the inverter and other electrical accessories are estimated.

2.4.5 Limitations of grid-tied solar PV system

Grid-tied solar PV technology has a significant impact on the distribution line, a phenomenon not taken into consideration when the electrical distribution networks were built (Haque and Wolfs 2016). As such, normal operation of the electrical distribution network can be interrupted by large amounts of solar PV penetration. Having a high number of rooftop grid-tied solar PV system can also cause technical challenges such as poor power quality to the grid (Haque and Wolfs 2016). Solar PV output fluctuates significantly over time, and this has negative impacts on the distribution network, as summarized below (Karimi et al. 2016):

- Can cause voltage rise or fall and imbalanced voltage, (i.e., voltage fluctuation in the grid).
- Can interrupt operation of voltage regulation equipment (i.e., capacitor banks, line voltage regulators).
- Can cause fluctuations in reactive power flow.
- Can introduce problems due to over-voltage and over-current protection operation of the grid.
- Creates harmonic distortion of current in the distribution system, which causes power loss through heating in the distribution network.

To prepare electrical distribution networks for future grid-tied solar PV systems, significant changes in overall design and implementation of electrical infrastructure is needed. Addressing the limitations of grid-tied solar PV requires technical solutions (capacitor bank or battery bank to stabilize the grid distribution line) as well as policy and regulatory frameworks (Passey et al. 2011).

2.4.6 Conclusion of literature review

The primary objective of the literature review was to develop an in-depth understanding of the various studies available in the area of design and optimization of solar PV systems and to identify gaps in the existing body of knowledge. The literature review encompassed design optimization, parameters of solar PV system, PSO modelling, and existing methodologies.

Important observations arising from the literature review are summarized as follows:

- No multi-objective optimization model exists by which to achieve total energy generation and energy per unit. Most of the prediction and optimization models are difficult to understand without technical knowledge, such that their implementation in real-world projects is challenging.
- No multi-objective optimization, considering energy generation and affiliated parameters, exists in the research to date.

The research presented herein thus contributes to improved design of grid-tied rooftop solar PV systems. This optimization identifies the configuration of solar PV parameters that maximizes total energy and energy per unit.

Finally this survey aims to serve as a convenient reference for future work in design optimization of solar PV system, assisting companies seeking to improve their PV design process.

CHAPTER THREE: METHODOLOGY OF OPTIMIZATION

3.1 Modification to existing models

A new and simple method is introduced in this thesis to build a relationship between tilt angle and shading effect with the power output. Awad et al. (2016) show that tilt angle and shading effect are correlated in flat roof solar PV systems, and also characterizes the effect of these parameters on the payback period, which forms the basis of their optimization. In the present research, the relationship between power output with the solar PV tilt angle and shading loss due to inter-row shading is used to model a new multi-objective optimization.

3.2 Data used for modelling the PV system

Based on the manufacturer's data sheet, PV output capacity, efficiency, and physical dimensions are collected. The parameters obtained from the data sheet of Conergy PH 255P (Conergy 2015) are presented in Table 1.

Table 1: Data for Conergy PH 255 P solar module

Technical Data	PH 255P
Peak Power-P_{MAX} (W)	255
Power Output Tolerance	0/+3
Module Efficiency (%)	15.5
Module Length (mm)	1,652
Module Width (mm)	994

Module Height (mm)	40

Inverter efficiency and power rating data from SMA Sunny Boy 5.0-US (SMA) are presented in Table 2.

Table 2: Data from SMA Sunny Boy 5.0-US

Technical Data	Sunny Boy 5.0-US
Maximum Usable DC Power (W)	5,150
Maximum Efficiency	97.5%
Power Factor	1
AC Grid Frequency	60 Hz / 50 Hz

3.3 Location details

In the present research, data is drawn from several geographic locations. Latitudes of various cities are used as locations in the model, and weather data from each given location is also used (see Table 3).

Table 3: Geographic locations of Canadian cities used in the model

City	Latitude (°)
Edmonton	53.54
Vancouver	49.28
Toronto	43.65
Ottawa	45.42

Montréal	45.50
Saskatoon	52.13
Winnipeg	49.89

In this research, a flat roof of 50 m × 40 m in size is used as the test subject. The tilt angle and distance between rows are adjusted throughout the study, but the azimuth angle is considered fixed. Given that Canada is in the Northern Hemisphere, the direction of all panels is considered to be south-facing.

In this research, for the fire safety of the solar PV system and roof a 1 m-wide perimeter is applied, with a 1 m-wide pathway through the center of the roof in each direction. Figure 12 shows the layout of the 1 m pathway and 1 m perimeter for a rooftop solar PV system.

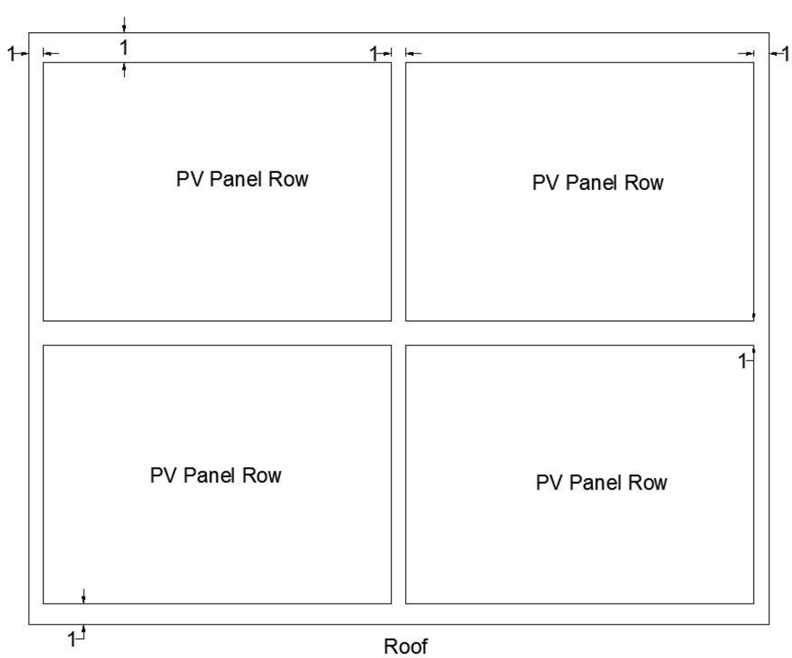

Figure 12: Rooftop solar PV system layout with safety measures (meter)

3.4 Solar radiation calculation

A method discussed by (Bakirci 2012) to calculate the average daily radiation for each calendar month on surfaces toward the equator is used in the present study. Monthly average daily solar radiation data is readily available for many geographic locations; however, there is no data available for radiation on a tilted surface.

Following is the method to calculate solar radiation on a tilted surface from (Bakirci 2012),

$$K_T = H/H_0 \tag{1}$$

Using the clearness index (K_T) and daily extraterrestrial radiation (H_0), the monthly average daily radiation on horizontal surface, H, can be derived. K_T can be expressed (in degrees) for each month.

$$H_0 = \frac{24}{\pi} * I_{SC}\left(1 + 0.033cos\frac{360n}{365}\right)(cos\varphi cos\delta sin\omega_S + \frac{\pi\omega_S}{180}sin\varphi sin\delta) \tag{2}$$

In Equation (2), I_{SC} is the universal solar constant, which has a value 1,360 W/m^2; n is the day of the year given for each month; δ is the solar declination angle; φ is the latitude; and ω_S is the hour angle. δ and ω_S can be derived from the following equation:

$$\delta = 23.45sin\left(\frac{360(n+284)}{365}\right) \tag{3}$$

$$\omega_S = cos^{-1}(-tan\delta tan\varphi) \tag{4}$$

H_T, the average daily radiation on a tilted surface, can be expressed as

$$H_T = RH \tag{5}$$

where R is the ratio of the daily average radiation on a tilted surface to that on a horizontal surface for each month. R is estimated by considering beam, diffuse, and reflected radiation received by a tilted surface, and can be expressed using Equation (6),

$$R = \left(1 - \frac{H_d}{H}\right) R_b + H_d \left(\frac{1+cos(\beta)}{2h}\right) + \rho(\frac{1- COS(\beta)}{2}) \quad (6)$$

where β is the tilt angle, R_b is calculated from the beam radiation on a tilted surface and ρ is the ground reflectance. H_d is the monthly average daily diffuse radiation, which can be expressed as

$$H_d = H(1 - 1.13K_T) \quad (7)$$

Beam radiation ratio, R_b, depends upon cloudiness, particulate concentration, and water vapour. R_b can be derived from Equation (8).

$$R_b = \frac{cos(\varphi-\beta)\, cos(\delta)\, sin(\omega_s') + \frac{\omega_s' \pi}{180} sin(\varphi-\beta)\, sin(\delta))}{cos(\delta)\, cos(\varphi)\, sin(\omega_s) + \left(\frac{\omega_s \pi}{180}\right) sin(\varphi)\, sin(\delta)} \quad (8)$$

where ω_s' is the sunset hour angle of a tilted surface and is expressed as

$$\omega_s' = \min[\omega_s, cos^{-1}[-tan\delta \tan(\varphi - \beta)] \quad (9)$$

Table 4 presents the ground albedo (reflectivity) data collected from (Iqbal 2012), as well as the monthly mean daily solar radiation on a horizontal surface collected from (Natural Resources Canada 2013).

Table 4. Monthly mean daily solar radiation on horizontal surface and monthly albedo of various locations in Canada

Month/City	Edmonton		Vancouver		Saskatoon		Winnipeg	
	monthly mean daily solar radiation on horizontal surface	Monthly Avg. Ground Albedo	monthly mean daily solar radiation on horizontal surface	Monthly Avg. Ground Albedo	monthly mean daily solar radiation on horizontal surface	Monthly Avg. Ground Albedo	monthly mean daily solar radiation on horizontal surface	Monthly Avg. Ground Albedo
Jan.	1.03	0.58	0.8	0.18	1.34	0.49	1.40	0.54
Feb.	2.05	0.57	1.54	0.17	2.48	0.5	2.36	0.55
Mar.	3.63	0.46	2.84	0.17	3.85	0.42	3.76	0.47
Apr.	4.8	0.32	4.28	0.14	5.21	0.24	4.90	0.31
May	5.92	0.26	5.59	0.14	6.16	0.18	5.77	0.20
Jun.	5.96	0.25	5.95	0.14	6.67	0.20	6.15	0.21
Jul.	6.11	0.25	6.26	0.14	6.52	0.21	6.33	0.21
Aug.	4.75	0.25	5.32	0.14	5.53	0.22	5.26	0.23
Sep.	3.46	0.26	3.69	0.14	3.85	0.22	3.61	0.23
Oct.	2.18	0.28	2.04	0.14	2.55	0.22	2.21	0.24
Nov.	1.29	0.39	0.97	0.15	1.40	0.27	1.30	0.32
Dec.	0.77	0.53	0.66	0.18	1.01	0.27	1.05	0.45

Table 4 (Continued):

Month/City	Toronto		Ottawa		Montréal	
	monthly mean daily solar radiation on horizontal surface	Monthly Avg. Ground Albedo	monthly mean daily solar radiation on horizontal surface	Monthly Avg. Ground Albedo	monthly mean daily solar radiation on horizontal surface	Monthly Avg. Ground Albedo
Jan	1.39	0.50	1.54	0.62	1.52	0.32
Feb	2.23	0.50	2.60	0.60	2.43	0.33
Mar	3.36	0.38	3.68	0.43	3.57	0.25
Apr	4.45	0.28	4.61	0.12	4.41	0.22
May	5.49	0.25	5.41	0.13	5.34	0.20
Jun	6.06	0.25	5.91	0.19	5.77	0.20
Jul	6.09	0.25	5.90	0.19	5.85	0.20
Aug	5.14	0.25	4.96	0.20	4.84	0.20
Sep	3.85	0.25	3.60	0.20	3.74	0.20
Oct	2.53	0.25	2.33	0.25	2.31	0.21
Nov	1.34	0.29	1.29	0.21	1.29	0.23
Dec	1.05	0.39	1.16	0.56	1.11	0.28

The radiation (H_T) results from Equation (1) are compared with the RETScreen results (Figure 14) given in Table 5 to show the competency of this radiation calculation (RETScreen 2005). For the purpose of this comparison, tilt angle (Figure 13) value is equal to latitude. Equation (1) to (9) is used to calculate this radiation.

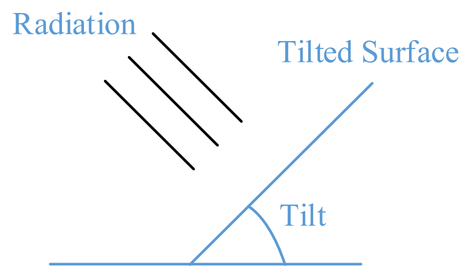

Figure 13: Tilted surface diagram

Table 5: Comparison of calculated monthly mean daily solar radiation with RETScreen data of 53° tilt in Edmonton and 49° tilt in Vancouver.

Month/City	**Edmonton (53° Tilt)**		**Vancouver (49° Tilt)**	
	Calculated Value ($kWh/m^2/day$)	RET Screen Value ($kWh/m^2/day$)	Calculated Value ($kWh/m^2/day$)	RET Screen Value ($kWh/m^2/day$)
Jan.	3.19	3.25	1.39	1.35
Feb.	4.70	4.75	2.33	2.35
Mar.	5.97	5.85	3.63	3.64
Apr.	5.47	5.45	4.43	4.57
May	5.51	5.60	5.01	5.21
Jun.	5.12	5.23	5.00	5.21
Jul.	5.43	5.54	5.42	5.64
Aug.	4.82	4.90	5.25	5.41
Sep.	4.49	4.48	4.43	4.49
Oct.	4.03	4.02	3.00	3.05
Nov.	3.69	3.69	1.63	1.60
Dec.	2.56	2.73	1.22	1.22

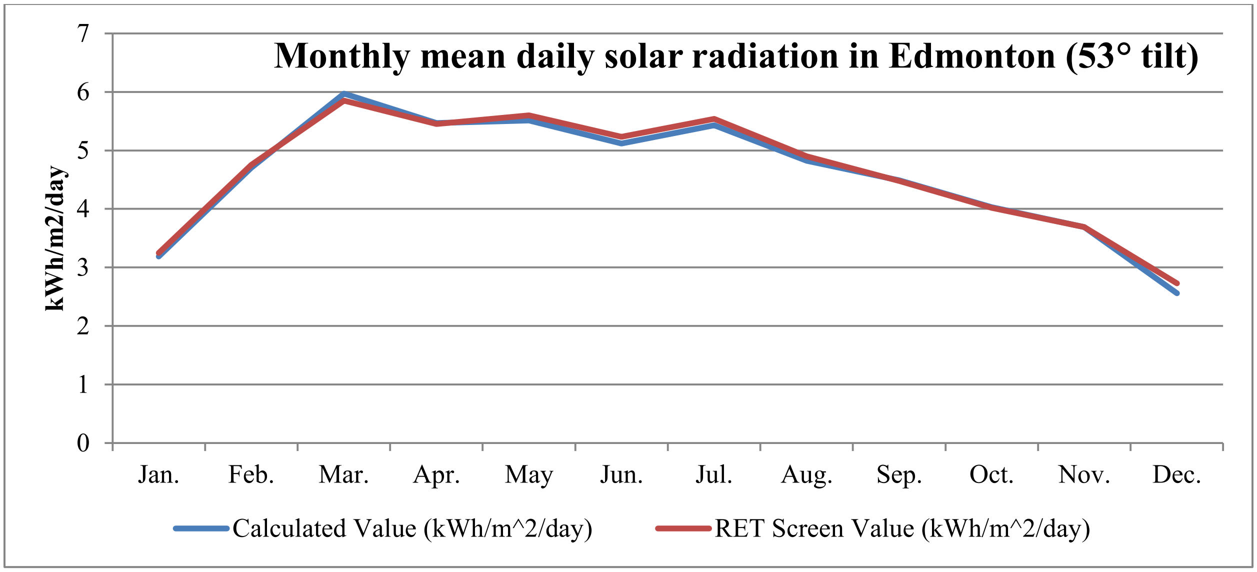

(a) Edmonton's radiation on a tilted surface with 53° tilt angle

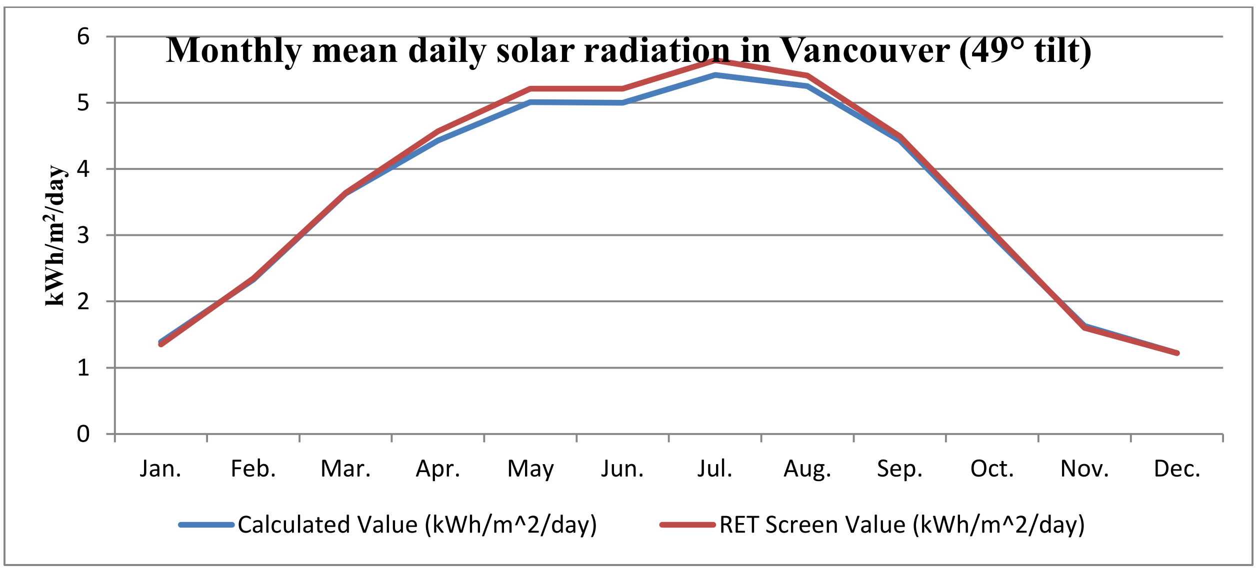

(b) Vancouver's radiation on a tilted surface with 49° tilt angle

Figure 14: Monthly mean daily solar radiation in kWh/m^2/day in (a) Edmonton, and (b) Vancouver

3.5 Solar PV panel output and shading length calculation

Solar PV output is derived using the calculated solar radiation and considering mismatch and wire loss, dust effect, DC-to-AC conversion factor, and inverter efficiency. This type of radiation is measured in m^2, thus PV panel area is used with conversion efficiency. The angles are measured in degrees.

$$E = A * r * H_T * PR \quad (10)$$

where

E = Energy (kWh)

A = Total solar panel area (m^2)

r = solar panel yield or efficiency (%)

H_T = Average solar radiation on tilted panels (shading not included)

PR = Performance loss

The amount of solar shading is calculated to determine the shading loss (Awad et al. 2016).

$$ALT = 90 - Zenith \quad (11)$$

$$Zenith = cos^{-1}(\cos\varphi * cos\delta * cos\omega_S + sin\varphi * sin\delta) \quad (12)$$

where ALT is the altitude angle of the sun and $Zenith$ is the zenith angle of the sun.

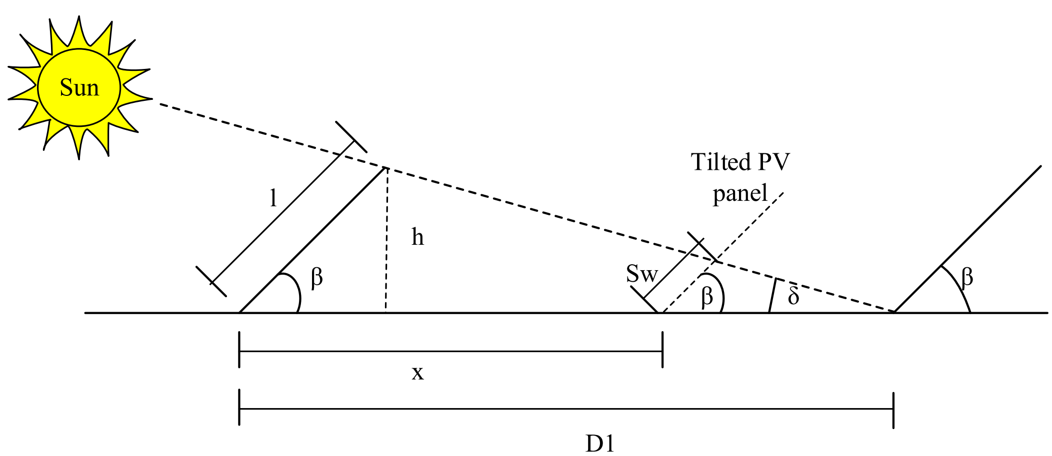

Figure 15: Shading effect for the row distance

The maximum shading distance for a for a given time and panel length can be expressed as,

$$D1 = \ l * [+(sin\beta * \cot(ALT))] \quad (13)$$

where l is the length of the panel and $D1$ is the distance between two consecutive rows where shading is not present. The model then calculates what would be the energy gain or loss for the shading within this space.

$$Sw = [(D1 - x) * sin(ALT)]/[sin\,(180 - ALT - \beta] \quad (14)$$

where x is the row distance, which is less than $D1$, and Sw is the amount of shading (Figure 15).

By deducting the energy loss due to this shading in the solar PV panel from that without shading, generation net energy gain can be obtained.

$$NetEnergy = E - (E * \frac{Sw}{l}) \quad (15)$$

The proposed model considers time for the hour angle (ω_S) and day number (n) for a month to be constant.

To achieve a commercially efficient design, PV system energy gain per unit (kW) is calculated. This indicates (in kWh/kW) the output efficiency of each panel but not of the overall system.

$$EnergyperKW = \frac{NetEnergy}{Systemsize} \quad (16)$$

$$Systemsize = Np * PO \quad (17)$$

where Np is the total number of PV panels in a system and PO is the power output rating of the PV panel given in the manufacturer's specifications.

3.6 Development of solar PV output optimization algorithm

3.6.1 Structure of the optimization model

To calculate the net energy gain from a given project using these equations, it is necessary to determine the number of panels to be installed for a given area, which is a tradeoff between used area and total number of PV panels. There are primarily two methods by which to determine the area. In the first method, PV panels are placed far apart and at an optimum tilt angle to ensure they are free from shading and that each panel can harvest the greatest amount of energy. However, this method results in unused space on the flat roof and lower energy production overall. The second method places the modules closer together with a smaller tilt angle and with shading. As a result, this method requires a much higher number of PV panels and high-rated peak energy. But, due to the shading, the individual panels are less productive, and the number of panels increases the installation and maintenance costs.

To balance the total output power of a system and effective output power of a solar PV panel, a new model is proposed subject to the following key factors.

- Variables necessary to run the model: the available area determines the system size; the system location determines the sun angles and row-to-row shading; solar panel manufacturer’s specifications give dimension and efficiency of that solar PV panel and, finally, the generated energy per unit solar PV system reflects a project’s fixed costs (the costs that remain constant regardless of the size of the system) and marginal costs (the scalable costs that change according to the module quantity, the wires, and the mounting system).

- Tilt and spacing of the panels are changed for the searching of the optimization goal, while other solar PV parameters are fixed. These two key variables are closely related, as the value for one determines the effects of the other; hence this is a joint optimization.

- In the optimization model one output is the **system size** (the module quantity, determined by the module spacing) while the other is **energy yield** (determined by the module specifications, solar insolation, and shading loss). System cost, revenue and, in turn, the payback period, can be calculated accordingly.

Figure 16 presents the structural diagram of the optimization model.

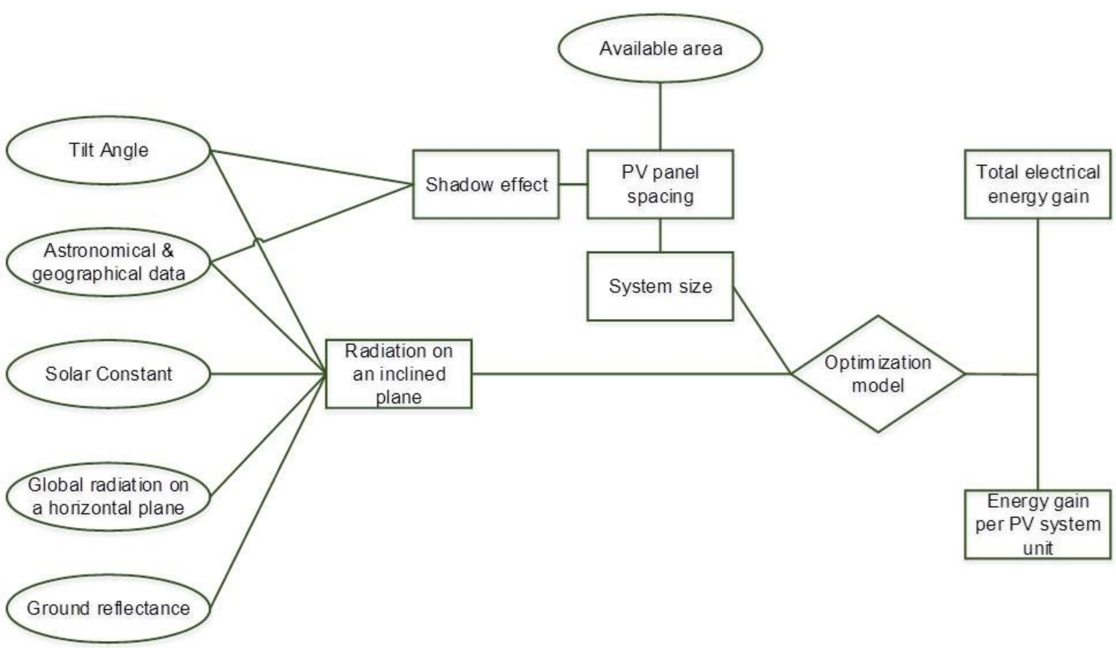

Figure 16: Multi-objective optimization model for energy gain on inclined solar PV system. The ellipses in the figure represent the input data while the rectangles are the steps in the calculation.

3.6.2 Objective functions

To increase the efficiency of the entire PV system, two objective functions are considered:

$$J_1 = \max\{E: E \in Net\ energy\ gain\} \tag{18}$$

$$J_2 = \max\{U: U \in Net\ energy\ gain\ per\ KW\} \tag{19}$$

Energy per kW can be low when the total energy output of the system is large. In a rooftop system, to increase the total energy gain the number of solar PV panel must be increased. The space between two consecutive rows is thus decreased, which increases the mutual shading loss. Then, the output of each panel will be less. Alternatively, if we consider the maximum output of each panel, then the panel will take more space. The total number of panels will be small and the total energy gain from the overall PV system will be low.

The design problem can be formulated as the following optimization problem:

$$\text{Optimize } J_1 \text{and } J_2 \tag{20}$$

Subject to

$$\text{Tilt}_{min} \leq \text{Tilt}_i \leq \text{Tilt}_{max} \tag{21}$$

$$x_{min} \leq x_i \leq x_{max} \tag{22}$$

General ranges of the optimized parameters are [0° to 90°] for Tilt_i and [1 m to 4 m] for x_i. Finally, Equation (18) and Equation (19) are optimized using PSO method.

3.7 Particle swarm optimization

Particle swarm optimization (PSO) is simple, computationally efficient, and easy to implement (Khare and Rangnekar 2013). PSO was introduced by Kennedy and Eberhart (Kennedy 2011; Kennedy 1997; Shi and Eberhart 1998). In PSO, a population of particles is used to run the searches. Particles move from one position to another in a multidimensional search space until a predefined condition is met or limitations are exceeded and each particle represents a candidate solution to the given problem. Particles share their information with one another to find the optimal solution. Every particle has a velocity by which it updates its position and position value.

3.7.1 Elements of PSO

Particle,X(t): Each particle's position value is a candidate for the solution, where *m* is the number of optimized parameters, and the j^{th} particle $X_j(t)$ can be shown at time *t*, $X_j(t) = [X_{j,1}(t), X_{j,2}(t), \ldots\ldots X_{j,m}(t)]$. Here, the *X*s are the optimized parameters, and $X_{j,k}(t)$ is the position of the j^{th} particle with respect to the k^{th} dimension (Abido 2002).

Population,pop(t): A set of particles at a given time is referred to as the population. $Pop(t) = [X_1(t), X_2(t), X_3(t), \ldots .Xn(t)]^T$, where *n* particles are in a set at time *t* (Abido 2002).

Swarm: A swarm is a group of disorganized particles moving randomly clustered together (Shi and Eberhart 1998).

Particle Velocity, V(t): Particle velocity is the velocity of moving particles; j^{th} particle velocity, $V_j(t)$, at time *t* is $V_j(t) = [v_{j,1}(t), v_{j,2}(t), \ldots\ldots\ldots\ldots, v_{j,m}(t)]$, where *m* is the number of parameters, and $v_{j,k}(t)$ is the velocity of j^{th} particle with respect to the k^{th} dimension. The velocity of the particle is limited by a maximum value and a minimum value. The limit of the velocity enhances local exploration of the problem. The equation for particle velocity is

$$v_{j,k}(t) = w(t)v_{j,k}(t-1) + c_1 r_1(x^*_{j,k}(t-1) - x_{j,k}(t-1)) + c_2 r_2(x_{j,k} ** (t-1) - x_{j,k}(t-1)) \quad (23)$$

where c_1 and c_2 are the cognitive and social parameters, respectively, and have positive constant values, and r_1 and r_2 are uniformly distributed random numbers.

Inertia weight, w(t): Controls the impact of previous velocities on the current velocity. It has an impact on the global and local exploration abilities of the particles (Shi and Eberhart 1998). Inertia weight should be reduced over time in order to move the search process global exploration to local exploration; $w(t) = a*w(t-1)$, where a is the decrement coefficient.

Individual best, $X^*(t)$: A particle in each position compares its fitness value to the best fitness value it has ever attained at any time. The best fitness value of that particle up to the present time is called the individual best, $X^*(t)$. Each particle determines and updates its individual best in the PSO. For the $j^{th}J^{th}$ particle, individual best can be expressed as $X_j^*(t) = [X_{j,1}^*(t), X_{j,2}^*(t), \ldots\ldots, X_{j,m}^*(t)]$, where $J_j^* = J[X_j^*(t)]$ (Abido 2002). Particles change their position and update their value according to the following equation:

$$x_{j,k}(t) = v_{j,k}(t) + x_{j,k}(t-1) \quad (24)$$

Global Best, $X^{**}(t)$: The best position among all the individual best positions is the global best. If $J^{**} = J[X^{**}(t)]$, then, for a maximization problem, $J[X^{**}(t)] \geq J[X_j^*(t), j = 1,2,\ldots.,n.$

Stopping Criterion: The condition which terminates the search process is the stopping criteria. In the optimization model of this research, the stopping criterion is the number of iterations.

3.7.2 Basic flowchart of the PSO

The working steps for the basic PSO algorithm are described in the flowchart presented in Figure 17.

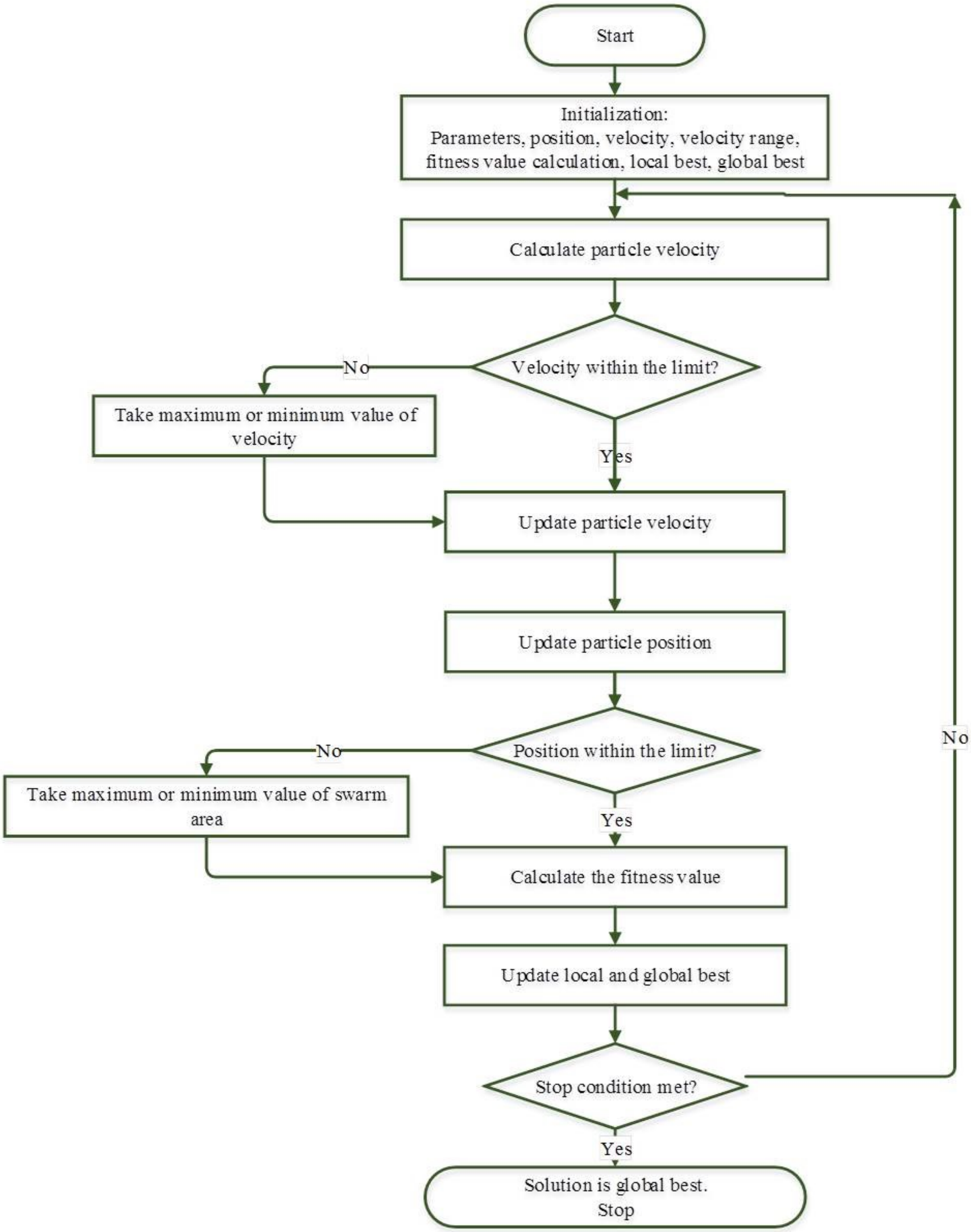

Figure 17: Flowchart of a general PSO technique

3.7.3 PSO implementation

The PSO-based optimization is implemented using the MATLAB platform. The optimization code is developed using MATLAB's m-file toolbox.

In the PSO search area, several combinations of particle numbers and iteration numbers are used to check the computing time and results, and then the number of particles is set to 50 and iteration number is set to 200. Other set parameters include inertia weight, $w = 1$; decrement constant, $a = 0.97$; and the cognitive and social parameters (respectively), $c_1 = c_2 = 2$. The optimization process terminates when the total number of iterations is complete. In this optimization, the two parameters, tilt angle and row distance, are two separate entities. For this reason, the velocities of these two inputs are different. The maximum and minimum velocity ranges can be expressed as per the following equations:

$$Velocity1_{max} = 0.0055*(swarm\ area\ of\ tilt) \tag{25}$$

$$Velocity1_{min} = -Velocity1_{max} \tag{26}$$

$$Velocity2_{max} = 0.011*(swarm\ area\ of\ row\ distance) \tag{27}$$

$$Velocity2_{min} = -Velocity2_{max} \tag{28}$$

The values of $Velocity1_{max}$ and $Velocity2_{max}$ are determined by the step size of the optimization area. In this optimization, the step size of the tilt angle is 0.5° and the step size of the row distance is 0.5 ft (0.152 m).

This proposed optimization model has been run for different solar PV system and the results have been analyzed. Findings of the results give the idea about this model's efficiency and accuracy.

CHAPTER FOUR: OPTIMIZATION RESULT AND FINDINGS

Solar PV design optimization which is developed in this thesis has been used on hypothetical solar PV system and existing real solar PV system. All the results from both type of system have been analyzed to check the consistency, efficiency, computing time. Finding of the results from this thesis has been discussed to understand this optimization's use.

4.1 Hypothetical setup

Test Case: To test the proposed optimization model, several grid-tied flat roof solar PV system test cases are created. The modelled PV system includes a Conergy PH 255P PV panel rated to 255 W at peak and an SMA Sunny Boy 5.0-US inverter rated to 5 kW. The tilt angle and space between two consecutive rows are optimized for different geographic locations (Edmonton, Vancouver, Winnipeg, Toronto, Ottawa, Montréal, and Saskatoon). Energy output, energy per unit system, total number of panels, and total system capacity are also checked in all locations and for different time periods (monthly and yearly).

In this proposed optimization method, PV panels are given a landscape orientation, given that this orientation is associated with less shading loss effect than is the portrait orientation. Typically, in crystalline PV panels two or three rows of PV cells are connected through one diode to the output. Based on this output diode configuration, landscape orientation can still generate energy if the bottom portion of the PV panel is under shading.

Input parameters to the proposed model include available area for the PV system, solar PV brand, solar inverter brand, location, and period (monthly, yearly). The proposed PSO model uses two optimization parameters (tilt, row distance) and five output parameters (energy output, energy per unit system, total number of panels, total system capacity, and time period).

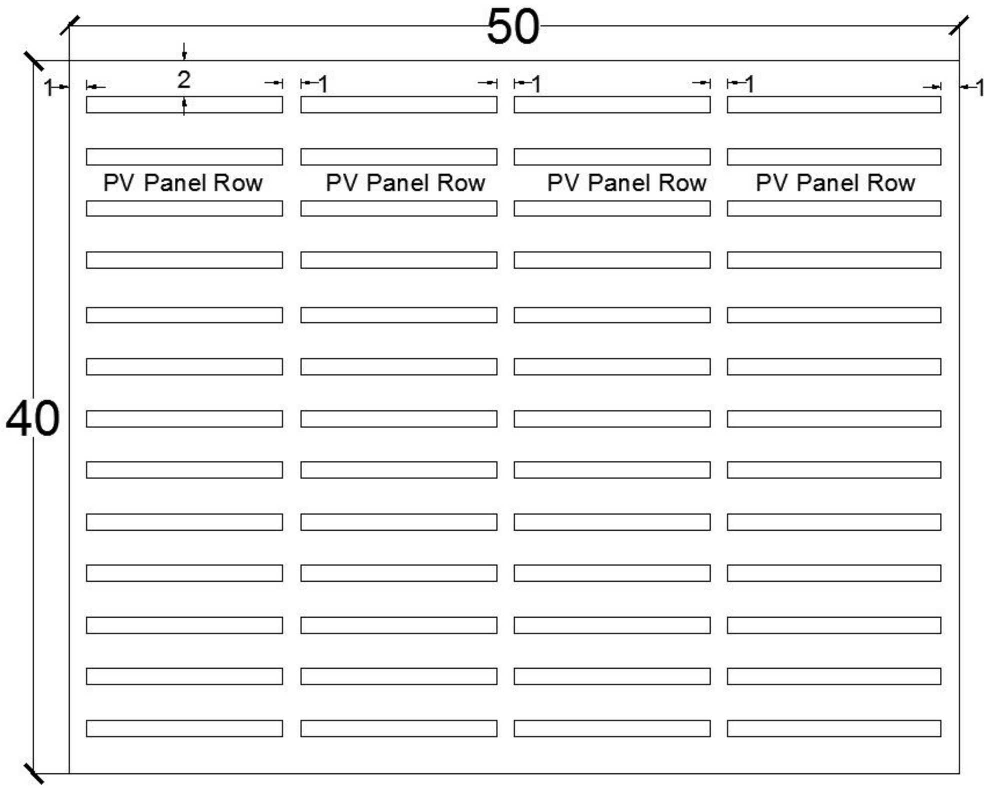

Figure 18: Rooftop PV system layout of Hypothetical setup (meters)

Model consistency

In this test case (Figure 18), an available flat roof area of 50 m length × 40 m width is considered. For maintenance and safety purposes, 1 m of free space is included on each side of the solar PV system, as well as a 1-m walkway in the center of the solar PV system array. Three passages, each 1 m in width, are considered in the project area for accessory and equipment space. The developed optimization model is used to design the parameters in Edmonton for monthly mean daily energy and yearly mean daily separately. The tilt angle range is 0° to 90°

while the row distance range is 1 m to 5 m. This model is run 100 times for the monthly mean daily energy and yearly mean daily value to check the model's consistency.

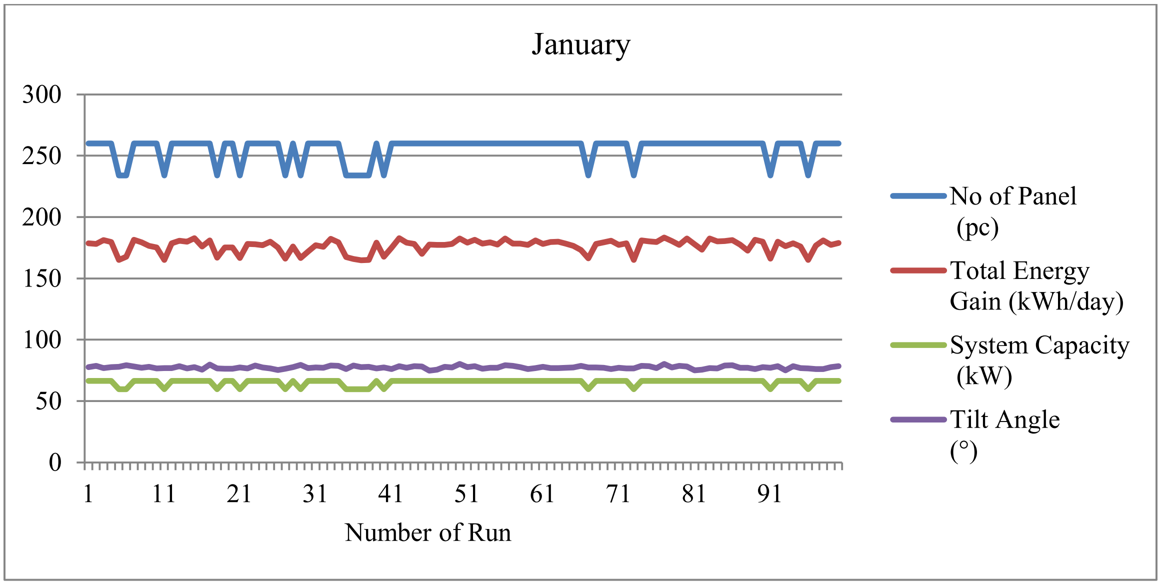

(a)

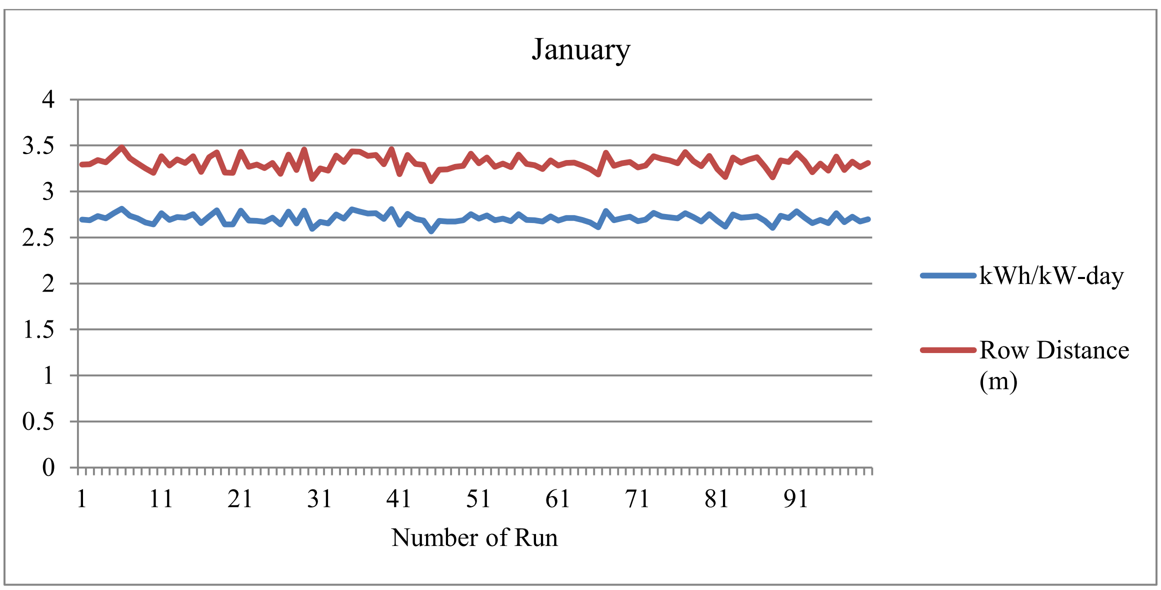

(b)

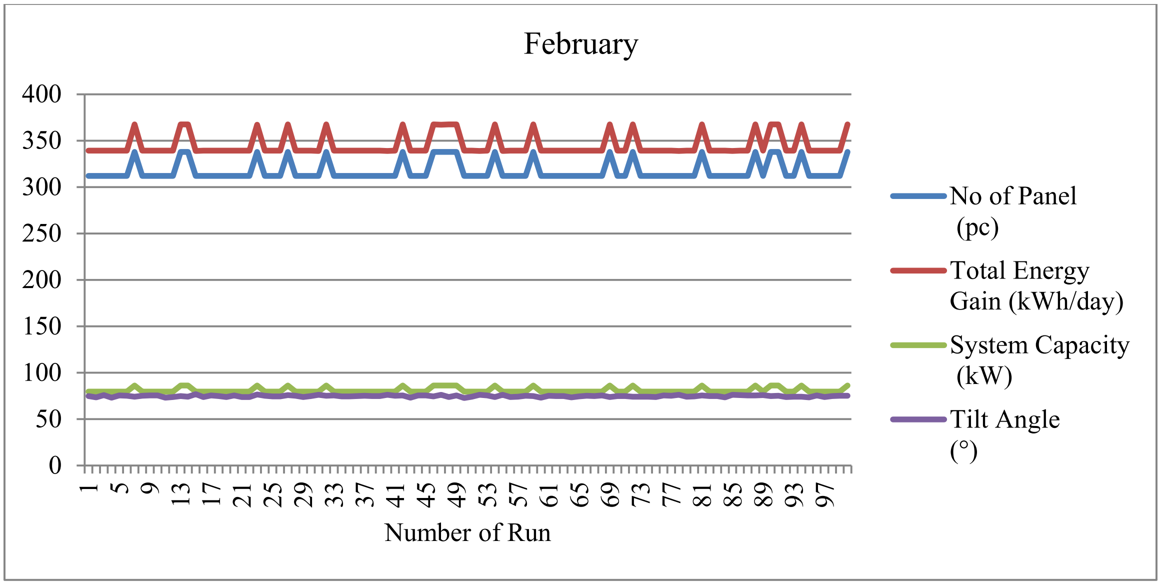
February
400
350
300
250
200
150
100
50
0
1 5 9 13 17 21 25 29 33 37 41 45 49 53 57 61 65 69 73 77 81 85 89 93 97
Number of Run
No of Panel (pc)
Total Energy Gain (kWh/day)
System Capacity (kW)
Tilt Angle (°)

(c)

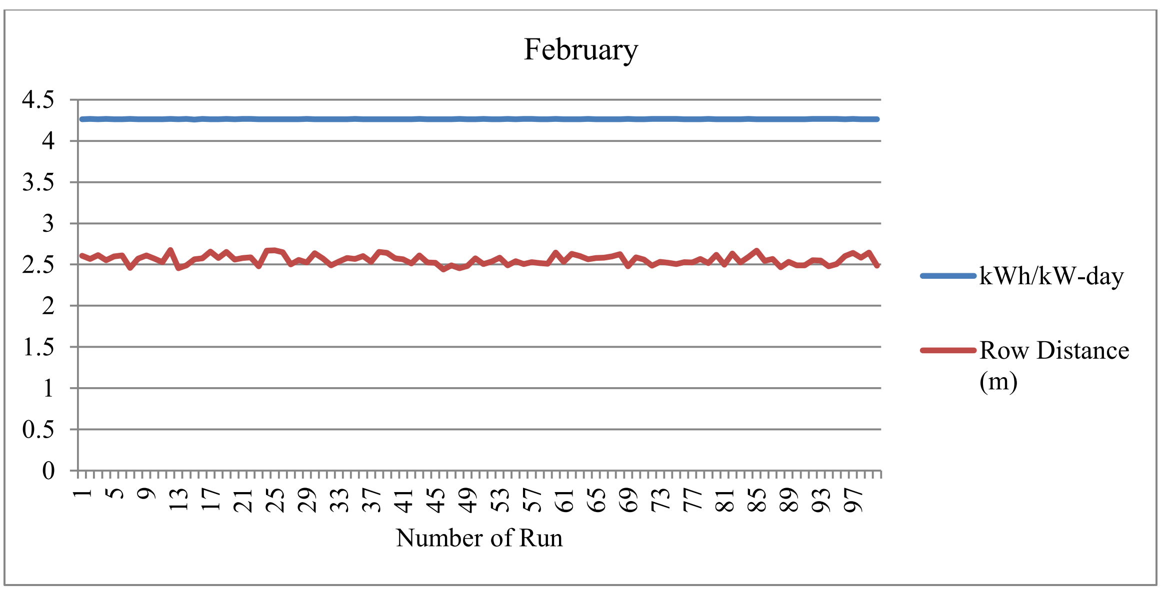
February
4.5
4
3.5
3
2.5
2
1.5
1
0.5
0
1 5 9 13 17 21 25 29 33 37 41 45 49 53 57 61 65 69 73 77 81 85 89 93 97
Number of Run
kWh/kW-day
Row Distance (m)

(d)

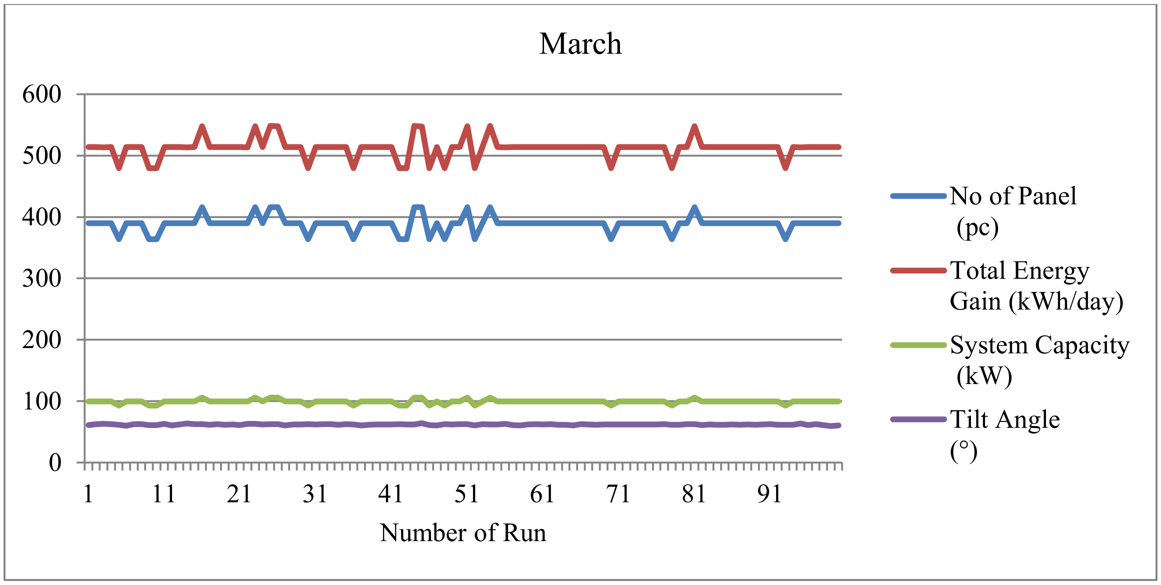
March
600
500
400
300
200
100
0
1
11
21
31
41
51
61
71
81
91
Number of Run
No of Panel (pc)
Total Energy Gain (kWh/day)
System Capacity (kW)
Tilt Angle (°)

(e)

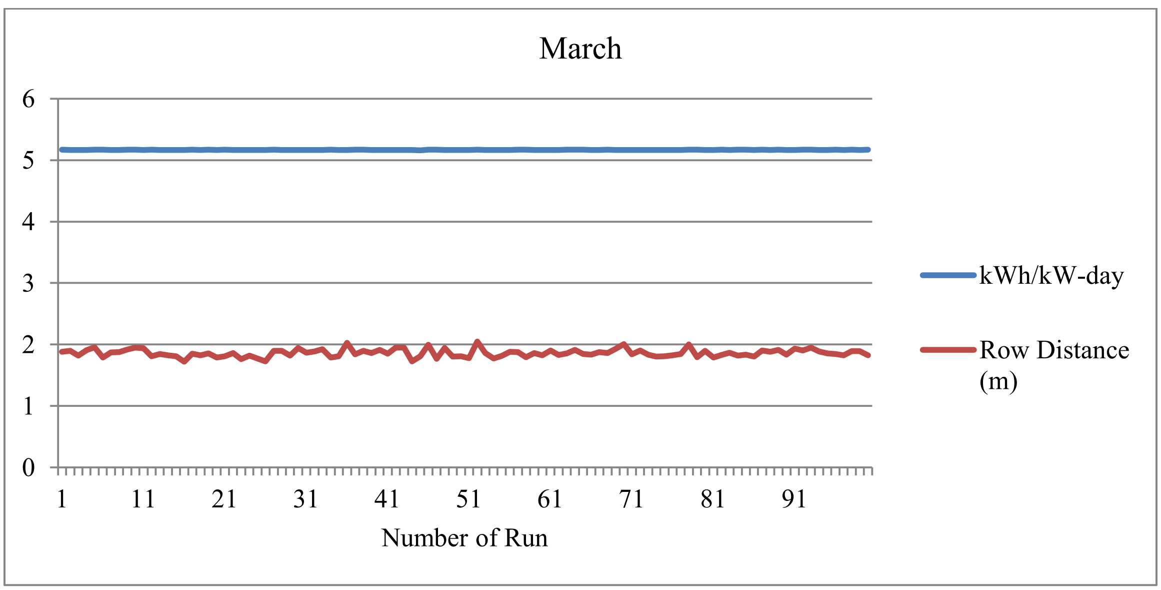
March
6
5
4
3
2
1
0
1
11
21
31
41
51
61
71
81
91
Number of Run
kWh/kW-day
Row Distance (m)

(f)

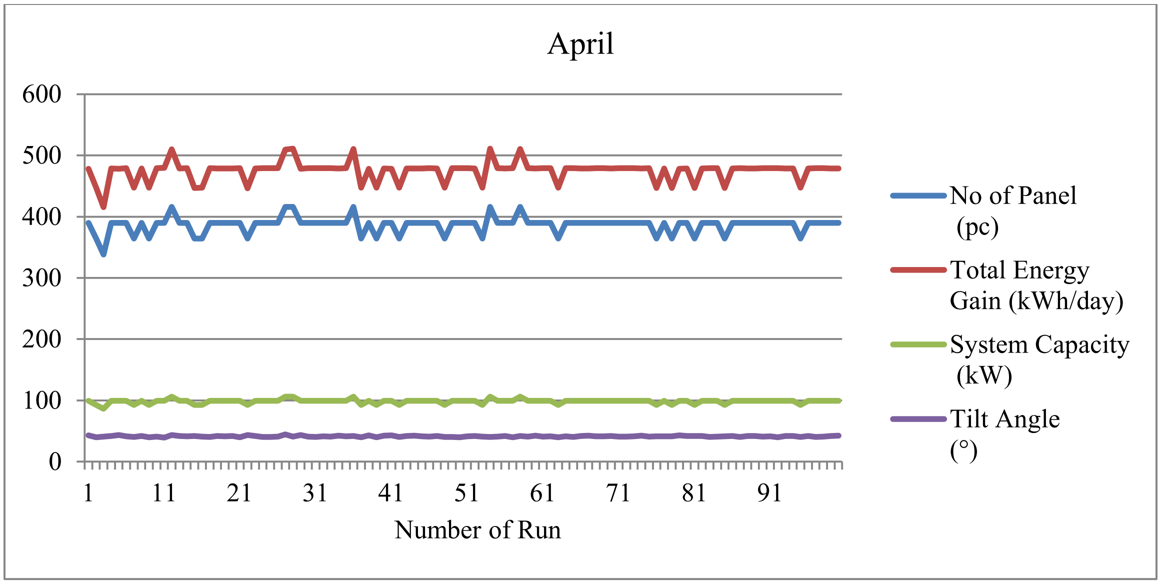
April
600
500
400
300
200
100
0
1
11
21
31
41
51
61
71
81
91
Number of Run
No of Panel (pc)
Total Energy Gain (kWh/day)
System Capacity (kW)
Tilt Angle (°)

(g)

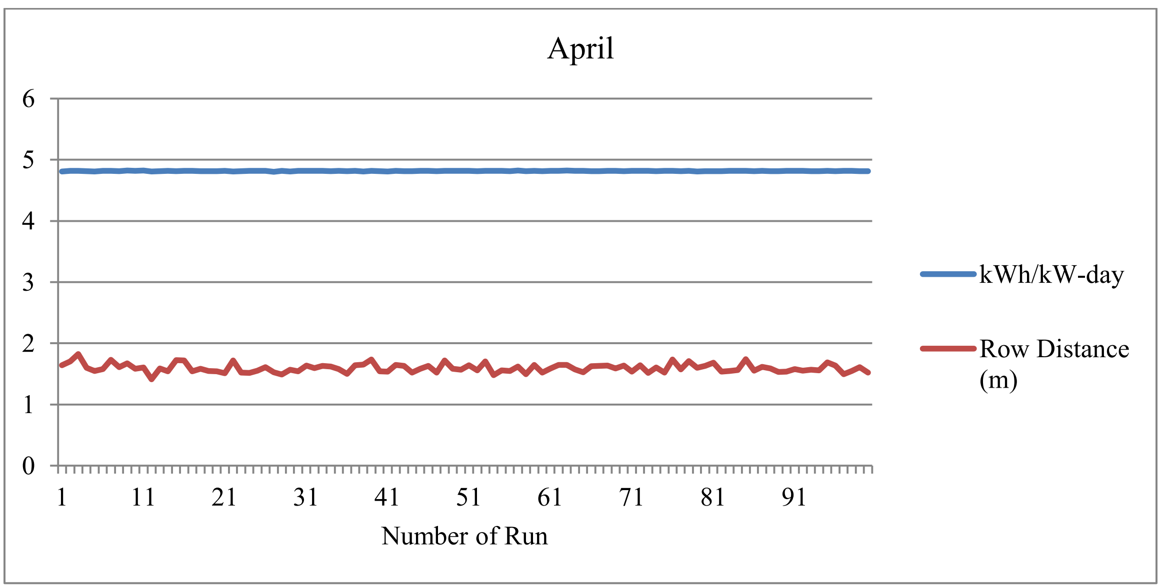
April
6
5
4
3
2
1
0
1
11
21
31
41
51
61
71
81
91
Number of Run
kWh/kW-day
Row Distance (m)

(h)

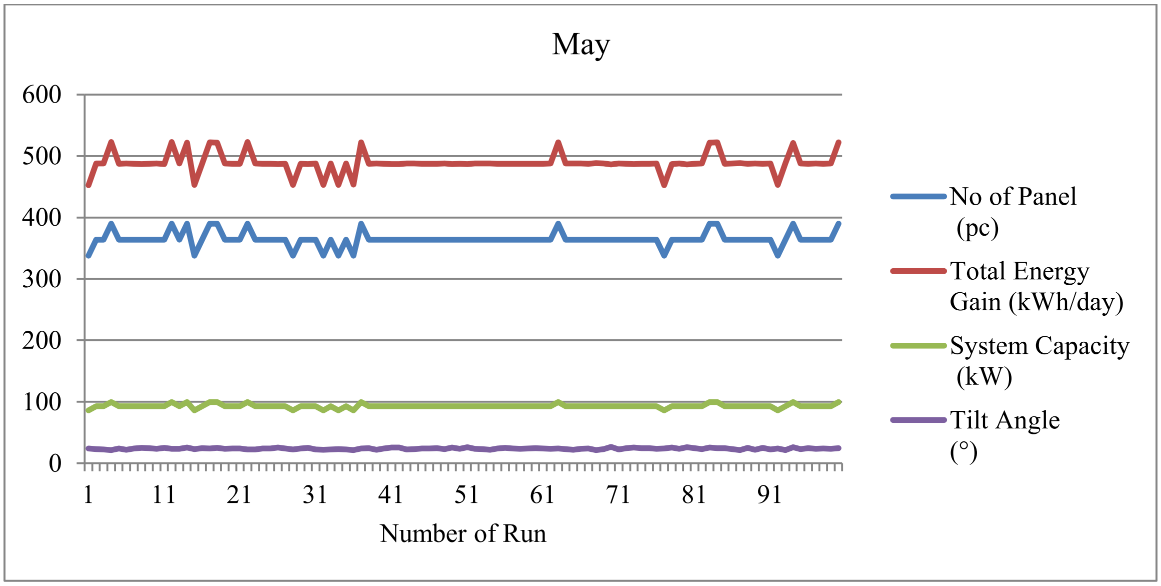
May
600
500
400
300
200
100
0
1
11
21
31
41
51
61
71
81
91
Number of Run
No of Panel (pc)
Total Energy Gain (kWh/day)
System Capacity (kW)
Tilt Angle (°)

(i)

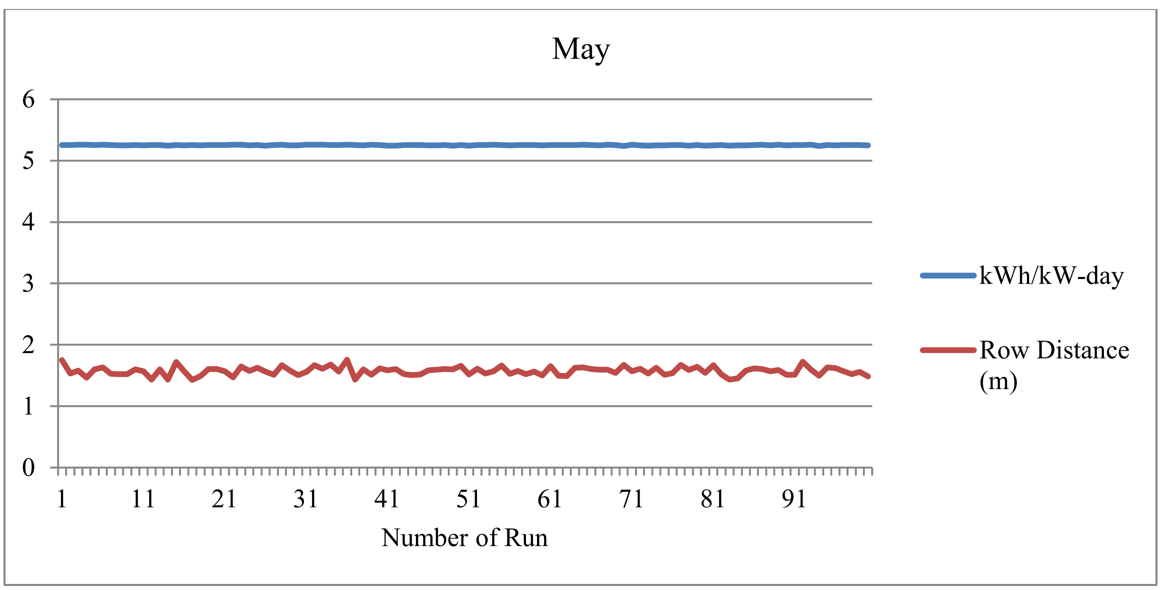
May
6
5
4
3
2
1
0
1
11
21
31
41
51
61
71
81
91
Number of Run
kWh/kW-day
Row Distance (m)

(j)

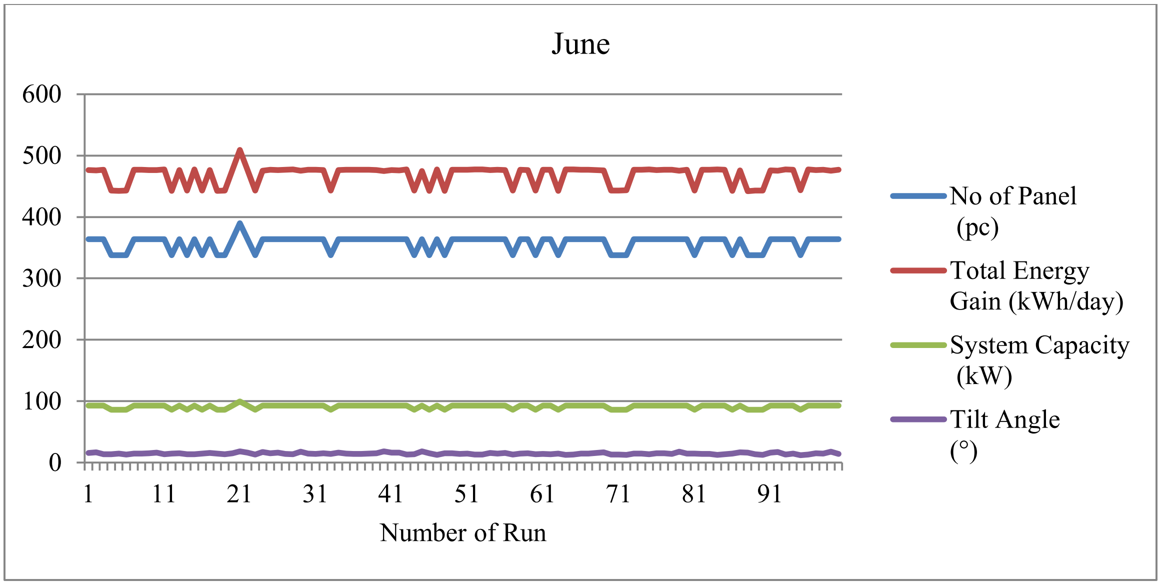
June
600
500
400
300
200
100
0
1
11
21
31
41
51
61
71
81
91
Number of Run
No of Panel (pc)
Total Energy Gain (kWh/day)
System Capacity (kW)
Tilt Angle (°)

(k)

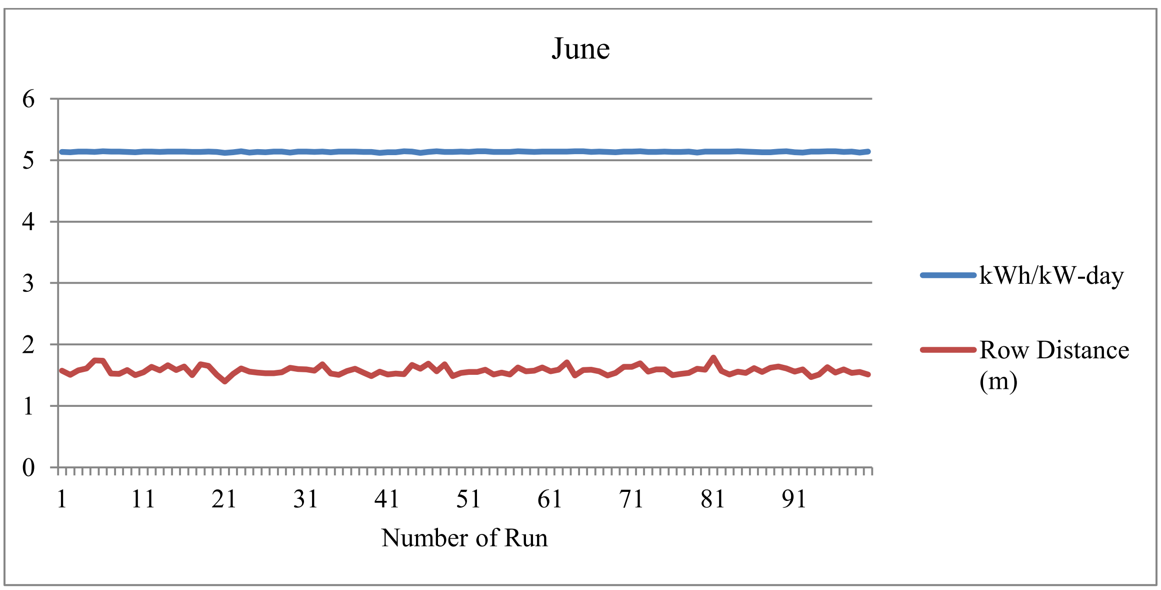
June
6
5
4
3
2
1
0
1
11
21
31
41
51
61
71
81
91
Number of Run
kWh/kW-day
Row Distance (m)

(l)

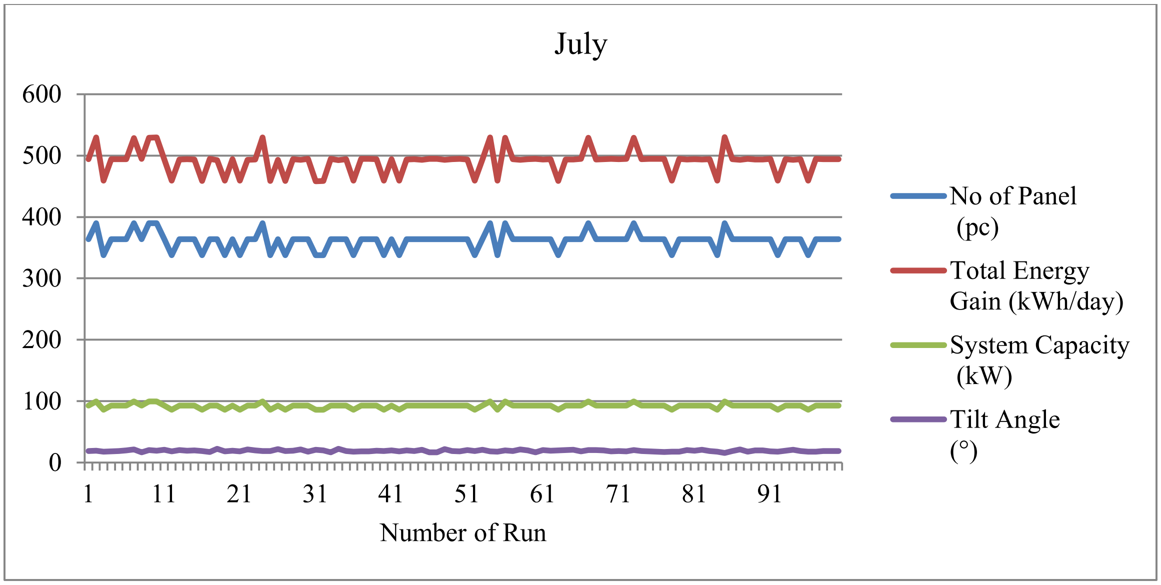
July
600
500
400
300
200
100
0
1
11
21
31
41
51
61
71
81
91
Number of Run
No of Panel (pc)
Total Energy Gain (kWh/day)
System Capacity (kW)
Tilt Angle (°)

(m)

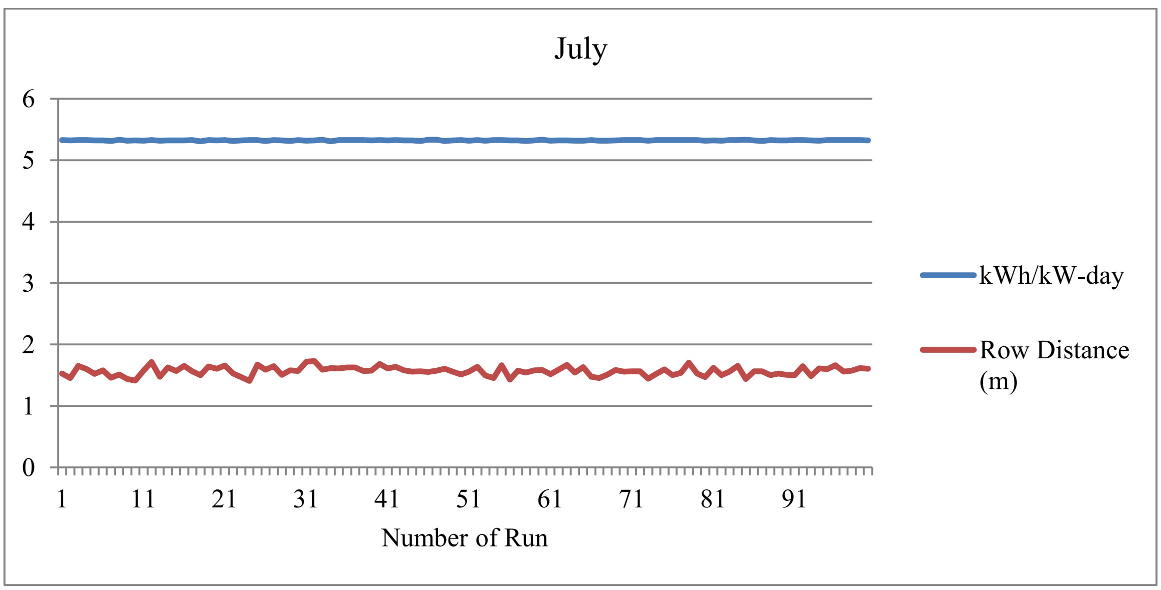
July
6
5
4
3
2
1
0
1
11
21
31
41
51
61
71
81
91
Number of Run
kWh/kW-day
Row Distance (m)

(n)

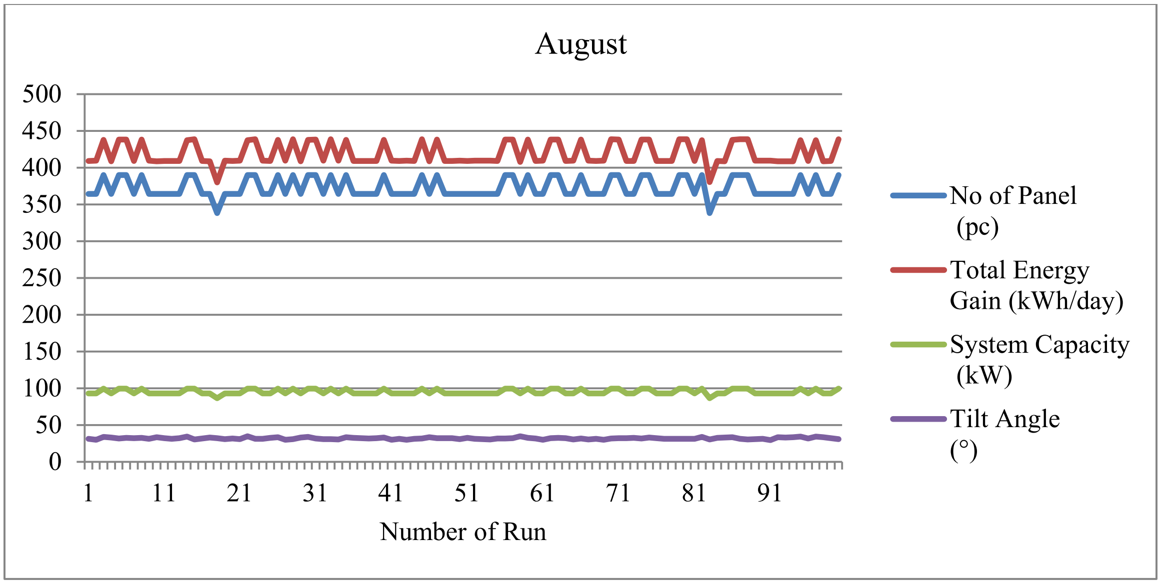
August
500
450
400
350
300
250
200
150
100
50
0
1
11
21
31
41
51
61
71
81
91
Number of Run
No of Panel (pc)
Total Energy Gain (kWh/day)
System Capacity (kW)
Tilt Angle (°)

(o)

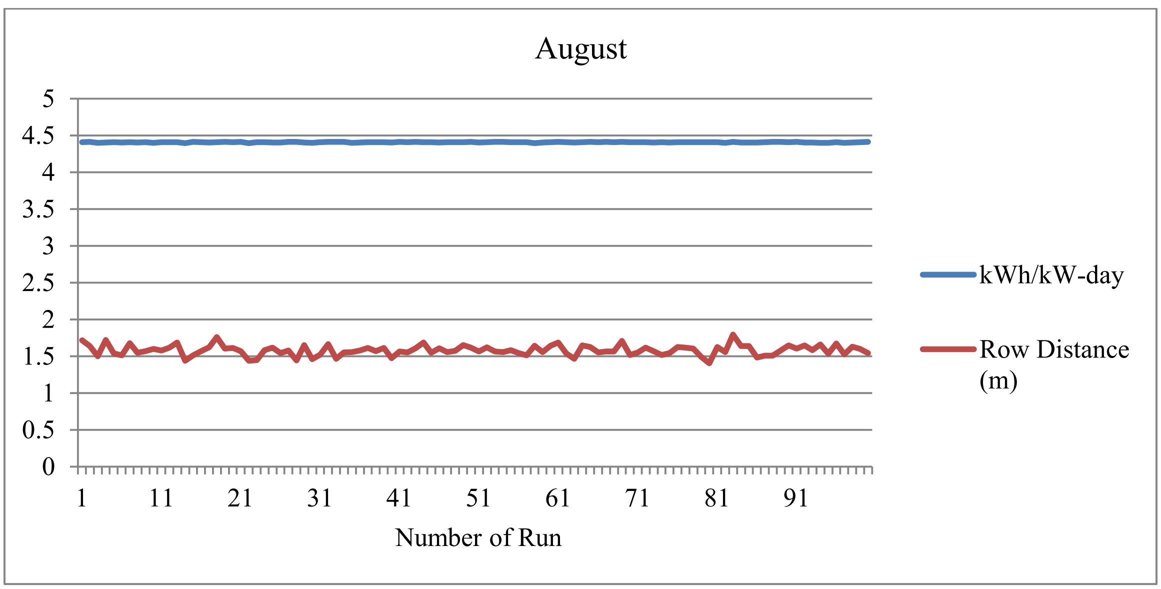
August
5
4.5
4
3.5
3
2.5
2
1.5
1
0.5
0
1
11
21
31
41
51
61
71
81
91
Number of Run
kWh/kW-day
Row Distance (m)

(p)

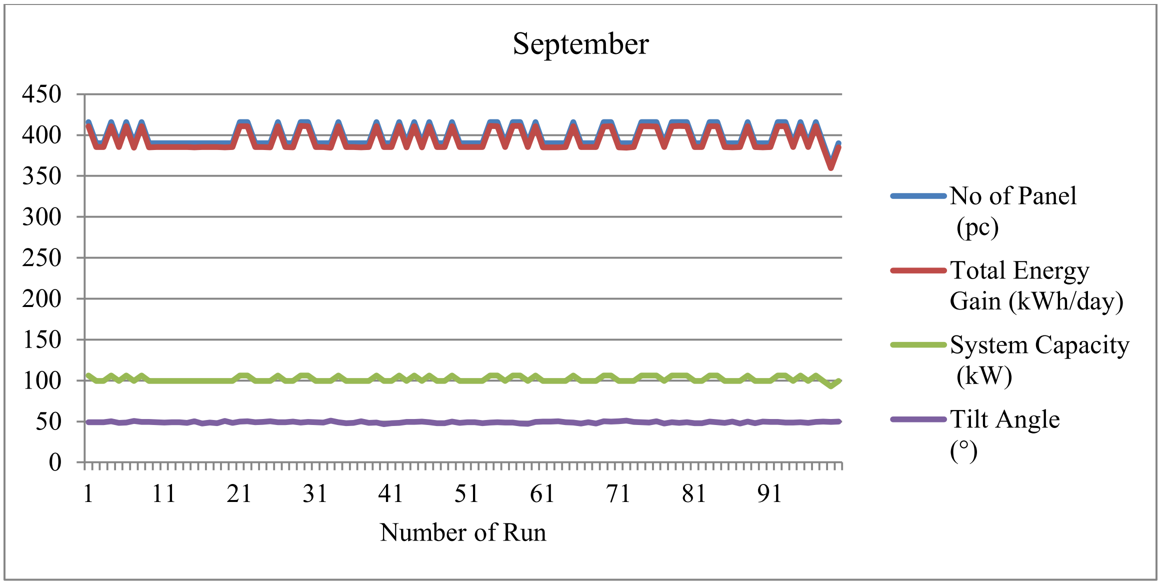
September
450
400
350
300
250
200
150
100
50
0
1
11
21
31
41
51
61
71
81
91
Number of Run
No of Panel (pc)
Total Energy Gain (kWh/day)
System Capacity (kW)
Tilt Angle (°)

(q)

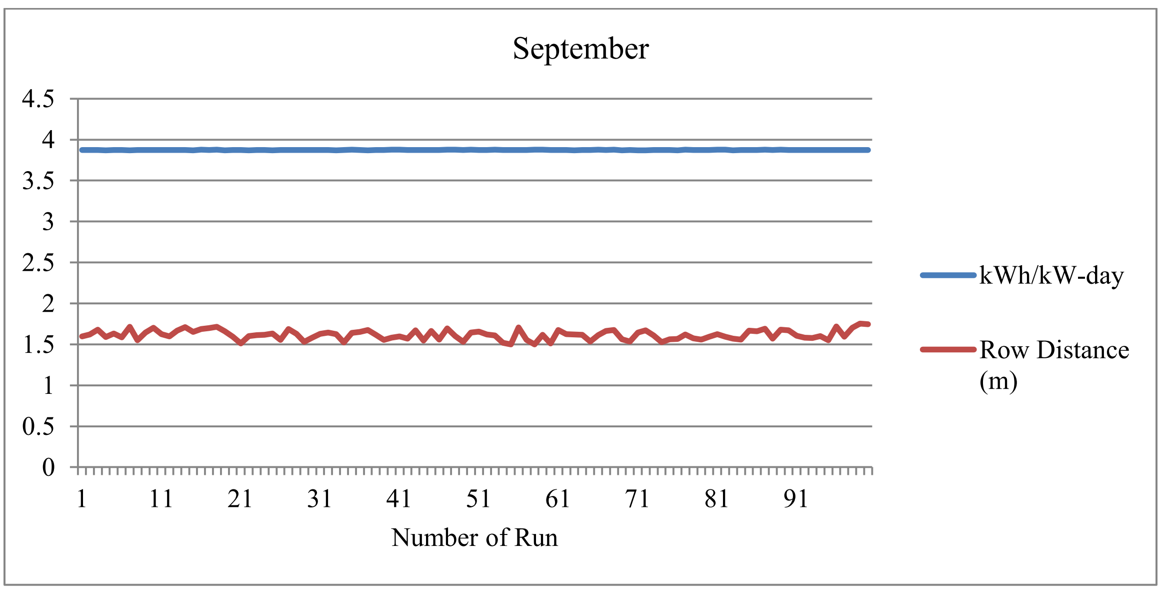
September
4.5
4
3.5
3
2.5
2
1.5
1
0.5
0
1
11
21
31
41
51
61
71
81
91
Number of Run
kWh/kW-day
Row Distance (m)

(r)

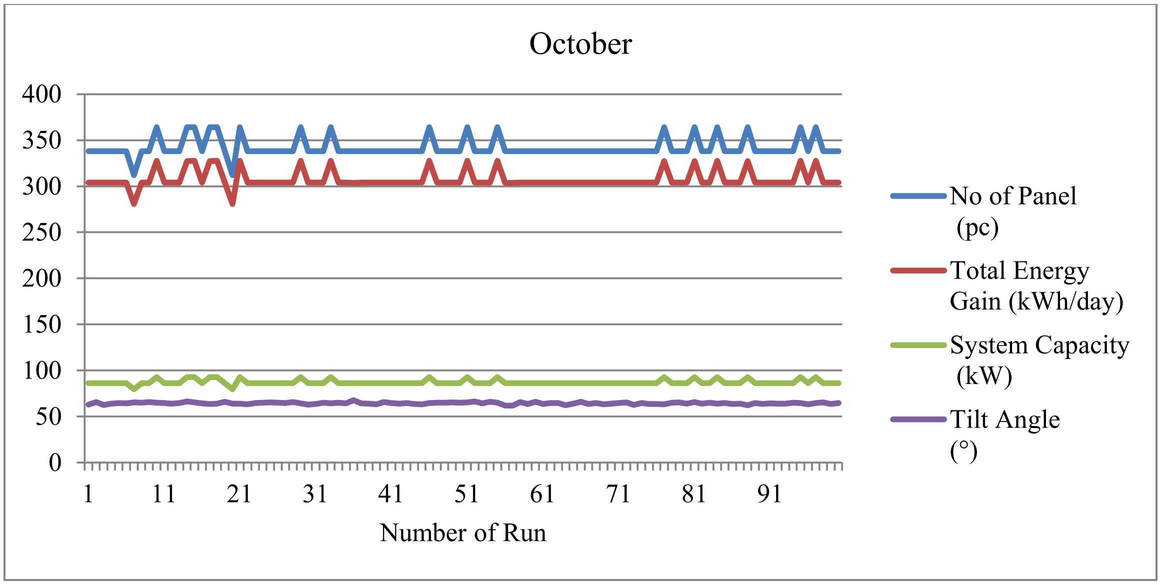
October
400
350
300
250
200
150
100
50
0
1
11
21
31
41
51
61
71
81
91
Number of Run
No of Panel (pc)
Total Energy Gain (kWh/day)
System Capacity (kW)
Tilt Angle (°)

(s)

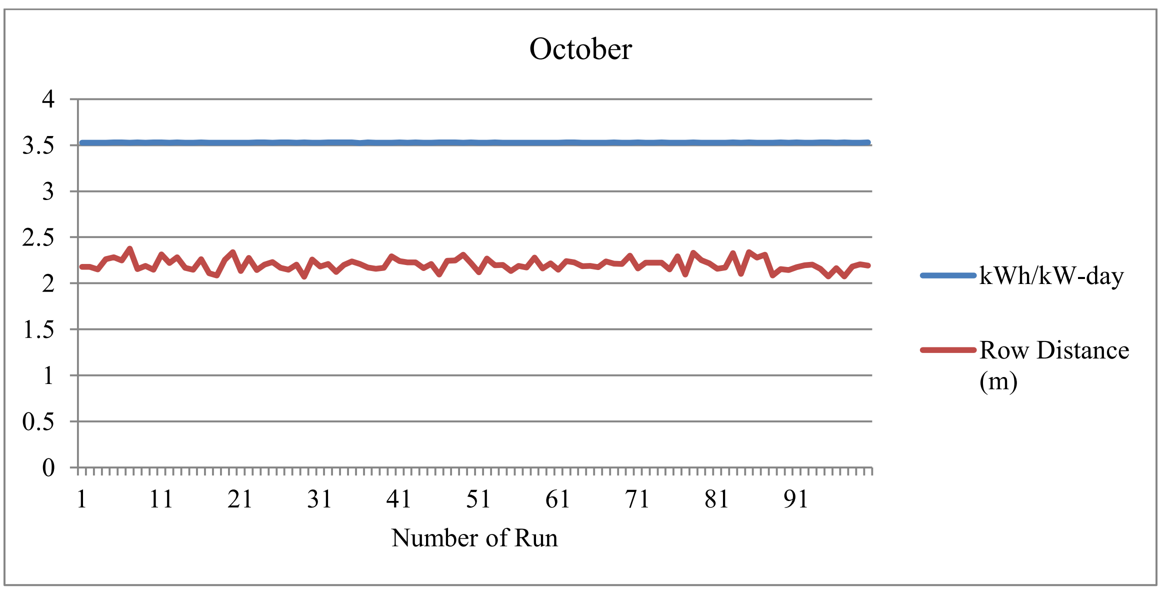
October
4
3.5
3
2.5
2
1.5
1
0.5
0
1
11
21
31
41
51
61
71
81
91
Number of Run
kWh/kW-day
Row Distance (m)

(t)

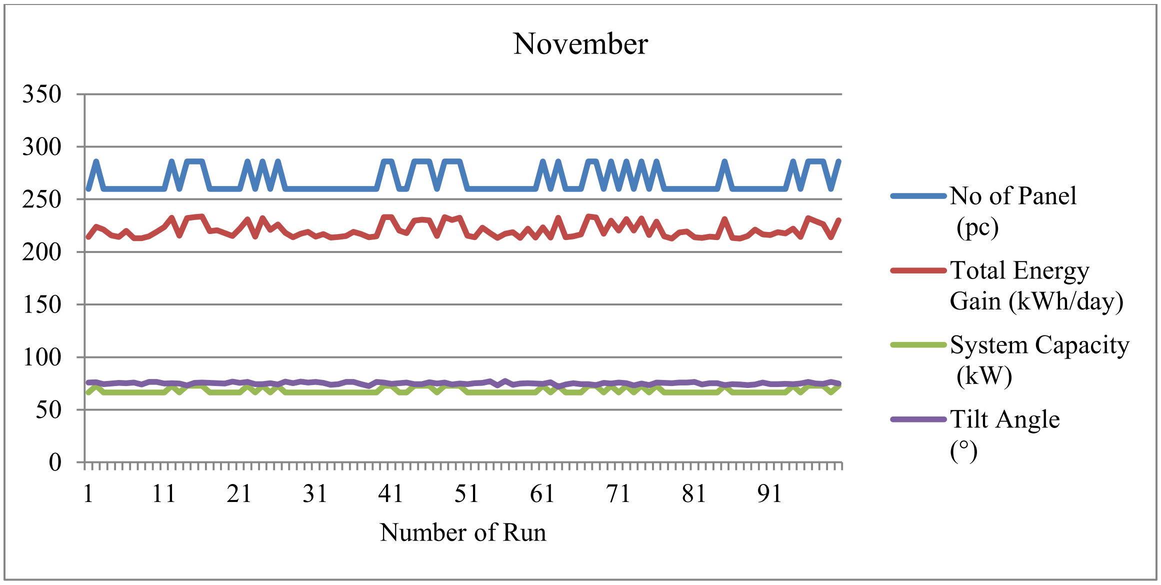
November
350
300
250
200
150
100
50
0
1
11
21
31
41
51
61
71
81
91
Number of Run
No of Panel (pc)
Total Energy Gain (kWh/day)
System Capacity (kW)
Tilt Angle (°)

(u)

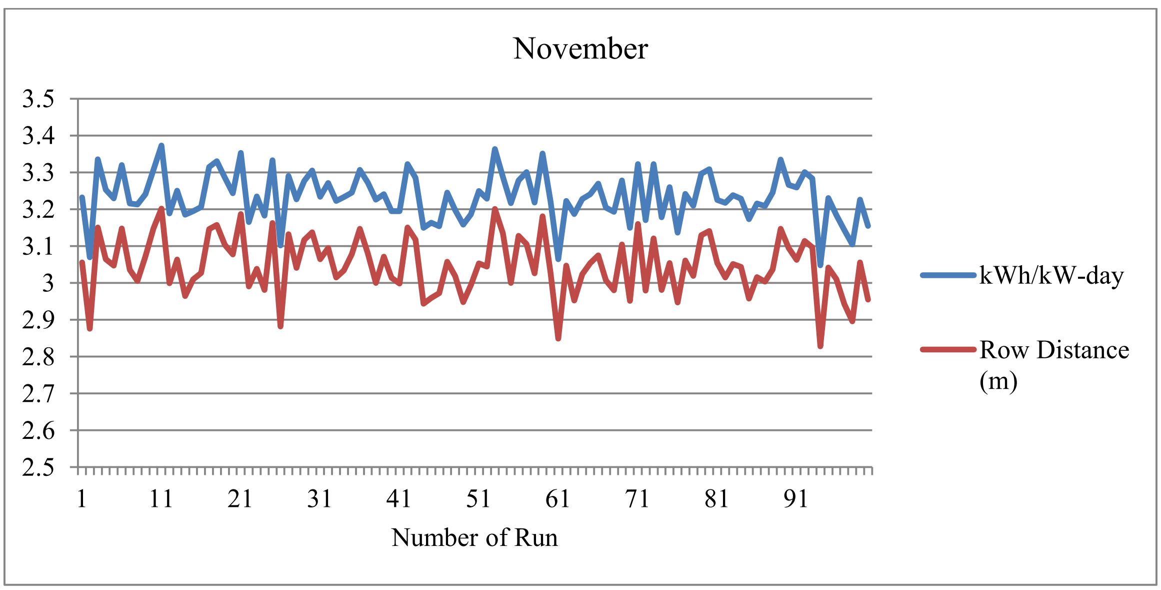
November
3.5
3.4
3.3
3.2
3.1
3
2.9
2.8
2.7
2.6
2.5
1
11
21
31
41
51
61
71
81
91
Number of Run
kWh/kW-day
Row Distance (m)

(v)

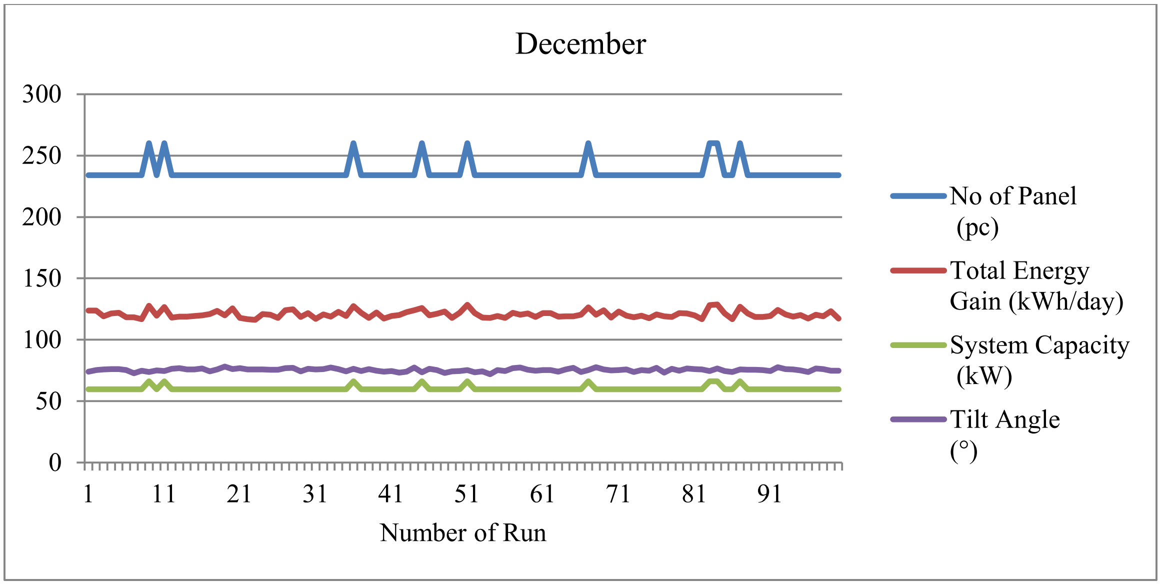

(w)

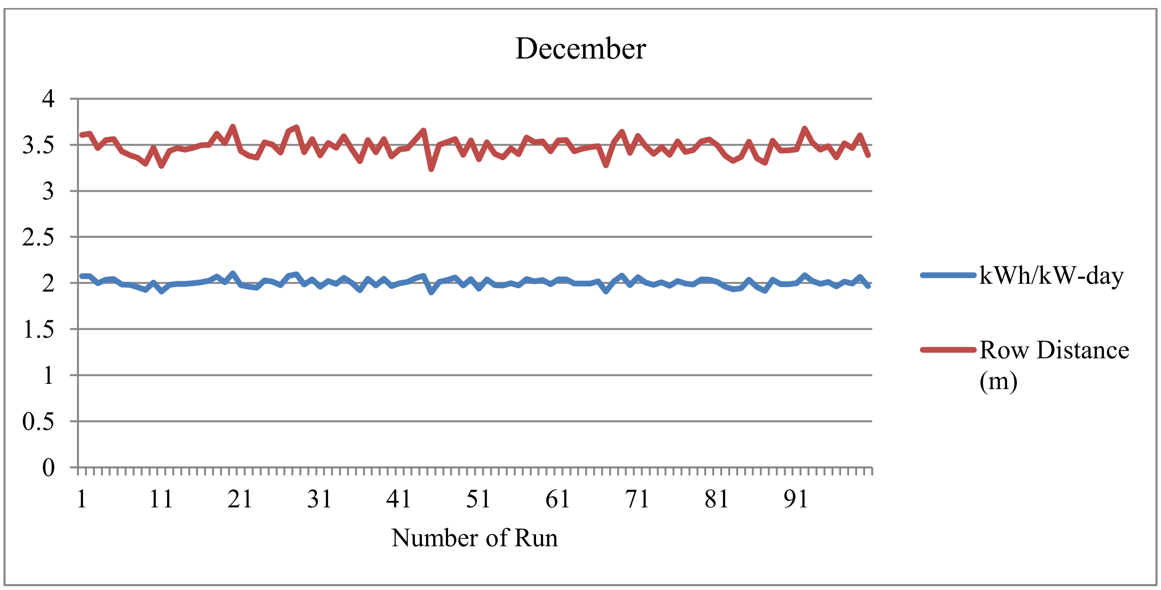

(x)

Figure 19 [(a) to (x)]: Results of 100 runs over twelve months

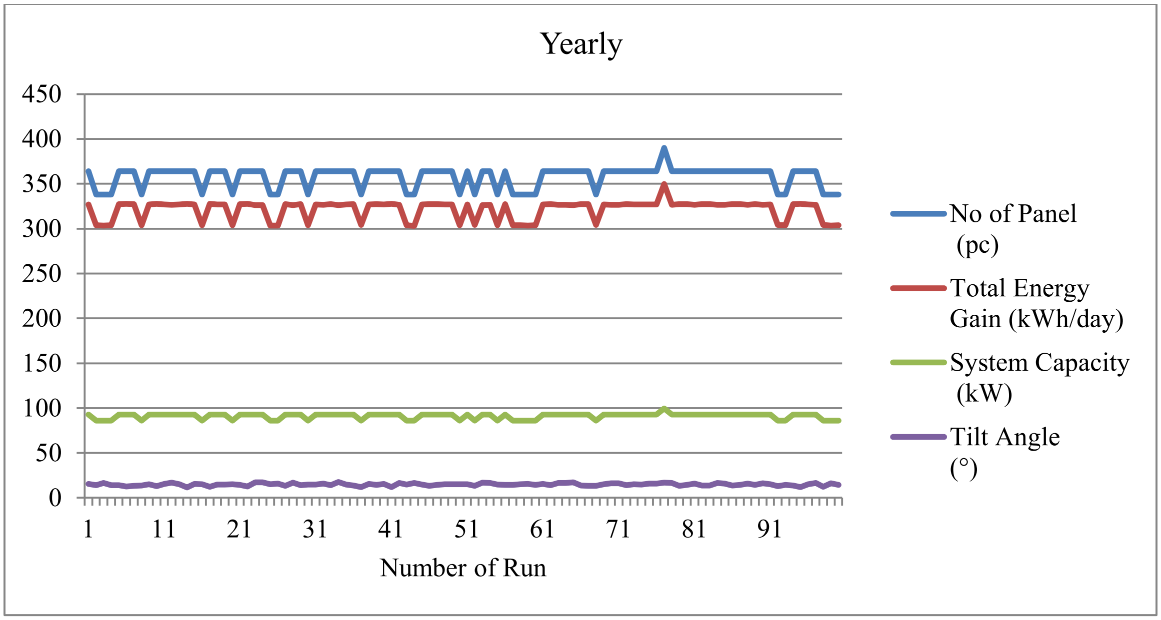

(a)

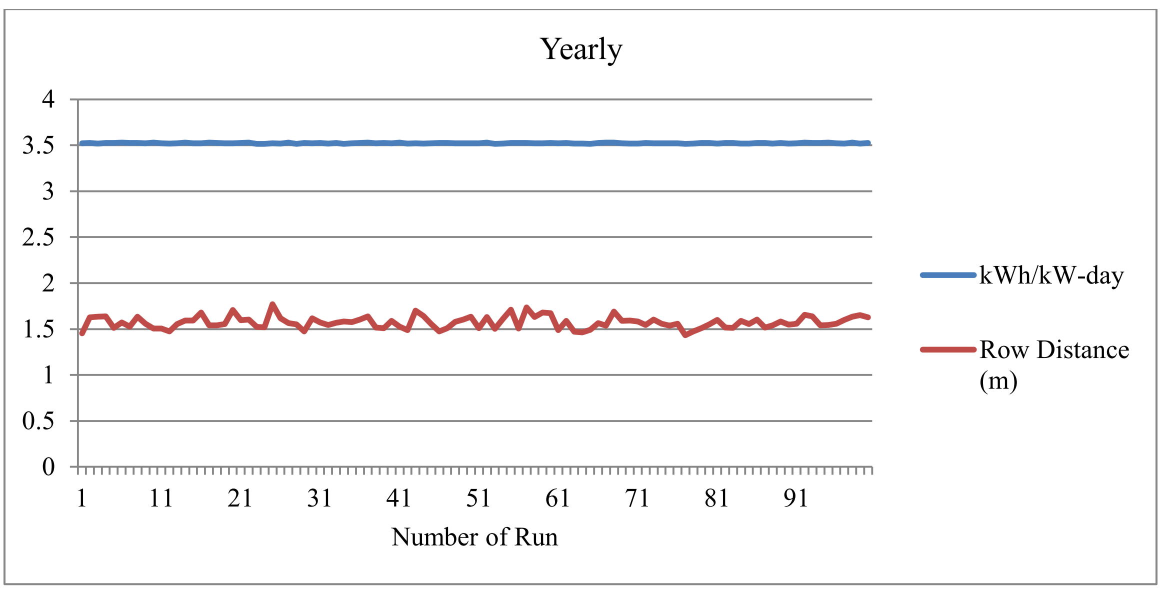

(b)

Figure 20 (a) and (b): Results of 100 runs for yearly optimization

Table 6: Monthly mean daily energy generation and yearly mean daily generation in Edmonton for test case

Month	No. of Panels (pc)	Total Energy Gain (kWh/day)	kWh/kW/day	System Capacity (kW)	Tilt Angle (°)	Row Distance (m)
1	260	175.22	2.76	66.3	77.35	3.30
2	312	339.20	4.26	79.56	75.07	2.57
3	390	513.71	5.17	99.45	62.65	1.85
4	390	479.23	4.82	99.45	40.48	1.60
5	364	487.50	5.25	92.82	23.83	1.49
6	364	476.61	5.13	92.82	15.12	1.51
7	364	495.13	5.32	92.82	20.38	1.55
8	364	409.28	4.41	92.82	30.67	1.56
9	390	385.29	3.87	99.45	48.60	1.60
10	338	304.08	3.53	86.19	63.81	2.18
11	260	220.61	3.39	66.3	75.26	3.00
12	234	124.55	2.00	59.67	75.64	3.40
Yearly Mean Daily	364	326.90	3.53	92.82	15.34	1.55

This optimization model provides the optimum number of panels, total energy, energy per unit solar PV, total system capacity, and tilt angle and row distance for the optimal solar PV system in a given geographic location. As can be observed in the figures (19 and 20), this model considers both energy gain and energy per unit solar PV as its maximization objectives. The monthly and yearly results [Figure 19(a) to (x) and Figure 20(a) to (b), respectively] of the optimization model are indicative of the consistency of the results. Among the 100 runs, the results for tilt angle and row gap vary less than 5%.

Shading loss effect on the model

To analyze the shading loss effect using the optimization model, each monthly mean daily energy gain and corresponding shading effect must be calculated. The test case is used to illustrate the calculation and analysis.

Table 7: Monthly mean daily energy generation with energy loss due to mutual shading in Edmonton

Month	No. of Panels (pc)	Total Energy Gain (kWh/day)	kWh/kW/day	System Capacity (kW)	Tilt Angle (°)	Row Distance (m)	Shading Loss-Monthly Mean Daily Energy (kWh/day)
1	260	175.22	2.76	66.30	77.35	3.39	15.3755
2	312	339.20	4.26	79.56	75.07	2.57	0
3	390	513.71	5.17	99.45	62.65	1.85	0
4	390	479.23	4.82	99.45	40.48	1.60	0
5	364	487.50	5.25	92.82	23.83	1.49	0
6	364	476.61	5.13	92.82	15.12	1.51	0
7	364	495.13	5.33	92.82	18.42	1.57	0
8	364	409.28	4.41	92.82	30.67	1.56	0
9	390	385.29	3.87	99.45	48.60	1.70	0
10	338	304.08	3.53	86.19	63.81	2.18	0
11	260	220.61	3.39	66.3	75.26	3.22	2.7227
12	260	124.55	1.88	66.3	77.64	3.25	37.5373

Table 7 reveals that this optimization model considers energy loss for the mutual shading to optimize the total power and power per unit. In the months of January, November, and December energy losses due to the shading effect in optimum conditions are, respectively, 15.3755 kWh/day, 2.7227 kWh/day, and 37.5373 kWh/day.

Location effect on the model

The test case is used to analyze the optimization model for various geographic locations in Canada.

Table 8: Yearly mean daily energy generation optimization data for different geographic locations in Canada with optimization time

Location	No. of Panels (pc)	Yearly Mean Total Energy Gain (kWh/day)	kWh/kW/day	System Capacity (kW)	Tilt Angle (°)	Row Distance (m)	Optimization Run time (seconds)
Edmonton	364	326.90	3.53	92.82	15.34	1.55	26.049
Vancouver	338	273.44	3.17	86.19	12.31	1.63	29.62
Toronto	364	308.20	3.32	92.82	12.50	1.45	25.43
Ottawa	364	308.32	3.33	92.82	13.30	1.55	25.17
Montréal	364	308.44	3.32	92.82	12.90	1.55	26.22
Saskatoon	364	334.50	3.60	92.82	13.47	1.53	25.84
Winnipeg	338	301.55	3.50	86.19	12.00	1.61	26.67

Table 8 shows different values of energy gain and energy per kW gain for the overall yearly average for various geographic locations in Canada with the same roof dimensions. Given that the position of the sun varies according to the geographic location, the tilt angle and shading loss also vary from one location to another. This model calculates the best tilt angle and row gap based on the location of the PV system.

Yearly output comparison with RETScreen results

RETScreen software was developed by the Government of Canada and is considered one of the best software tools for evaluating the economy of renewable energy projects. For the hypothetical setup, all the parameters suggested by optimization model for the various geographic locations under study are fed into the RETScreen, and then the output (yearly total output power in MWh) of RETScreen is compared with the output of the optimization model.

Table 9: Yearly total comparison with RETScreen output

Location	No. of Panels (pc)	System Capacity (kW)	Tilt Angle (°)	Proposed Optimization Results (MWh/Year)	RETScreen Results (MWh/Year)	Accuracy (%)
Edmonton	364	92.82	15.34	119.32	120.43	99.07
Vancouver	338	86.19	12.31	99.81	95.46	95.65
Toronto	364	92.82	12.5	112.49	111.91	99.48
Ottawa	364	92.82	13.3	112.54	114.66	98.11
Montréal	364	92.82	12.9	112.58	112.13	99.60
Saskatoon	364	92.82	13.47	122.09	132.37	91.58
Winnipeg	338	86.19	12	110.07	112.33	97.94

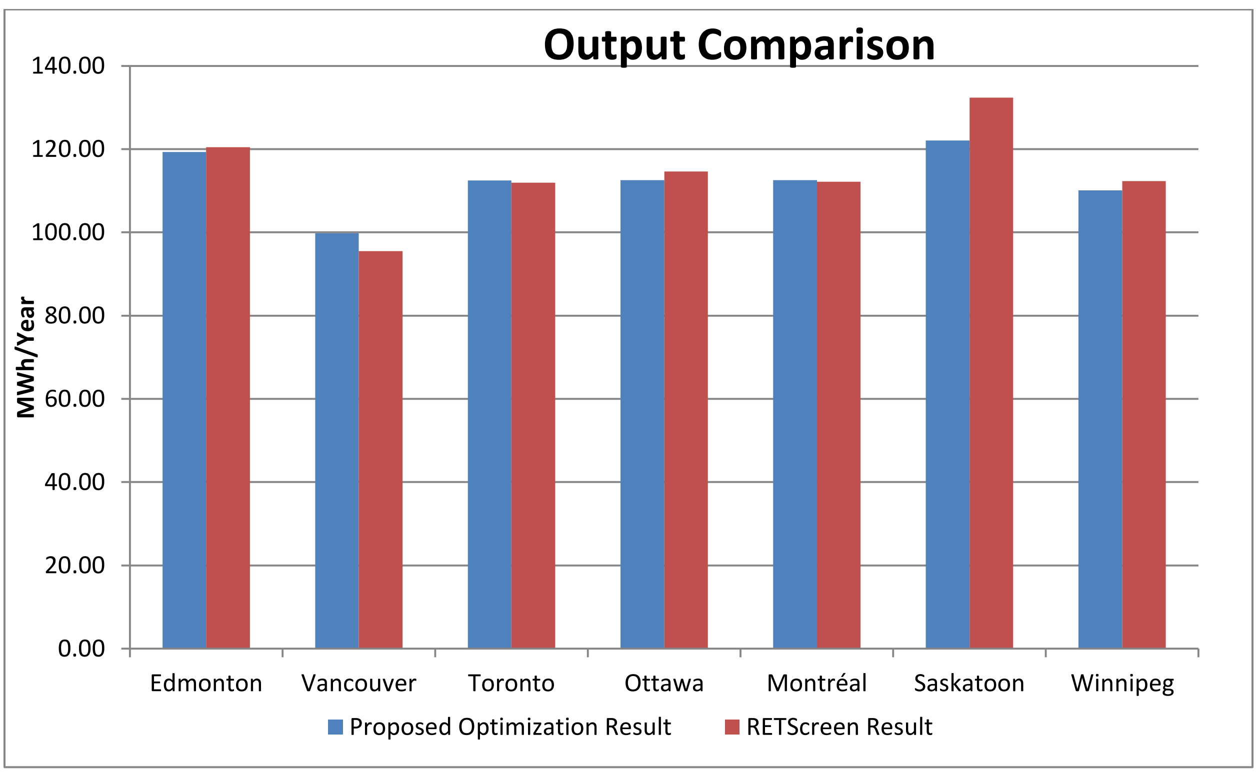

Figure 21: Comparison of results of the optimization and RETScreen

Figure 21 and Table 9 shows the accuracy of the proposed model output result based on the RETScreen output. The average accuracy of the optimization model is found to be 97%.

4.2 Demonstration of proposed model

The efficacy of the developed optimization model is demonstrated using an existing solar PV system: a flat roof solar PV project located at the Landmark Business Centre in Edmonton, Alberta, Canada (Figure 22 and Table 10). Landmark Business Centre has architectural awnings made of 153 pieces solar PV panels (Figure 23) and rooftop solar PV system made of 351 pcs solar PV panels (Figure 24). In this research, it should be noted, only rooftop solar PV system data is used—architectural awnings are not considered. The rooftop solar PV system is divided into five parts connected to the grid via five inverters. A Conergy PH 255P PV panel rated to 255 W at peak and a Sunny Tripower 20000TL-US-10 and Sunny Tripower 12000TL-US-10 rated power 25 kW DC and 15 kW DC are used in this project. The total number of PV panels in the project is 351, with 4 pc Tripower 20000TL-US-10 inverters and 1 pc Tripower 12000TL-US-10. The project capacity is 91.26 kW, and the effective area for the solar PV of the flat rooftop is approximately 1,895 m^2. Figure 25 shows the design layout of the roof.

Figure 22: Solar PV system in Landmark Business Centre

Table 10: Landmark Business Centre solar PV system details

Location	System Type	Number of PV panels	System Capacity (kW)	Solar PV System Area (m^2)	Solar PV Location	Annual Production (Approx. kWh)
Edmonton	Grid-tied	351	91.26	1895	Rooftop	100,386

Figure 23: Wall-mounted solar PV panels at Landmark Business Centre

Figure 24: Rooftop solar PV system at Landmark Business Centre

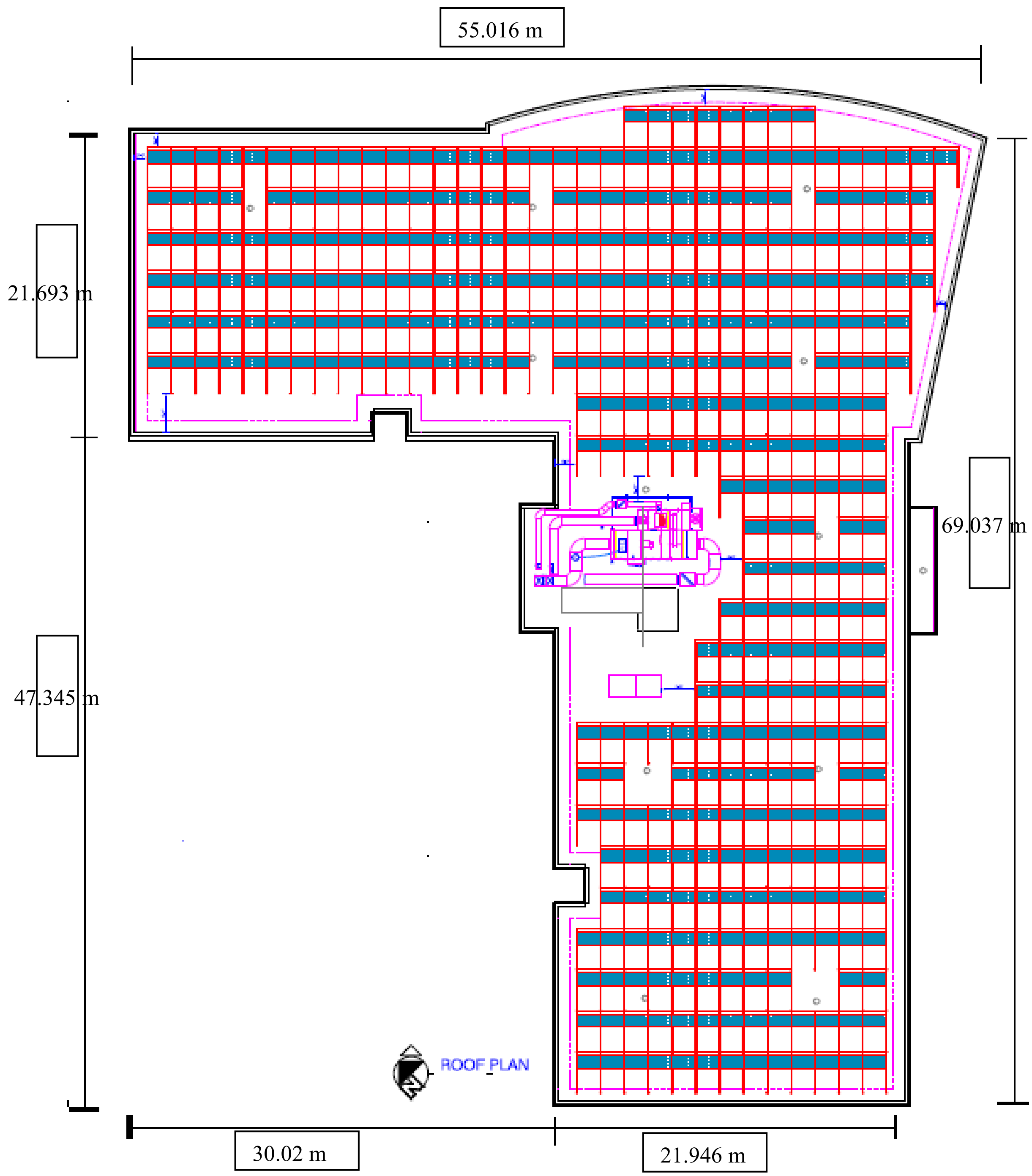

Figure 25: Design layout of Landmark office building solar PV system

Output data from all the inverters is collected and stored on the Sunny Portal database at regular intervals. Using the Sunny Portal web-based service, data is extracted from the cloud server for use in analyzing the optimization model. (For this project, it should be noted, the tilt angle, row distance, azimuth angle, and other parameters were designed by professional engineers using proper calculations.)

Most flat roofs have penetrations and, to install a solar PV system on a flat roof, these penetrations must be properly addressed. Segmentation of the roof is a very basic solution to this problem, and one with inherent deficiencies. However, there do exist more advanced techniques to address penetrations. The linear programming and Geographic Information System (GIS) can provide better implementation and integration of spatial data analysis. Guerra and Lewis, for instance, use a linear programming algorithm to analyze spatial requirements for identifying suitable sites for wildlife species (Guerra and Lewis 2002).

Density-based spatial optimization can also be used to optimize flat roof space. (Ligmann-Zielinska et al. 2008) develop a density-based design constraint, and then use it in their multi-objective optimization model, thereby encouraging efficient utilization of urban space through infill development. (Badarudin et al. 2012) describe the design of an algorithm-based solution for selecting a planting lining technique. Their algorithm is designed to divide an area into blocks and calculate the number of trees to plant. (Sengupta et al. 2012) develop a probabilistic model for developing a solar wind hybrid system that satisfies the energy generation requirement by optimal allocation of the land.

Landmark Business Centre's roof, it should be noted, differs in size and shape from the roof used in the hypothetical setup. For the purpose of carrying out the optimization, Landmark Business Centre's roof is thus divided into four segments. All the segments are optimized in the same model with different lengths and widths. For the lack of experimental data spatial optimization is not used in this research. Only segmentation is used for the demonstration of the proposed model.

The proposed optimization model is used to optimize the tilt angle and row distance for this project considering the geographic location and using the solar PV equipment data. Monthly and yearly results of the proposed optimization model are used to optimize the tilt angle and row distance for this project using geographic location and solar PV equipment data, as shown in Figure 26 and 27.

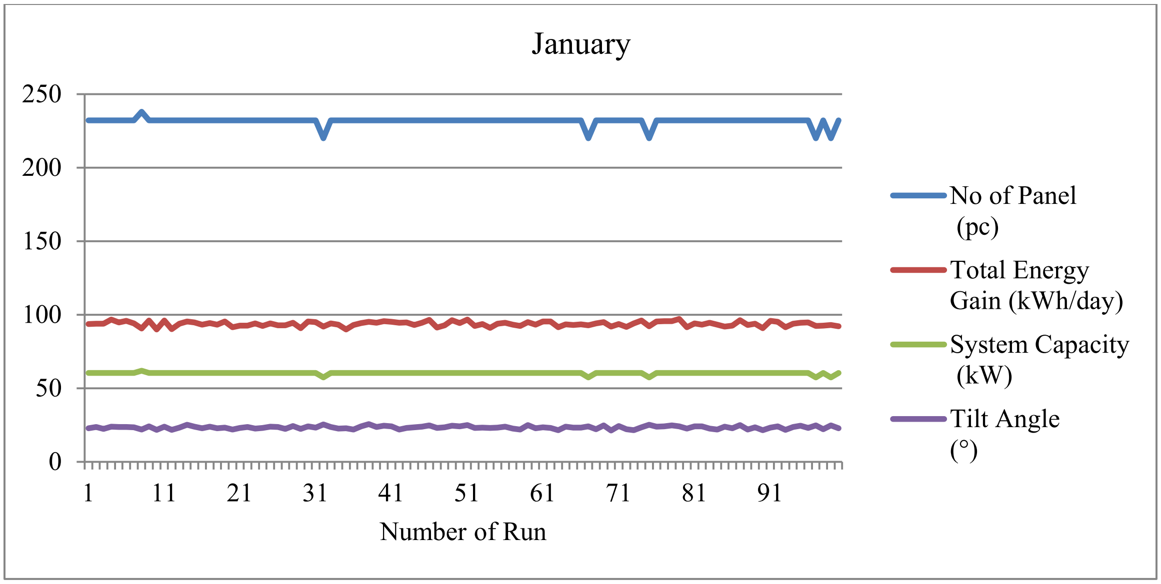
January
250
200
150
100
50
0
1
11
21
31
41
51
61
71
81
91
Number of Run
No of Panel (pc)
Total Energy Gain (kWh/day)
System Capacity (kW)
Tilt Angle (°)

(a)

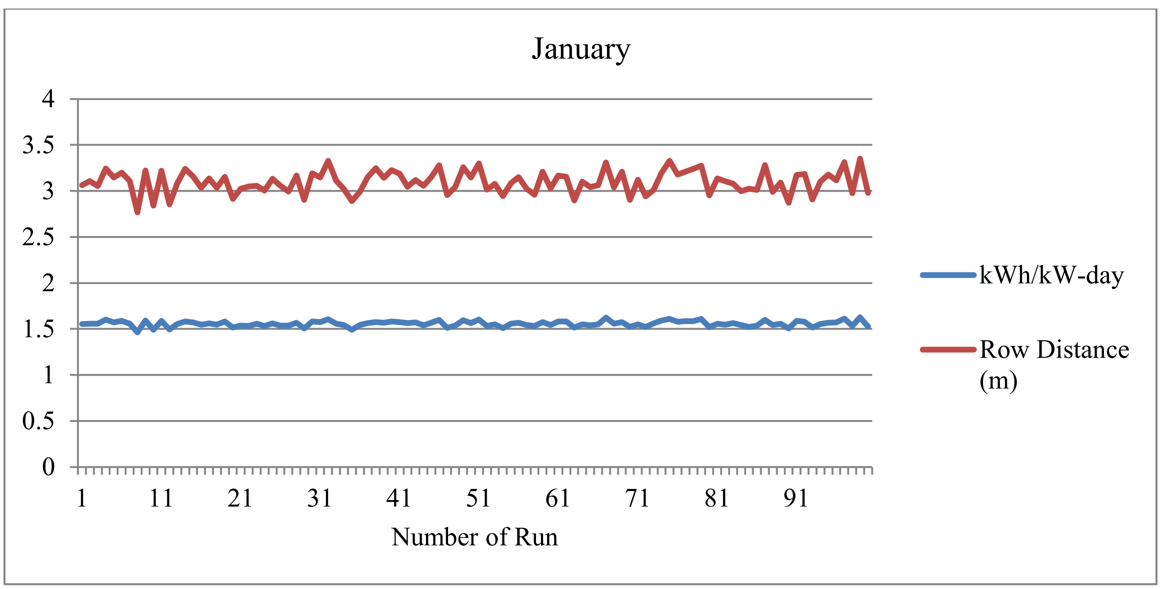
January
4
3.5
3
2.5
2
1.5
1
0.5
0
1
11
21
31
41
51
61
71
81
91
Number of Run
kWh/kW-day
Row Distance (m)

(b)

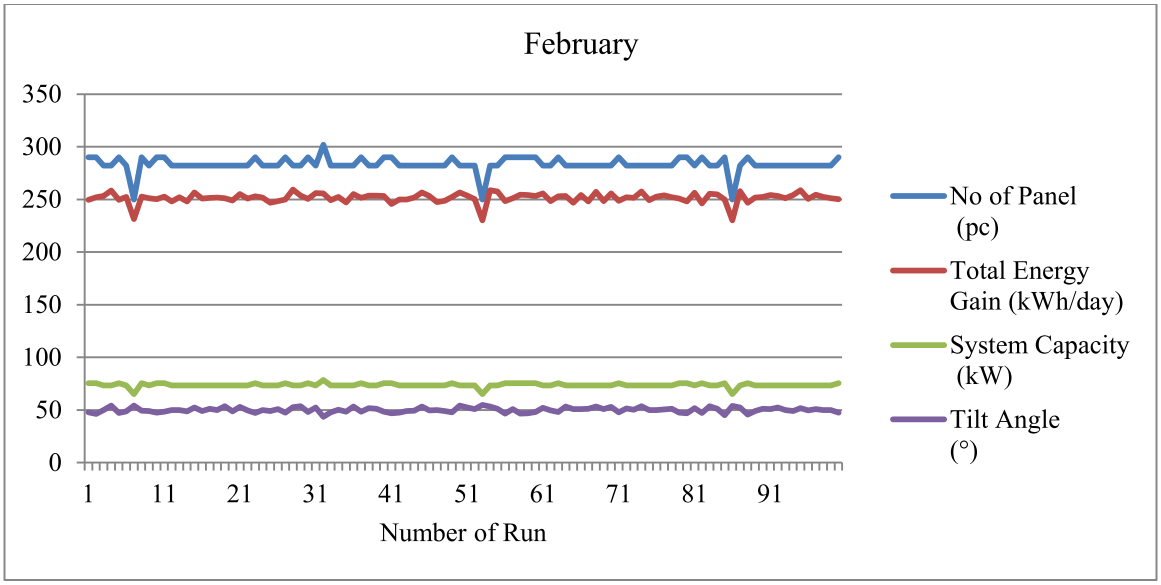
February
350
300
250
200
150
100
50
0
1
11
21
31
41
51
61
71
81
91
Number of Run
No of Panel (pc)
Total Energy Gain (kWh/day)
System Capacity (kW)
Tilt Angle (°)

(c)

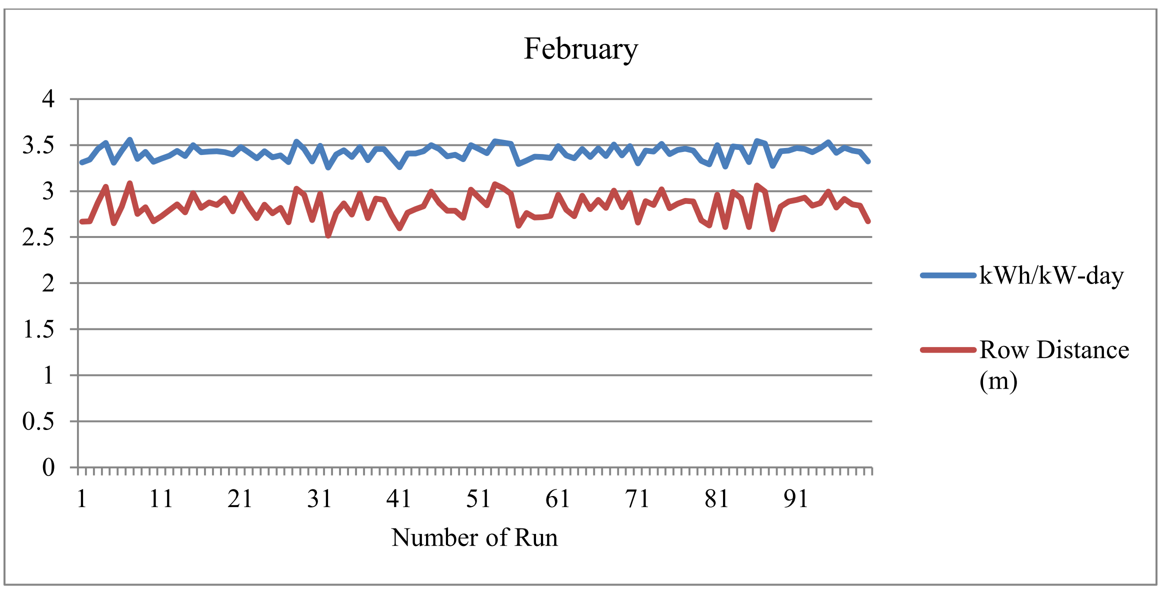
February
4
3.5
3
2.5
2
1.5
1
0.5
0
1
11
21
31
41
51
61
71
81
91
Number of Run
kWh/kW-day
Row Distance (m)

(d)

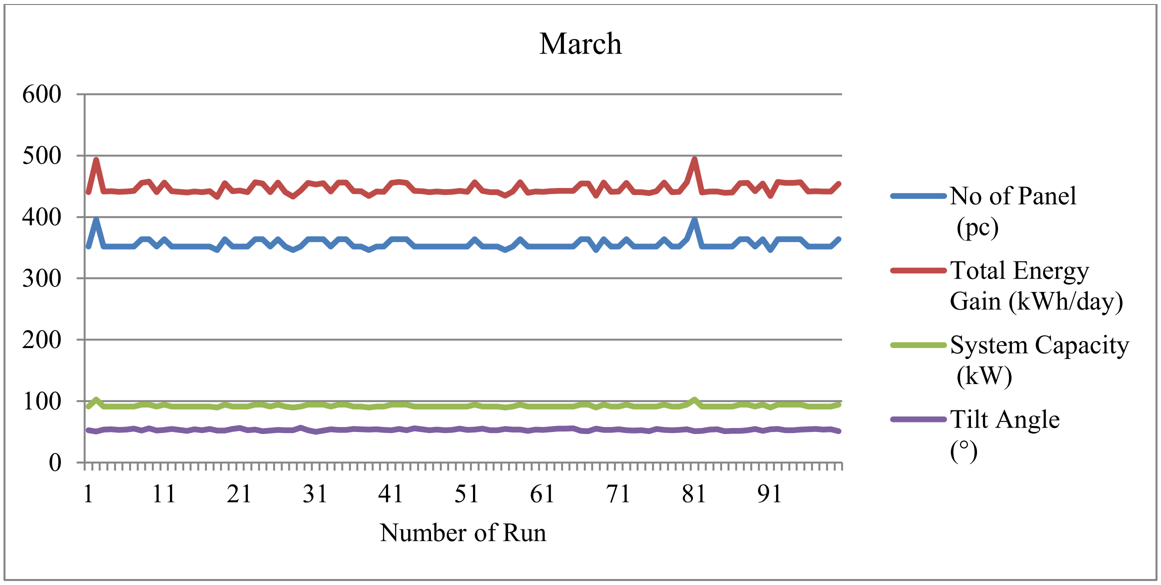
March
600
500
400
300
200
100
0
1
11
21
31
41
51
61
71
81
91
Number of Run
No of Panel (pc)
Total Energy Gain (kWh/day)
System Capacity (kW)
Tilt Angle (°)

(e)

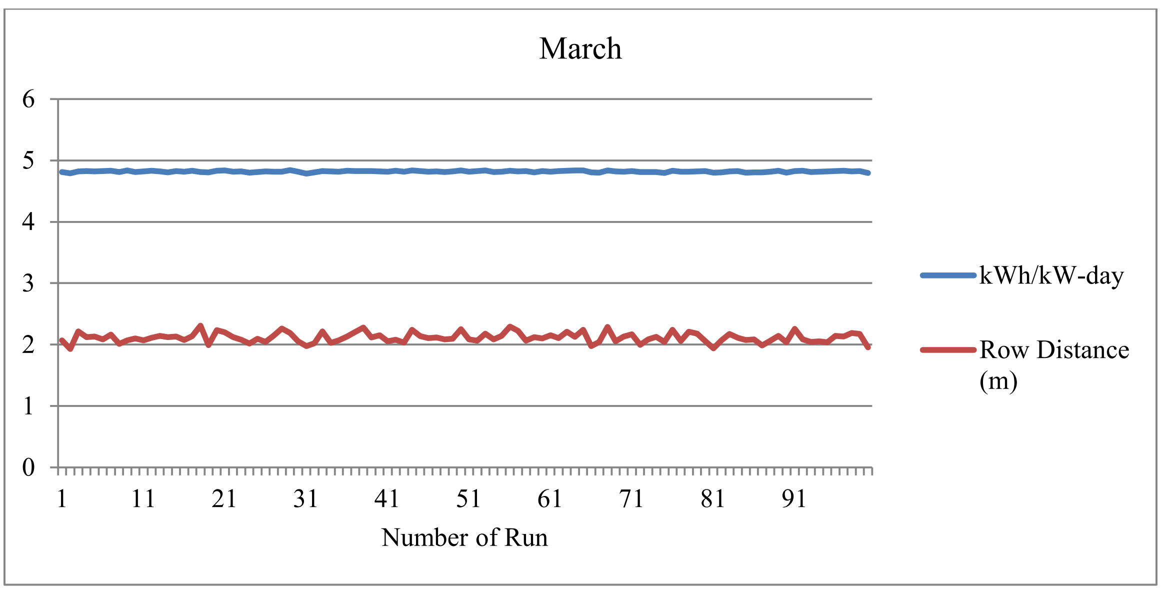
March
6
5
4
3
2
1
0
1
11
21
31
41
51
61
71
81
91
Number of Run
kWh/kW-day
Row Distance (m)

(f)

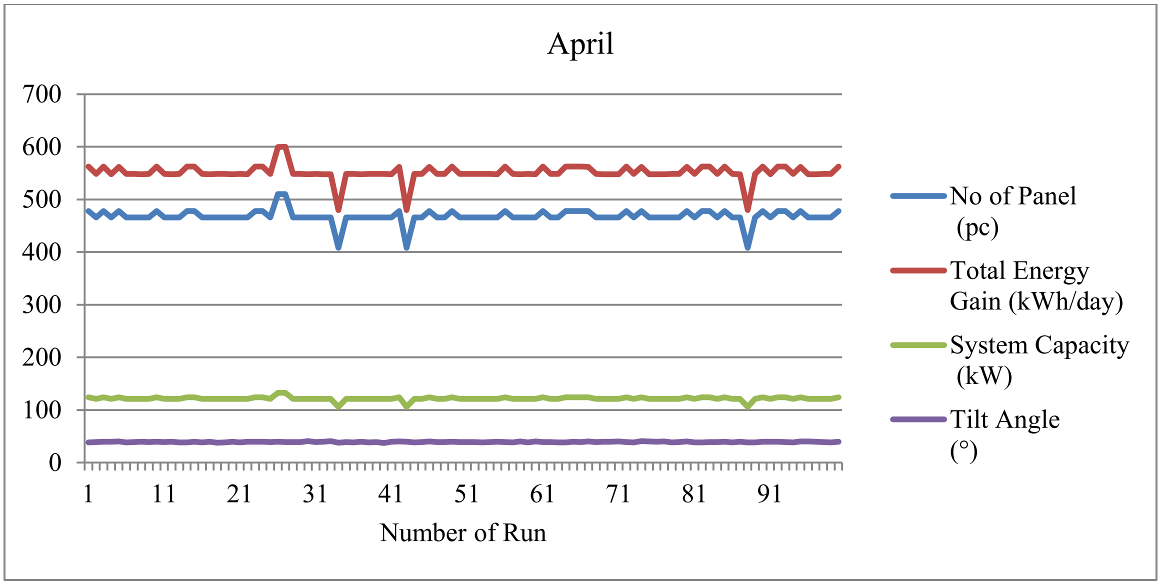
April
700
600
500
400
300
200
100
0
1
11
21
31
41
51
61
71
81
91
Number of Run
No of Panel (pc)
Total Energy Gain (kWh/day)
System Capacity (kW)
Tilt Angle (°)

(g)

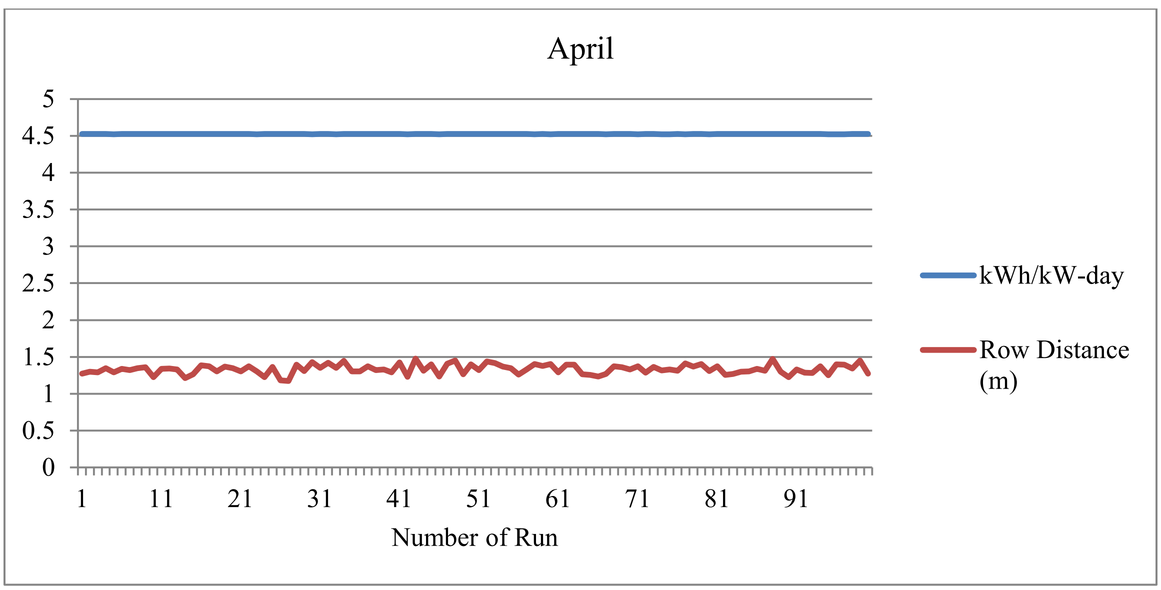
April
5
4.5
4
3.5
3
2.5
2
1.5
1
0.5
0
1
11
21
31
41
51
61
71
81
91
Number of Run
kWh/kW-day
Row Distance (m)

(h)

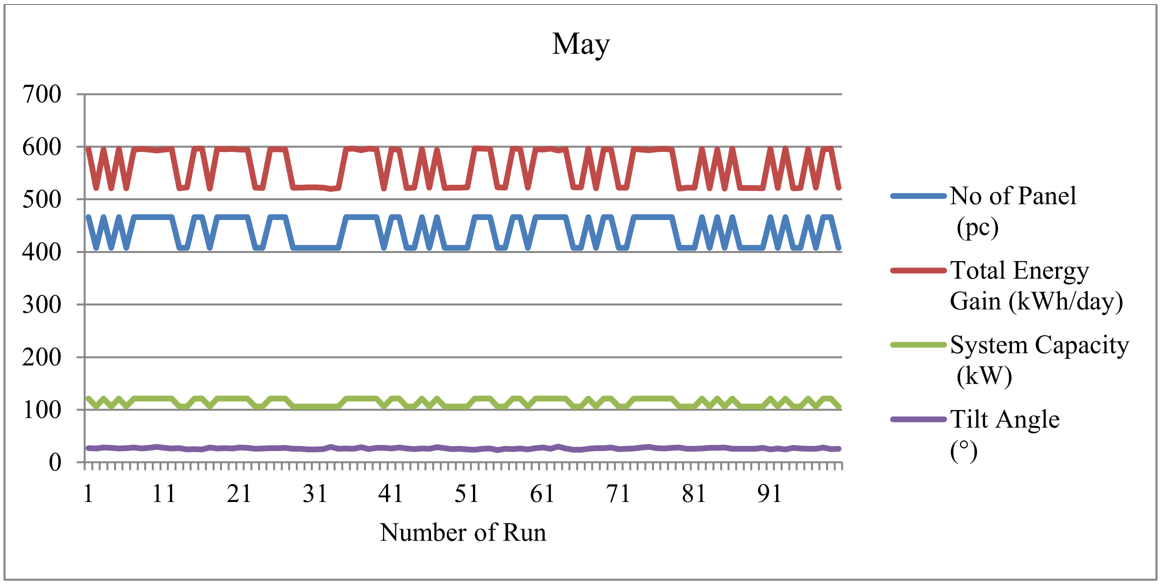

May
700
600
500
400
300
200
100
0
1
11
21
31
41
51
61
71
81
91
Number of Run
No of Panel (pc)
Total Energy Gain (kWh/day)
System Capacity (kW)
Tilt Angle (°)

(i)

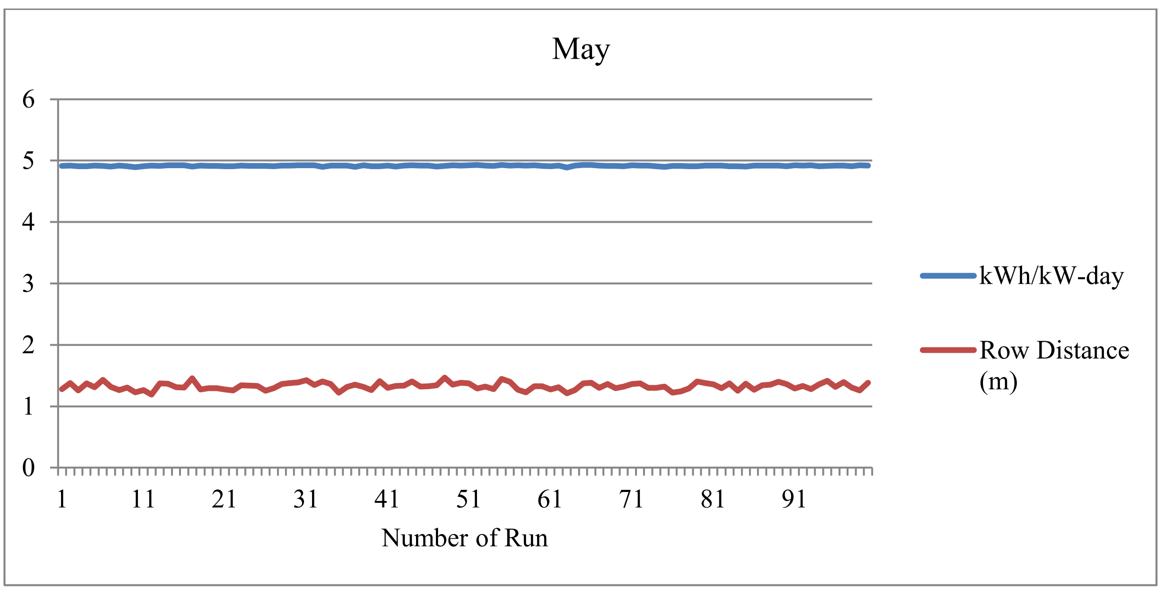

May
6
5
4
3
2
1
0
1
11
21
31
41
51
61
71
81
91
Number of Run
kWh/kW-day
Row Distance (m)

(j)

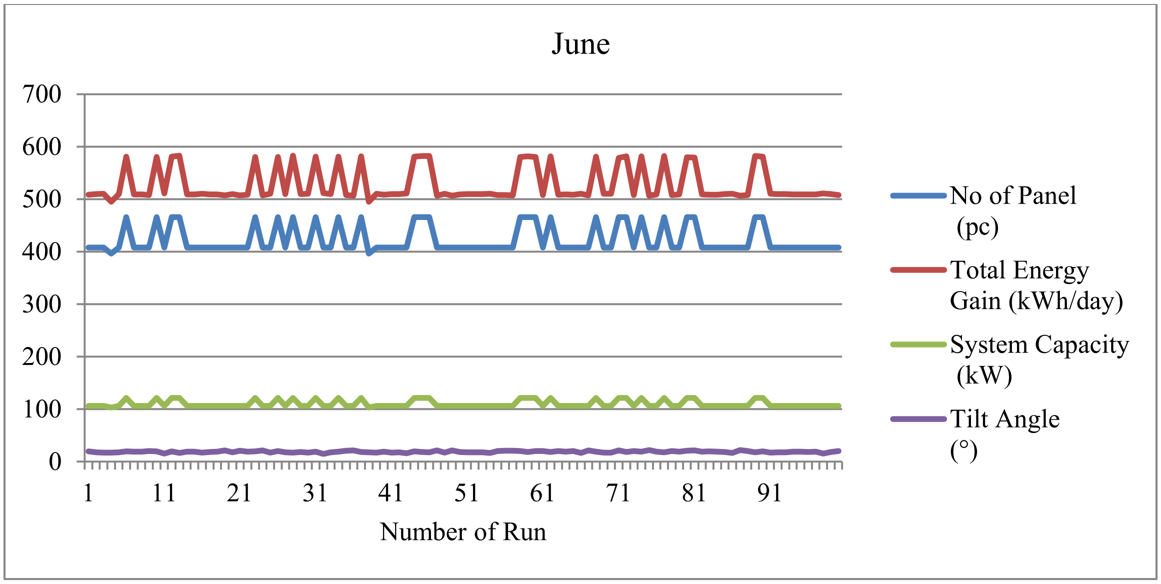
June
700
600
500
400
300
200
100
0
1
11
21
31
41
51
61
71
81
91
Number of Run
No of Panel (pc)
Total Energy Gain (kWh/day)
System Capacity (kW)
Tilt Angle (°)

(k)

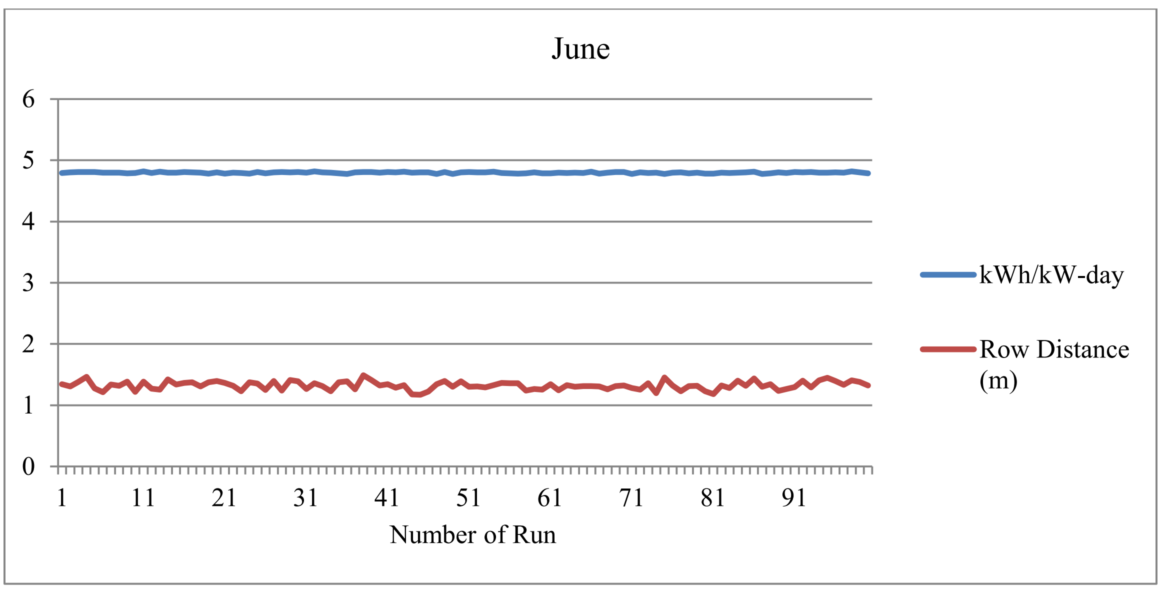
June
6
5
4
3
2
1
0
1
11
21
31
41
51
61
71
81
91
Number of Run
kWh/kW-day
Row Distance (m)

(l)

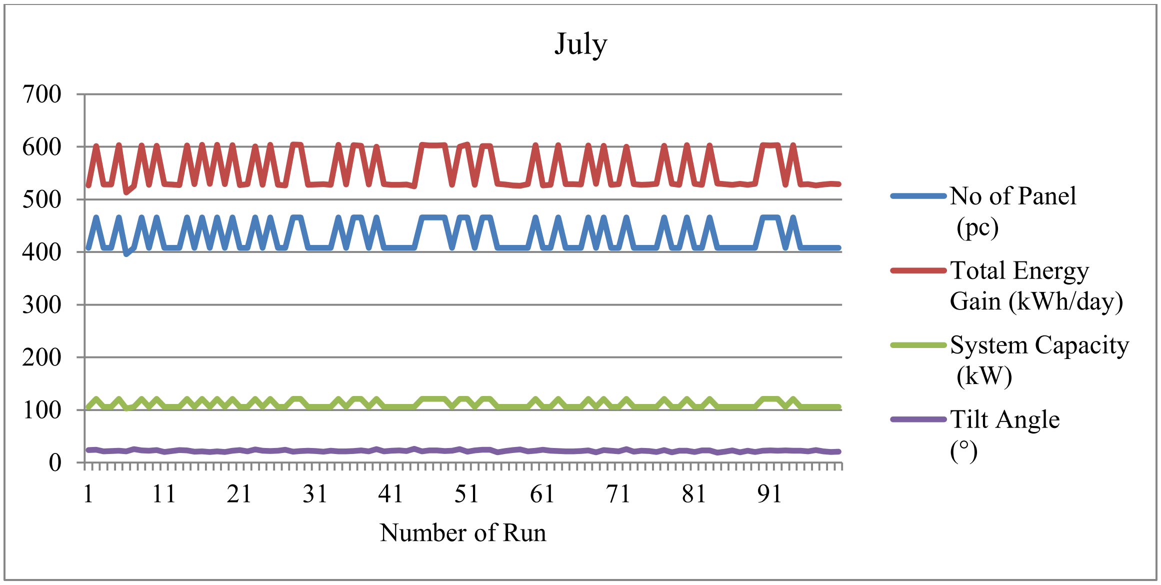
July
700
600
500
400
300
200
100
0
1
11
21
31
41
51
61
71
81
91
Number of Run
No of Panel (pc)
Total Energy Gain (kWh/day)
System Capacity (kW)
Tilt Angle (°)

(m)

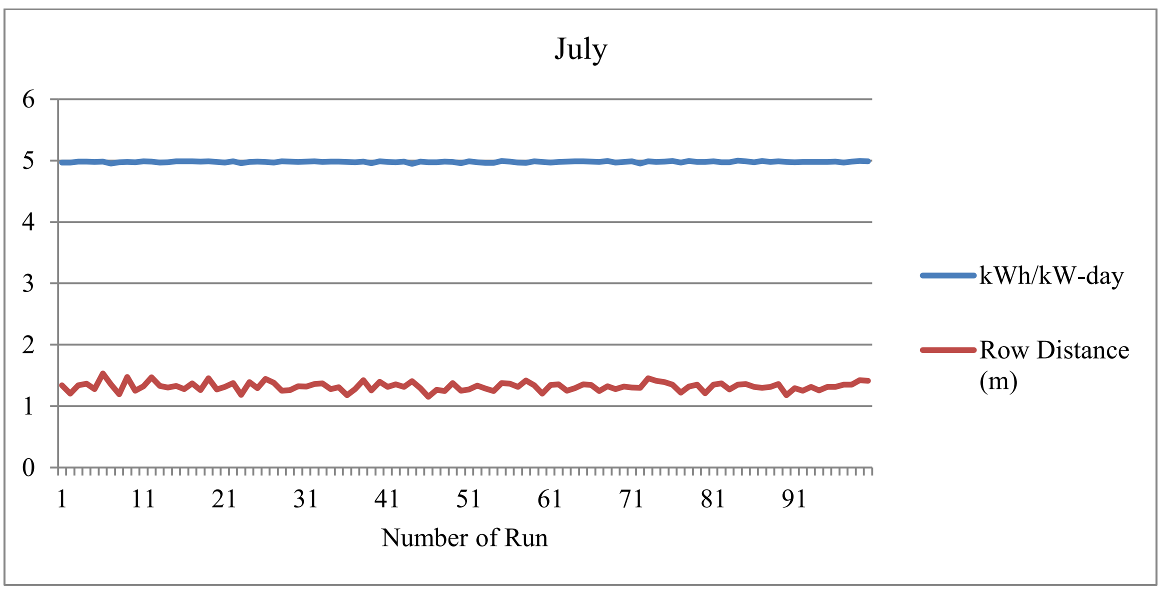
July
6
5
4
3
2
1
0
1
11
21
31
41
51
61
71
81
91
Number of Run
kWh/kW-day
Row Distance (m)

(n)

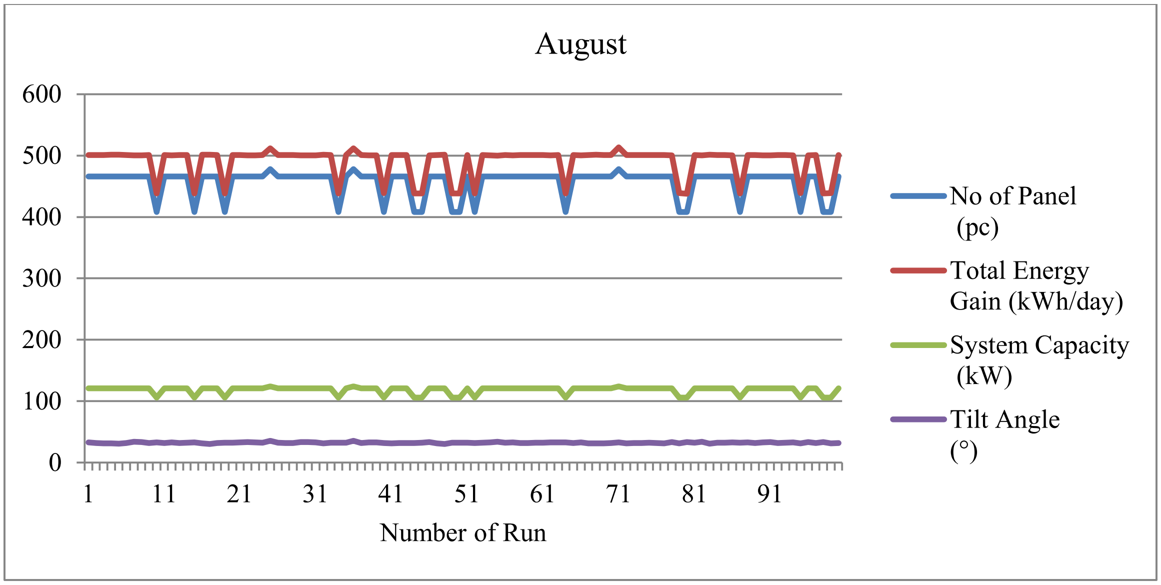
August
600
500
400
300
200
100
0
1
11
21
31
41
51
61
71
81
91
Number of Run
No of Panel (pc)
Total Energy Gain (kWh/day)
System Capacity (kW)
Tilt Angle (°)

(o)

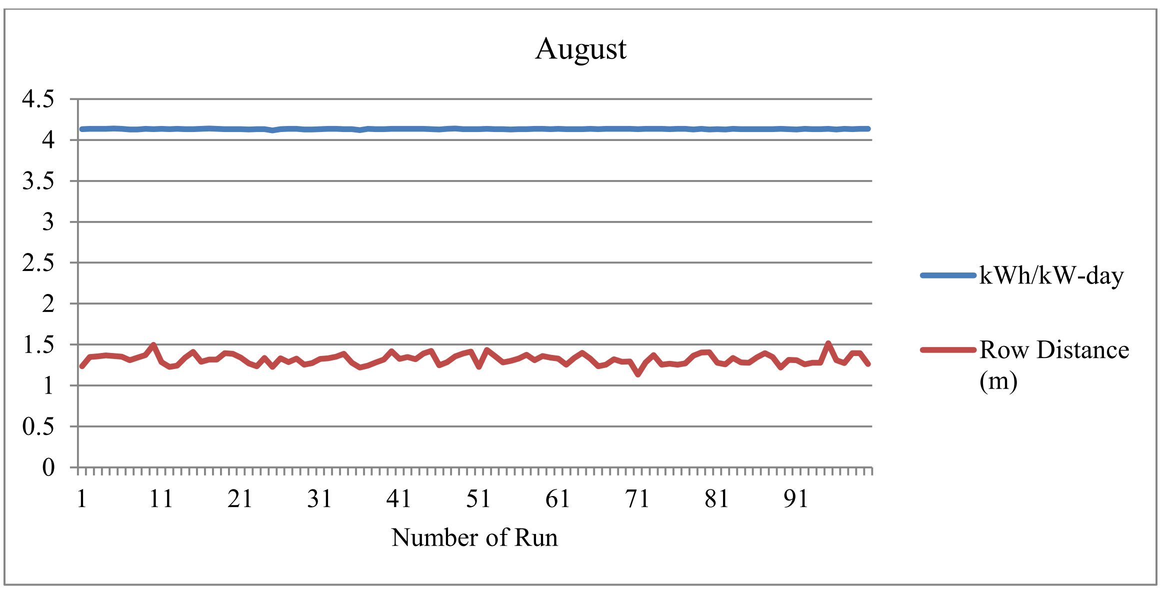
August
4.5
4
3.5
3
2.5
2
1.5
1
0.5
0
1
11
21
31
41
51
61
71
81
91
Number of Run
kWh/kW-day
Row Distance (m)

(p)

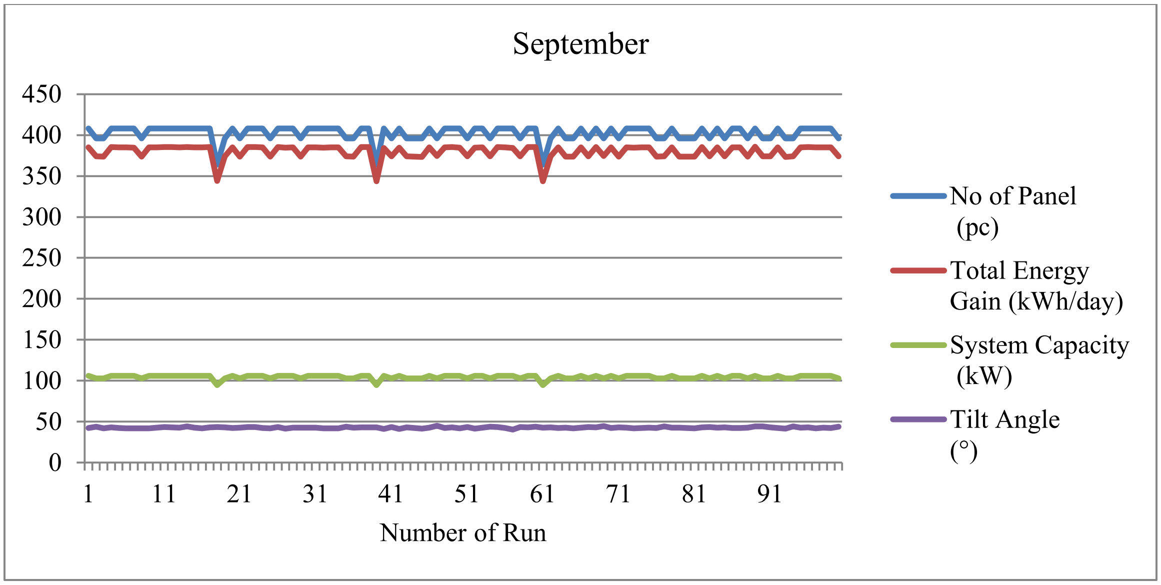
September
450
400
350
300
250
200
150
100
50
0
1
11
21
31
41
51
61
71
81
91
Number of Run
No of Panel (pc)
Total Energy Gain (kWh/day)
System Capacity (kW)
Tilt Angle (°)

(q)

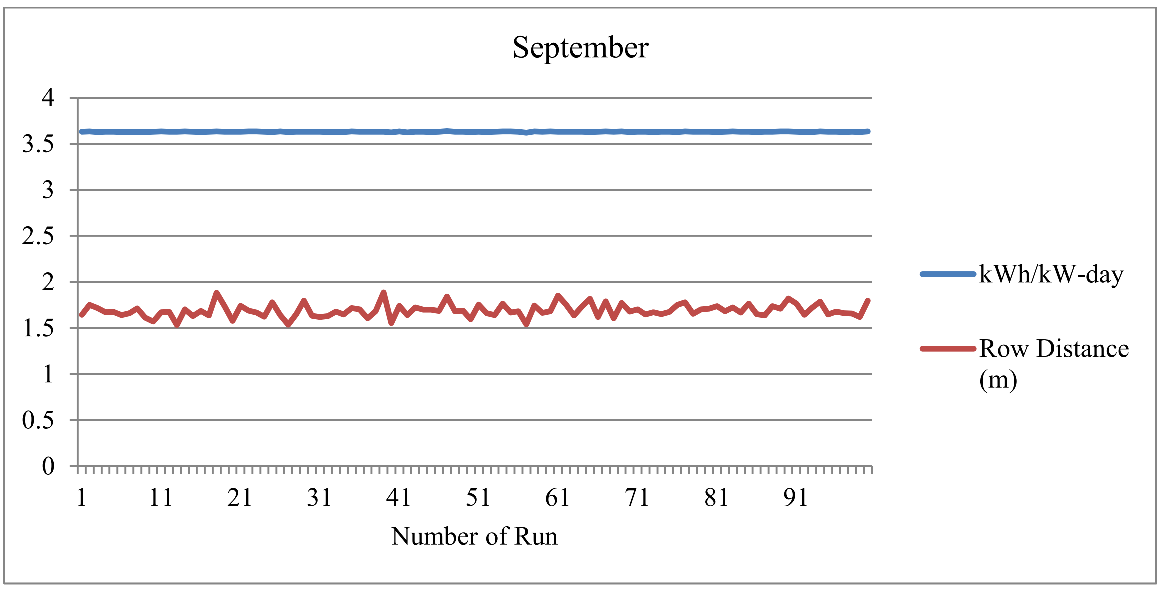
September
4
3.5
3
2.5
2
1.5
1
0.5
0
1
11
21
31
41
51
61
71
81
91
Number of Run
kWh/kW-day
Row Distance (m)

(r)

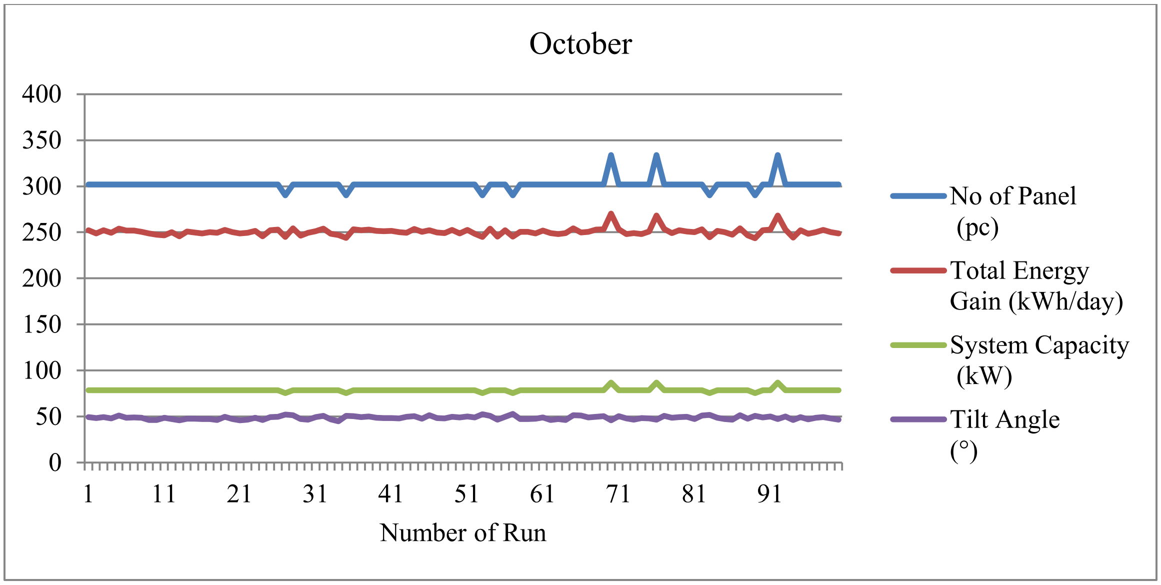
October
400
350
300
250
200
150
100
50
0
1
11
21
31
41
51
61
71
81
91
Number of Run
No of Panel (pc)
Total Energy Gain (kWh/day)
System Capacity (kW)
Tilt Angle (°)

(s)

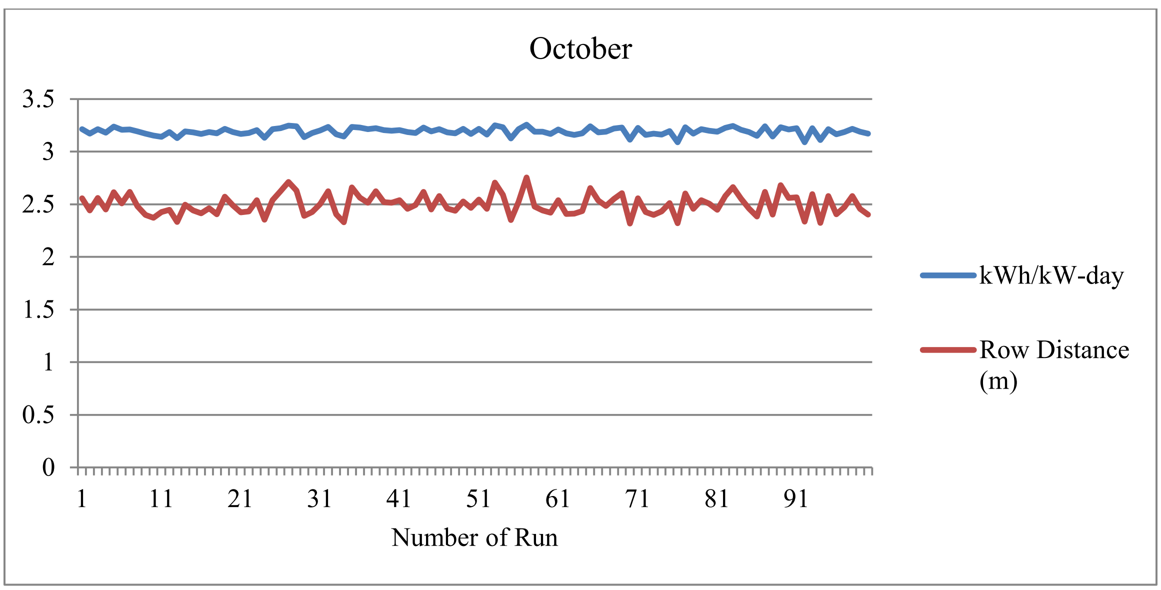
October
3.5
3
2.5
2
1.5
1
0.5
0
1
11
21
31
41
51
61
71
81
91
Number of Run
kWh/kW-day
Row Distance (m)

(t)

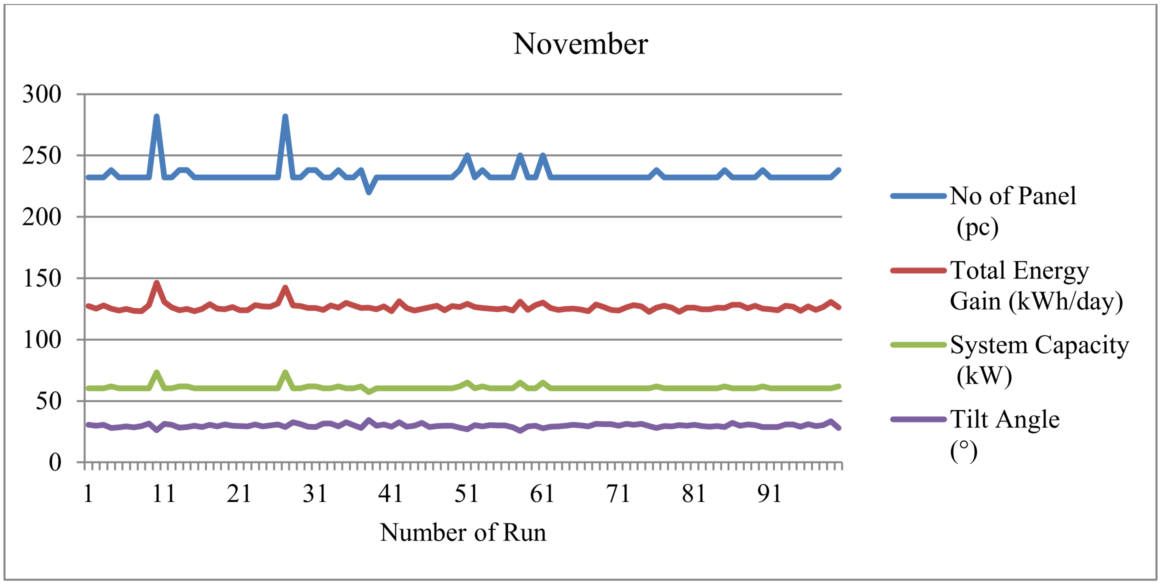
November
300
250
200
150
100
50
0
1
11
21
31
41
51
61
71
81
91
Number of Run
No of Panel (pc)
Total Energy Gain (kWh/day)
System Capacity (kW)
Tilt Angle (°)

(u)

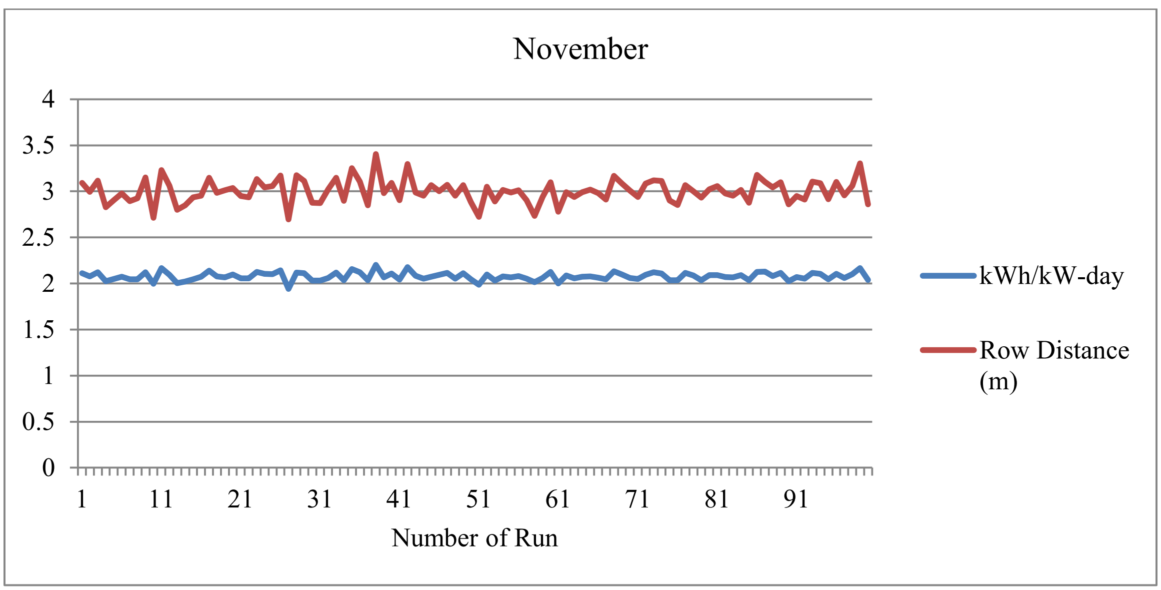
November
4
3.5
3
2.5
2
1.5
1
0.5
0
1
11
21
31
41
51
61
71
81
91
Number of Run
kWh/kW-day
Row Distance (m)

(v)

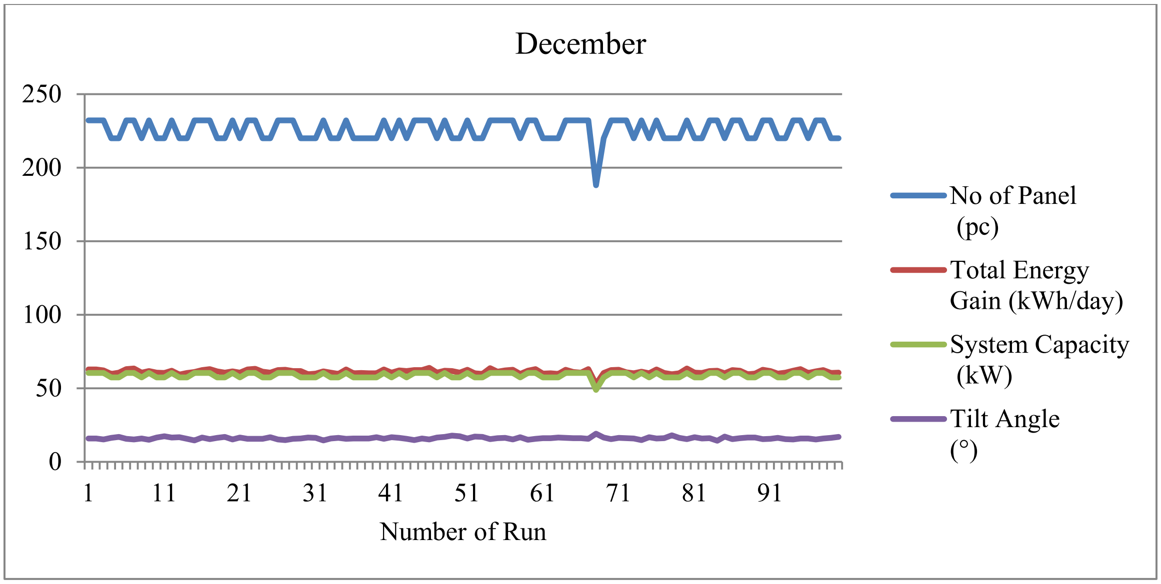

(w)

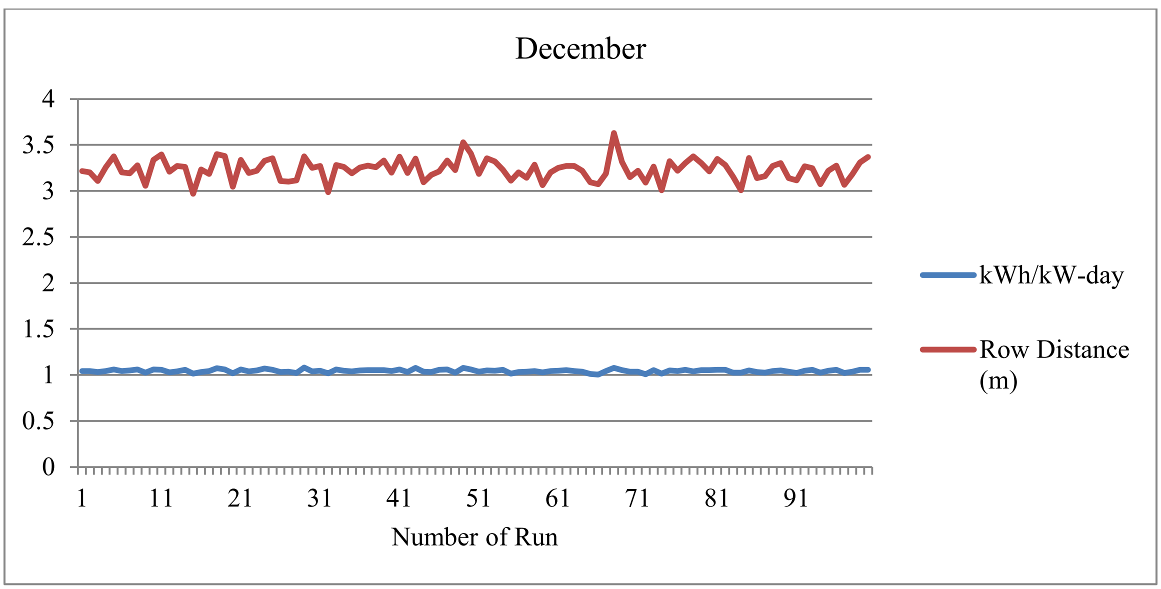

(x)

Figure 26 [(a) to (x)]: Results of 100 runs over twelve months

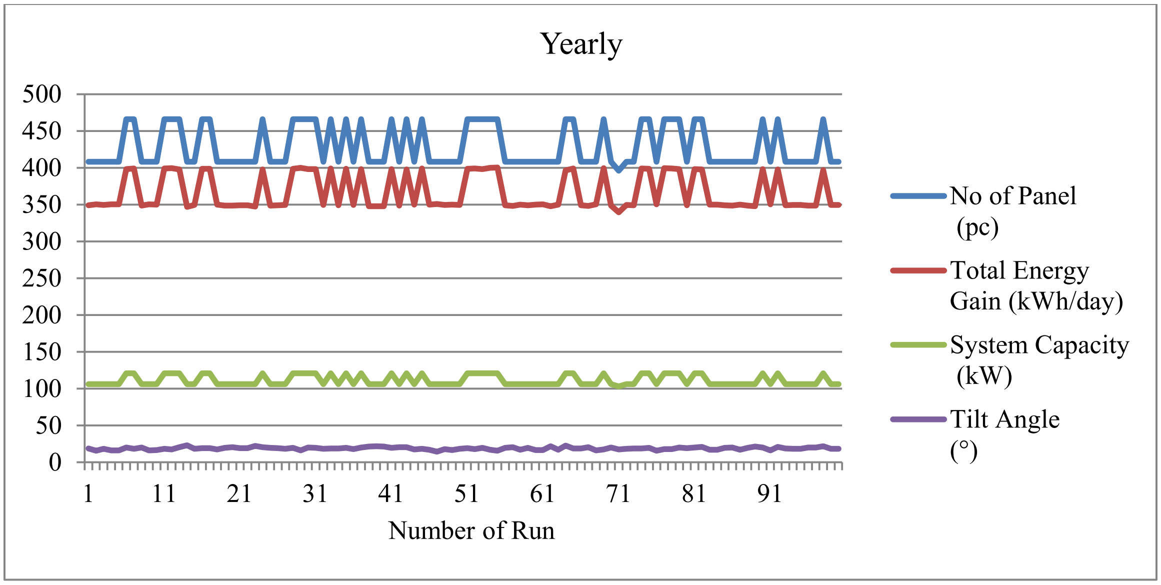

(a)

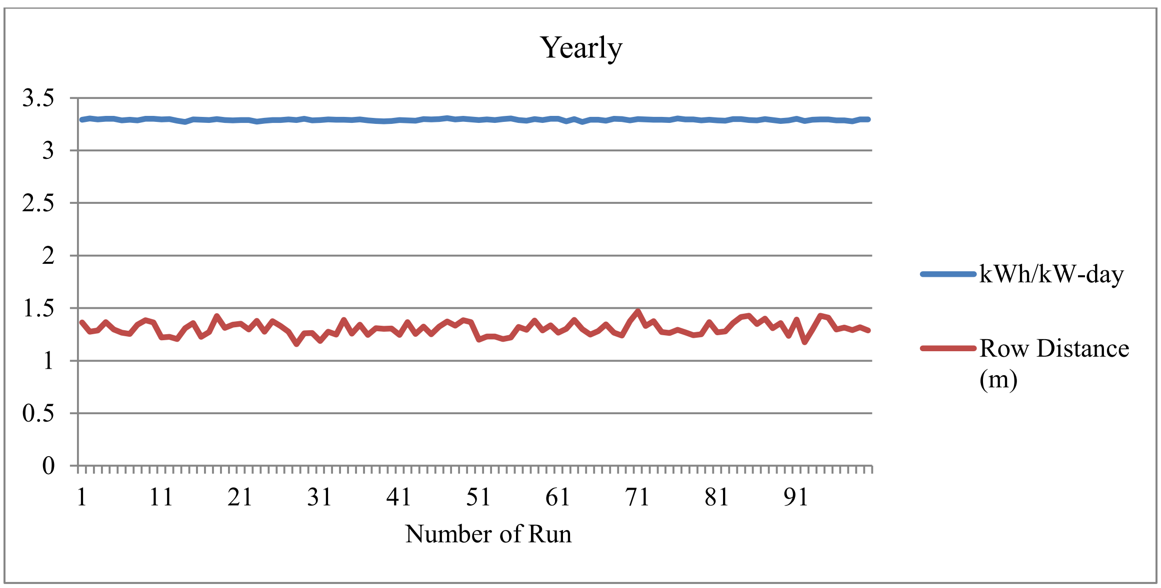

(b)

Figure 27(a) and (b): Results of 100 runs for yearly optimization

Figures 26 and 27 provide an overview of the results of the optimization model implemented for an existing solar PV system. The figures summarize the parameters optimized by the model and illustrate its consistency and reliability.

Table 11: Comparison between actual data and optimization model results for case project

Real Project Data (2016)					
No. of Panels (pc)	Yearly Mean Daily Energy (kWh/day)	kWh/kW/day	System Capacity (kW)	Tilt Angle (°)	Row Distance (m)
351	313.00	3.42	91.26	25.00	1.66
Optimization Model Results					
No. of Panels (pc)	Yearly Mean Daily Energy (kWh/day)	kWh/kW/day	System Capacity (kW)	Tilt Angle (°)	Row Distance (m)
408	350	3.29	106.08	19.83	1.37

Table 11 presents a comparison between the data collected from a real project and the optimization results for the same project. Based on the results of the optimization model, it can be observed that the total system capacity and energy gain can be improved by following this optimization suggestion. Although the energy per unit may decrease by this optimization, the overall energy generation would increase by following this optimization suggestion. The tilt angle and row distance from the optimization results, it should be noted, are similar to the calculated design used in the project, which proves the acceptability of the optimization results. This analysis proves the accuracy of the optimization model and also demonstrates its practical applicability.

CHAPTER FIVE: DISCUSSION OF RESULTS AND CONCLUSION

5.1 Conclusion

In the developed optimization algorithm, the optimum row number result is an integer value. When the model finds fractional values for row number in the optimization process, it suggests the closest integer values. It should also be noted that, in multiple runs, this model can suggest different row numbers as the optimal value. In such a case we consider the result which is suggested most frequently by the optimization model in multiple runs. For example: in 100 runs targeting the yearly mean daily energy of the hypothetical experiment, 338 panels is suggested as the optimal result in some runs while 364 panels is suggested in others. The row number for 338 panels is 13 and for 364 panels is 14. It also suggests different PV system sizes (86.19 kW and 92.82 kW) in different runs. For such a case, the optimal row number result is between 13 and 14. Since 14 is suggested more frequently than is 13 in 100 runs, we can take 14 as the number of rows and corresponding values for other parameters as the optimal result.

The discussion in Chapter 2 indicates that researchers and manufacturers have done some optimization on this field. The analysis of the proposed methods, though, reveals the differences from the other methods to design a solar PV system. An analysis of the results proves that the developed optimization model can be used in any geographic location and for different PV panels and inverters to optimize the system. It can also be used to find the radiation and the feasibility of the energy output for individual locations for grid-tied solar PV systems. It can also be used to calculate monthly and yearly average daily energy gain. As a result, the proposed model aids in determining the optimum parameter design solutions for grid-tied solar PV systems in different seasons or in a particular time of year separately. The optimization process can be carried out quickly (20 seconds on average).

5.2 Contributions

The developed solar PV design optimization can assist both researchers and users in several respects. It allows researchers to check their results quickly in order to find the optimal value. This model can also be used for any location, and this gives the researchers and commercial users flexibility to design a solar PV system. Commercial users will benefit from the developed model's useful and efficient design with optimized parameters. It is also worth noting that this proposed model can be applied on a mobile platform for easy access.

5.3 Limitations

Followings are the limitations of this research:

- This optimization model does not consider energy consumption characteristics.
- Roof top area optimization is not included for penetration.
- Grid power cut off is not considered in this research.

5.4 Proposed future work

- An extension of this research can focus on experimental setup and validation.
- Different types of roofs can be introduced to the model.
- Battery storage bank and off-grid solar PV system can be incorporated into the optimization.

REFERENCES

Abedi, S., Ahangar, H. G., Nick, M., and Hosseinian, S. H. (2011). "Economic and reliable design of a hybrid PV-wind-fuel cell energy system using differential evolutionary algorithm." *Proceedings of the 19th IEEE Iranian Conference on Electrical Engineering*, *Tehran, Iran,* 6 pages.

Abido, M. (2002). "Optimal design of power-system stabilizers using particle swarm optimization."*IEEE Trans.Energy Convers.,*17(3), 406-413.

Anapode Solar. "On-Grid vs. Off-Grid Solar." https://www.anapode.com/content/On-GridVsOff-Grid (16 August 2017).

Appelbaum, J. and Bany, J. (1979). "Shadow effect of adjacent solar collectors in large scale systems." *Solar Energy*, 23(6), 497-507.

Awad, H., Gül, M., Ritter, C., Verma, P., Chen, Y., Salim, K. E., Al-Hussein, M., Yu, H., and Kasawski, K. (2016). "Solar photovoltaic optimization for commercial flat rooftops in cold regions." *Proceedings of the IEEE Conference on Technologies for Sustainability*, *Phoenix, AZ, USA,* 39-46.

Badarudin, I. M., Sultan, A. B. M., bin Sulaiman, M. N., bin Mamat, A., and bin Tengku Muda, Mohamed Mahmud. (2012). "An algorithm for the selection of planting lining technique towards optimizing land Area: An algorithm for planting lining technique selection." *Proceedings of the 4th IEEE Conference on Data Mining and Optimization*, 28-34.

Bakirci, K. (2012). "General models for optimum tilt angles of solar panels: Turkey case study." *Renewable and Sustainable Energy Reviews,* 16(8), 6149-6159.

Bakirci, K. (2009). "Models of solar radiation with hours of bright sunshine: A review." *Renewable and Sustainable Energy Reviews*, 13(9), 2580-2588.

Bany, J. and Appelbaum, J. (1987). "The effect of shading on the design of a field of solar collectors." *Solar Cells*, 20(3), 201-228.

Barra, O., Conti, M., Santamata, E., Scarmozzino, R., and Visentin, R. (1977). "Shadows' effect in a large scale solar power plant." *Solar Energy,* 19(6), 759-762.

Bashir, M. and Sadeh, J. (2012). "Size optimization of new hybrid stand-alone renewable energy system considering a reliability index." *Proceedings of the 11th IEEE International Conference on Environment and Electrical Engineering*, *Venice, Italy,* 989-994.

Belfkira, R., Hajji, O., Nichita, C., and Barakat, G. (2007). "Optimal sizing of stand-alone hybrid wind/PV system with battery storage." *Proceedings of the IEEE European Conference on Power Electronics and Applications*, *Aalborg, Denmark,* 10 pages.

Bourennani, F., Rizvi, R., and Rahnamayan, S. (2010). "Optimal Photovoltaic Solar Power Farm Design using the Differential Evolution Algorithm."

Calabrò, E. (2009). "Determining optimum tilt angles of photovoltaic panels at typical north-tropical latitudes." *Journal of Renewable and Sustainable Energy*, 1(3), 033104.

Castellano, N. N., Parra, J. A. G., Valls-Guirado, J., and Manzano-Agugliaro, F. (2015). "Optimal displacement of photovoltaic array's rows using a novel shading model." *Appl.Energy,* 144, 9 pages.

Chandel, S. S. and Aggarwal, R. K. (2011). "Estimation of hourly solar radiation on horizontal and inclined surfaces in Western Himalayas." *Smart Grid and Renewable Energy*, 2(1), 45.

Chandel, S., Aggarwal, R., and Pandey, A. (2005). "New correlation to estimate global solar radiation on horizontal surfaces using sunshine hour and temperature data for Indian sites." *Journal of Solar Energy Engineering*, 127(3), 417-420.

Chen, Y., Lee, C., and Wu, H. (2005). "Calculation of the optimum installation angle for fixed solar-cell panels based on the genetic algorithm and the simulated-annealing method." *IEEE Trans.Energy Convers.*, 20(2), 467-473.

Cheng, C., Jimenez, C. S. S., and Lee, M. (2009). "Research of BIPV optimal tilted angle, use of latitude concept for south orientated plans." *Renewable Energy*, 34(6), 1644-1650.

Conergy. (2015). "Photovoltaic Modules Technical Data." https://www.solaris-shop.com/content/Conergy%20PH%20255P%20Specs.pdf (08/17, 2017).

Deline, C., Dobos, A., Janzou, S., Meydbray, J., and Donovan, M. (2013). "A simplified model of uniform shading in large photovoltaic arrays." *Solar Energy*, 96, 274-282.

Demain, C., Journée, M., and Bertrand, C. (2013). "Evaluation of different models to estimate the global solar radiation on inclined surfaces." *Renewable Energy*, 50, 710-721.

Dixit, T.V., Yadav. A., and Gupta, S. (2016). "Annual Optimum Tilt Angle Prediction of Solar Collector Using PSO Estimator." *Proceedings of the International Conference on Advanced Material Technologies (ICAMT)-2016*, Dadi Institute of Engineering and Technology (DIET), India.

El-Sebaii, A., Al-Hazmi, F., Al-Ghamdi, A., and Yaghmour, S. J. (2010). "Global, direct and diffuse solar radiation on horizontal and tilted surfaces in Jeddah, Saudi Arabia." *Appl.Energy*, 87(2), 568-576.

EnergyTrend.(2011). "Introduction of Solar Inverters." http://pv.energytrend.com/knowledge/Solar_Inverter_Introduction.html (16 August 2017).

Fernández-Infantes, A., Contreras, J., and Bernal-Agustín, J. L. (2006). "Design of grid connected PV systems considering electrical, economical and environmental aspects: A practical case." *Renewable Energy*, 31(13), 2042-2062.

Goss, B., Cole, I., Betts, T., and Gottschalg, R. (2014). "Irradiance modelling for individual cells of shaded solar photovoltaic arrays." *Solar Energy*, 110, 410-419.

Groumpos, P. P. and Khouzam, K. (1987). "A generic approach to the shadow effect of large solar power systems." *Solar Cells*, 22(1), 29-46.

Guerra, G. and Lewis, J. (2002). "Spatial optimization and GIS." *Locating and Optimal Habitat for Wildlife Reintroduction*. McGill University, Montréal, QC, Canada.

Halasah, S. A., Pearlmutter, D., and Feuermann, D. (2013). "Field installation versus local integration of photovoltaic systems and their effect on energy evaluation metrics." *Energy Policy*, 52, 462-471.

Haque, M. M. and Wolfs, P. (2016). "A review of high PV penetrations in LV distribution networks: Present status, impacts and mitigation measures." *Renewable and Sustainable Energy Reviews*, 62, 1195-1208.

Hussein, H., Ahmad, G., and El-Ghetany, H. (2004). "Performance evaluation of photovoltaic modules at different tilt angles and orientations." *Energy Conversion and Management*, 45(15), 2441-2452.

IFC (2015). *Utility-Scale Solar Photovoltaic Power Plants.* International Finance Corporation, Washington, D.C.

Iqbal, M. (2012). *An Introduction to Solar Radiation.* Elsevier

Jäger-Waldau, A. (2016). "PV Status Report 2016."

S. Joe, and Windy, D. (2007). "Ask the expert: PV longevity & degradation ." https://www.homepower.com/articles/solar-electricity/equipment-products/ask-experts-pv-longevity-degradation (08/15, 2017).

Jones, R. and Burkhart, J. (1981). "Shading effects of collector rows tilted toward the equator." *Solar Energy*, 26(6), 563-565.

Kanters, J. and Davidsson, H. (2014). "Mutual shading of PV modules on flat roofs: A parametric study." *Energy Procedia*, 57, 1706-1715.

Karimi, M., Mokhlis, H., Naidu, K., Uddin, S., and Bakar, A. (2016). "Photovoltaic penetration issues and impacts in distribution network: A review." *Renewable and Sustainable Energy Reviews*, 53, 594-605.

Kennedy, J. (2011). "Particle swarm optimization." *Encyclopedia of Machine Learning,* Springer, 760-766.

Kennedy, J. (1997). "The particle swarm: Social adaptation of knowledge." *Proceedings of the IEEE International Conference on Evolutionary Computation*, *Indianapolis, IN, USA,* 303-308.

Khare, A., and Rangnekar, S. (2013). "A review of particle swarm optimization and its applications in solar photovoltaic system." *Applied Soft Computing,* 13(5), 2997-3006.

Khatib, T., Mohamed, A., and Sopian, K. (2013). "A review of photovoltaic systems size optimization techniques." *Renewable and Sustainable Energy Reviews*, 22 454-465.

Kornelakis, A. and Koutroulis, E. (2009). "Methodology for the design optimisation and the economic analysis of grid-connected photovoltaic systems." *IET Renewable Power Generation*, 3(4), 476-492.

Kornelakis, A. and Marinakis, Y. (2010). "Contribution for optimal sizing of grid-connected PV-systems using PSO." *Renewable Energy*, 35(6), 1333-1341.

Ligmann-Zielinska, A., Church, R. L., and Jankowski, P. (2008). "Spatial optimization as a generative technique for sustainable multiobjective land-use allocation." *Int.J.Geogr.Inf.Sci.,* 22(6), 601-622.

Mondal, M. A. H. and Islam, A. S. (2011). "Potential and viability of grid-connected solar PV system in Bangladesh." *Renewable Energy*, 36(6), 1869-1874.

Mondol, J. D., Yohanis, Y. G., and Norton, B. (2007). "Comparison of measured and predicted long term performance of grid a connected photovoltaic system." *Energy Conversion and Management*, 48(4), 1065-1080.

Natural Resources Canada (2013). "RETScreen 4".

Notton, G., Lazarov, V., and Stoyanov, L. (2010). "Optimal sizing of a grid-connected PV system for various PV module technologies and inclinations, inverter efficiency characteristics and locations." *Renewable Energy*, 35(2), 541-554.

Passey, R., Spooner, T., MacGill, I., Watt, M., and Syngellakis, K. (2011). "The potential impacts of grid-connected distributed generation and how to address them: A review of technical and non-technical factors." *Energy Policy*, 39(10), 6280-6290.

Photovoltaic Software (2014). "Professional Photovoltaic Softwares." http://photovoltaic-software.com/professional.php (5 December 2017).

Poissant, Y., Dignard-Bailey, L., and Bateman, P. (2016). "Photovoltaic technology status and prospects: Canadian annual report 2015."

PV Education.ORG. (2017) "Azimuth angle." http://www.pveducation.org/pvcdrom/2-properties-sunlight/azimuth-angle (17 August 2017).

PV Education.ORG. (2017) "Module materials." http://pveducation.org/pvcdrom/modules/module-materials (16 August 2017).

PVPS, IEA. (2016). "A snapshot of global PV." *Report IEA PVPS T1-29*.

Quaschning, V. and Hanitsch, R. (1998). "Increased energy yield of 50% at flat roof and field installations with optimized module structures." *Proceedings of the 2nd World Conference and Exhibition on Photovoltaic Solar Energy Conversion*, 1993-1996.

Ramaprabha, R. and Mathur, B. (2012). "A comprehensive review and analysis of solar photovoltaic array configurations under partial shaded conditions." *International Journal of Photoenergy*.

RETScreen (2005). *Clean energy project analysis.* Natural Resources Canada, Ottawa, ON, Canada.

Sadineni, S., Boehm, R. F., and Hurt, R. (2008). "Spacing analysis of an inclined solar collector field." *Proceedings of the 2nd ASME International Conference on Energy Sustainability, Jacksonville, FL, USA.*

Sengupta, N., Das, K., Jayram, T., and Seetharam, D. P. (2012). "Optimal allocation of land area for a hybrid solar wind power plant." *3rd IEEE International Conference on Smart Grid Communications*, *Tainan, Taiwan*, 522-527.

Shi, Y. and Eberhart, R. C. (1998). "Parameter selection in particle swarm optimization." *Proceedings of the International Conference on Evolutionary Programming*, Springer, 591-600.

Siraki, A. G. and Pillay, P. (2012). "Study of optimum tilt angles for solar panels in different latitudes for urban applications." *Solar Energy*, 86(6), 1920-1928.

Society of Research Administrators. (2015). "Technical assistance: Solar power analysis and design specifications." 12-13-16.

Solar Energy Society of Alberta (2017). https://solaralberta.ca/ (21 March 2017).

Solar Power Engineering (2010). "How to choose the right PV power inverter." https://www.solarpowerworldonline.com/2010/07/how-to-choose-the-right-pv-power-inverter/ (15 August 2017).

Solar Guy. (2014). "What are the disadvantages of solar power?" http://solarpanelsvenue.com/disadvantages-of-solar-power/ (3 December 2017).

Strzalka, A., Alam, N., Duminil, E., Coors, V., and Eicker, U. (2012). "Large scale integration of photovoltaics in cities." *Appl.Energy*, 93, 413-421.

Tudu, B., Majumder, S., Mandal, K. K., and Chakraborty, N. (2011). "Comparative performance study of genetic algorithm and particle swarm optimization applied on off-grid renewable hybrid energy system." *Proceedings of the International Conference on Swarm, Evolutionary, and Memetic Computing*, Springer, 151-158.

Wang, L. and Singh, C. (2007). "Compromise between cost and reliability in optimum design of an autonomous hybrid power system using mixed-integer PSO algorithm." *Proceedings of the IEEE International Conference on Clean Electrical Power*, 682-689.

Weinstock, D. and Appelbaum, J. (2009). "Optimization of solar photovoltaic fields." *Journal of Solar Energy Engineering*, 131(3), 031003.

Weinstock, D. and Appelbaum, J. (2004a). "Optimal solar field design of stationary collectors." *Journal of Solar Energy Engineering*, 126(3), 898-905.

Weinstock, D. and Appelbaum, J. (2004b). "Shadow variation on photovoltaic collectors in a solar field." *Proceedings of the 23rd IEEE Convention of Electrical and Electronics Engineers in Tel-Aviv, Israel*, 354-357.

Yang, H. and Lu, L. (2007). "The optimum tilt angles and orientations of PV claddings for building-integrated photovoltaic (BIPV) applications." *Journal of Solar Energy Engineering,* 129(2), 253-255.

Zaman, H. U. (2016). "*A framework for improving the productivity of operational preventive maintenance activities for wastewater collection system*"

Zhang, B., Yang, Y., and Gan, L. (2008). "Dynamic control of wind/photovoltaic hybrid power systems based on an advanced particle swarm optimization." *Proceedings of the IEEE International Conference on Industrial Technology*, 6 pages.